

MECHANICAL CHARACTERISTICS OF ANTRIM SHALE

Interim Report for Period April 1977 - January 1978

Kunsoo Kim
(Principal Investigator)

Department of Mining Engineering
Michigan Technological University
Houghton, MI 49931

NOTICE

This report was prepared as an account of work sponsored by the United States Government. Neither the United States nor the United States Department of Energy, nor any of their employees, nor any of their contractors, subcontractors, or their employees, makes any warranty, express or implied, or assumes any legal liability or responsibility for the accuracy, completeness or usefulness of any information, apparatus, product or process disclosed, or represents that its use would not infringe privately owned rights.

Date Published - February 1978

MASTER

Prepared For

The Dow Chemical Company

Under DOE Contract No. EX-76-C-01-2346

EP

DISCLAIMER

This report was prepared as an account of work sponsored by an agency of the United States Government. Neither the United States Government nor any agency thereof, nor any of their employees, makes any warranty, express or implied, or assumes any legal liability or responsibility for the accuracy, completeness, or usefulness of any information, apparatus, product, or process disclosed, or represents that its use would not infringe privately owned rights. Reference herein to any specific commercial product, process, or service by trade name, trademark, manufacturer, or otherwise does not necessarily constitute or imply its endorsement, recommendation, or favoring by the United States Government or any agency thereof. The views and opinions of authors expressed herein do not necessarily state or reflect those of the United States Government or any agency thereof.

DISCLAIMER

Portions of this document may be illegible in electronic image products. Images are produced from the best available original document.

ABSTRACT

A laboratory investigation has been conducted to determine the basic mechanical properties of Antrim oil shale. The strength and deformation properties were studied in quasi-static uniaxial compression, ultrasonic velocity, point load strength and surface hardness tests.

Young's modulus and compressive strength were found to decrease with increasing kerogen content while Poisson's ratio remained at a fairly constant level. The density decreased in a linear fashion with increasing kerogen content. The floor rocks showed much greater strength, Young's modulus and Poisson's ratio in comparison with oil shale.

A distinct characteristic of Antrim shale was the extreme weakness of the bedding plane which caused a great difficulty in sample preparation. This strength anisotropy would be of great importance in the design of bed preparation methods such as massive hydraulic fracturing and explosives fracturing.

TABLE OF CONTENTS

	Page
Abstract	i
List of Figures	iii
List of Tables	vi
1.0 Introduction	1
2.0 Experimental	1
2.1 Uniaxial Compression	1
2.1.1 Specimen preparation	1
2.1.2 Test procedure	2
2.1.3 Test results	3
2.2 Ultrasonic Wave Velocity Measurements	28
2.2.1 Test procedure	28
2.2.2 Test results	28
2.3 Point Load Strength Index	47
2.3.1 Test procedure	47
2.3.2 Test results	48
2.4 Scleroscope Hardness	48
2.4.1 Test procedure	48
2.4.2 Test results	61
3.0 Summary	61
References	75
Appendix	76

LIST OF FIGURES

Figure	Page
1 Typical stress, strain and time curves monitored during tests	4
2a Typical stress-strain curves of oil shale (Specimen No. 102-1375.0)	5
2b Typical stress-strain curves of oil shale (Specimen No. 102-1397.5)	6
2c Typical stress-strain curves of floor rock (Specimen No. 102-1436.0)	7
2d Typical stress-strain curves of floor rock (Specimen No. 101-1517.2)	8
2e Stress-strain curves of some selected specimens	9
3a Variation of static Young's moduli with depth (Well No. Dow/ERDA 100)	13
3b Variation of static Young's moduli with depth (Well No. Dow/ERDA 101)	14
3c Variation of static Young's moduli with depth (Well No. Dow/ERDA 102)	15
4a Variation of static Poisson's ratio with depth (Well No. Dow/ERDA 100)	16
4b Variation of static Poisson's ratio with depth (Well No. Dow/ERDA 101)	17
4c Variation of static Poisson's ratio with depth (Well No. Dow/ERDA 102)	18
5a Variation of uniaxial compressive strength with depth (Well No. Dow/ERDA 100)	19
5b Variation of uniaxial compressive strength with depth (Well No. Dow/ERDA 101)	20
5c Variation of uniaxial compressive strength with depth (Well No. Dow/ERDA 102)	21
6 Density vs. % wt. loss	24
7 Compressive strength vs. % wt. loss	25
8 Static Young's modulus vs. % wt. loss	26
9 Static Poisson's ratio vs. % wt. loss	27
10a Variation of dynamic Young's modulus with depth (Well No. Dow/ERDA 100)	34

LIST OF FIGURES (continued)

Figure	Page
10b Variation of dynamic Young's modulus with depth (Well No. Dow/ERDA 101)	35
10c Variation of dynamic Young's modulus with depth (Well No. Dow/ERDA 102)	36
11a Variation of dynamic Poisson's ratio with depth (Well No. Dow/ERDA 100)	37
11b Variation of dynamic Poisson's ratio with depth (Well No. Dow/ERDA 101)	38
11c Variation of dynamic Poisson's ratio with depth (Well No. Dow/ERDA 102)	39
12a Variation of shear modulus with depth (Well No. Dow/ERDA 100)	40
12b Variation of shear modulus with depth (Well No. Dow/ERDA 101)	41
12c Variation of shear modulus with depth (Well No. Dow/ERDA 102)	42
13 P-wave velocity vs. % wt. loss	43
14 S-wave velocity vs. % wt. loss	44
15 Dynamic Young's modulus vs. % wt. loss	45
16 Dynamic Poisson's ratio vs. % wt. loss	46
17 Variation of point load strength index with depth (Well No. Dow/ERDA 100)	55
18 Variation of point load strength index with depth (Well No. Dow/ERDA 101)	56
19 Variation of point load strength index with depth (Well No. Dow/ERDA 102)	57
20 Variation of density with depth (Well No. Dow/ERDA 100) . . .	58
21 Variation of density with depth (Well No. Dow/ERDA 101) . . .	59
22 Variation of density with depth (Well No. Dow/ERDA 102) . . .	60
23 Variation of scleroscope hardness with depth (Well No. Dow/ERDA 100)	68
24 Variation of scleroscope hardness with depth (Well No. Dow/ERDA 101)	69
25 Variation of scleroscope hardness with depth (Well No. Dow/ERDA 102)	70

LIST OF FIGURES (continued)

Figure	Page
26 Point load strength index vs. scleroscope hardness no. (Well No. Dow/ERDA 100)	71
27 Point load strength index vs. scleroscope hardness no. (Well No. Dow/ERDA 101)	72
28 Point load strength index vs. scleroscope hardness no. (Well No. Dow/ERDA 102)	73

LIST OF TABLES

Table		Page
1	Uniaxial Compression Test Results (Specimens from Well No. Dow/ERDA 100)	10
2	Uniaxial Compression Test Results (Specimens from Well No. Dow/ERDA 101)	11
3	Uniaxial Compression Test Results (Specimens from Well No. Dow/ERDA 102)	12
4	Weight Loss After Roasting in Air at 500°C	23
5	Dynamic Elastic Constants Measured by Ultrasonic Method (Specimens from Well No. Dow/ERDA 100)	29
6	Dynamic Elastic Constants Measured by Ultrasonic Method (Specimens from Well No. Dow/ERDA 101)	31
7	Dynamic Elastic Constants Measured by Ultrasonic Method (Specimens from Well No. Dow/ERDA 102)	33
8	Point Load Test Results (Specimens from Well No. Dow/ERDA 100)	49
9	Point Load Test Results (Specimens from Well No. Dow/ERDA 101)	51
10	Point Load Test Results (Specimens from Well No. Dow/ERDA 102)	53
11	Scleroscope Hardness Test Results (Specimens from Well No. Dow/ERDA 100)	62
12	Scleroscope Hardness Test Results (Specimens from Well No. Dow/ERDA 101)	63
13	Scleroscope Hardness Test Results (Specimens from Well No. Dow/ERDA 102)	66

1.0 INTRODUCTION

The prime objectives of this investigation were to determine the basic mechanical properties of Antrim shale and to study its behavior under various conditions as part of the in-situ oil shale retorting research program. The following tests were conducted in the first year of the study:

1. Unconfined compression tests for uniaxial compressive strength, Young's modulus and Poisson's ratio;
2. point load tests for point load strength index;
3. scleroscope hardness tests for surface hardness number; and
4. ultrasonic velocity measurements for dynamic Young's modulus and Poisson's ratio

Some selected specimens were subjected to retorting condition after completing the foregoing tests to find the kerogen content. The parameters obtained from the mechanical property tests were plotted against the kerogen content to study the relationships between them.

Specimens were prepared from the 3½ inch diameter cores obtained from the Dow/ERDA Wells No. 100, 101 and 102 located on the Dow test site in Sanilac County, Michigan. Approximately 900 ft long cores, 300 ft from each well, were provided to the University for this study. These cores consisted of cap rocks, floor rocks and oil shale.

It is planned to carry out triaxial compression, diametral compression, fracture toughness and laboratory hydraulic fracturing tests in the succeeding years.

This report describes the test methods employed and results obtained during the first year.

2.0 EXPERIMENTAL

2.1 Uniaxial Compression

2.1.1 Specimen Preparation

Specimens for uniaxial compression tests were prepared from the 3½ inch diamond drill cores provided. The ASTM Designation D2938-71¹ was used as a guideline.

It was originally planned to obtain a specimen at every 10 ft interval from the 900 ft cores. Visual inspection of cores revealed that the quality of the cores in the interval from 1200 to 1300 ft was so poor that no NX specimen that fulfilled the ASTM specifications (length to diameter ratio 2-2.5) could be obtained. This interval represents the cap rock overlying Antrim shale. Our effort to secure specimens was, therefore, concentrated on the intervals below the 1300 ft level.

The specimen preparation involved coring, diamond saw cutting and surface grinding. A large number of specimens were broken during these preparation processes due to the inherent weakness in the bedding planes which are approximately perpendicular to the core axis. In core 100, only sixteen specimens (2 1/8" diameter x 5 1/4" length) from nine intervals were obtained after making more than 60 attempts. This low rate of success in specimen preparation made us alter our original plan of having at least one specimen from each interval.

The physical dimensions and weight were measured when specimen preparation was finished. It was ensured that test specimens have ends flat within 0.001 inch and sides smooth within .005". Before conducting the actual test, the color, nature and volumetric intrusion of foreign materials, etc. were recorded. Specimens were stored in room temperature until test was ready.

2.1.2 Test Procedure

The tests were conducted to determine the strength and deformation properties in uniaxial compression.

Four foil type strain gages* were mounted on the specimen surface free from irregularities or abnormalities, two in the axial direction and the other two in the lateral direction. Each pair of strain gages in the axial and lateral direction were oriented at diametrically opposite points to compensate for possible asymmetrical loading.

We used an ultra-stiff closed loop servo-controlled hydraulic testing system[†] coupled with a processor interface, three transducers/conditioners

*Micro-Measurement type CEA-06-250UW-120.

[†]MTS Rock Mechanics Test System.

and a small digital computer to enable automated testing and data acquisition. The load capacity of this test system was 5 MN.

The computer program used for this series of tests provided:

(i) a constant rate of loading approximately 0.69 MPa/sec (100 psi/sec),
(ii) graphical displays of stress vs axial strain, stress vs circumferential strain and axial strain vs circumferential strain, etc. Data was stored in a floppy disc and a hard copy unit facilitated copies of all plots. The system was backed by two x-y recorders in order to cover the risk due to accidental malfunctioning of the computer.

A specimen was set up in the testing machine and each pair of strain gages was connected to form a half bridge temperature compensated circuit. The bridge circuits were shunt calibrated to provide 12,000 $\mu\epsilon$ for axial and 3,000 $\mu\epsilon$ for lateral strain. The excitation voltage was adjusted to yield an output voltage of 10 volts. Maximum loading range was 0.5 MN (112,400 lbs). After adjusting the output voltage the x-y recorder range was adjusted to provide an adequate strain resolution.

Testing was started by initiating the pre-programmed computer program. The stress-strain curves were displayed on a cathode ray tube (CRT) terminal during testing while all the data were continuously stored in the floppy disc mass storage unit until test is completed. Typical plots are given in Fig. 1.

The test was automatically stopped at failure of specimen.

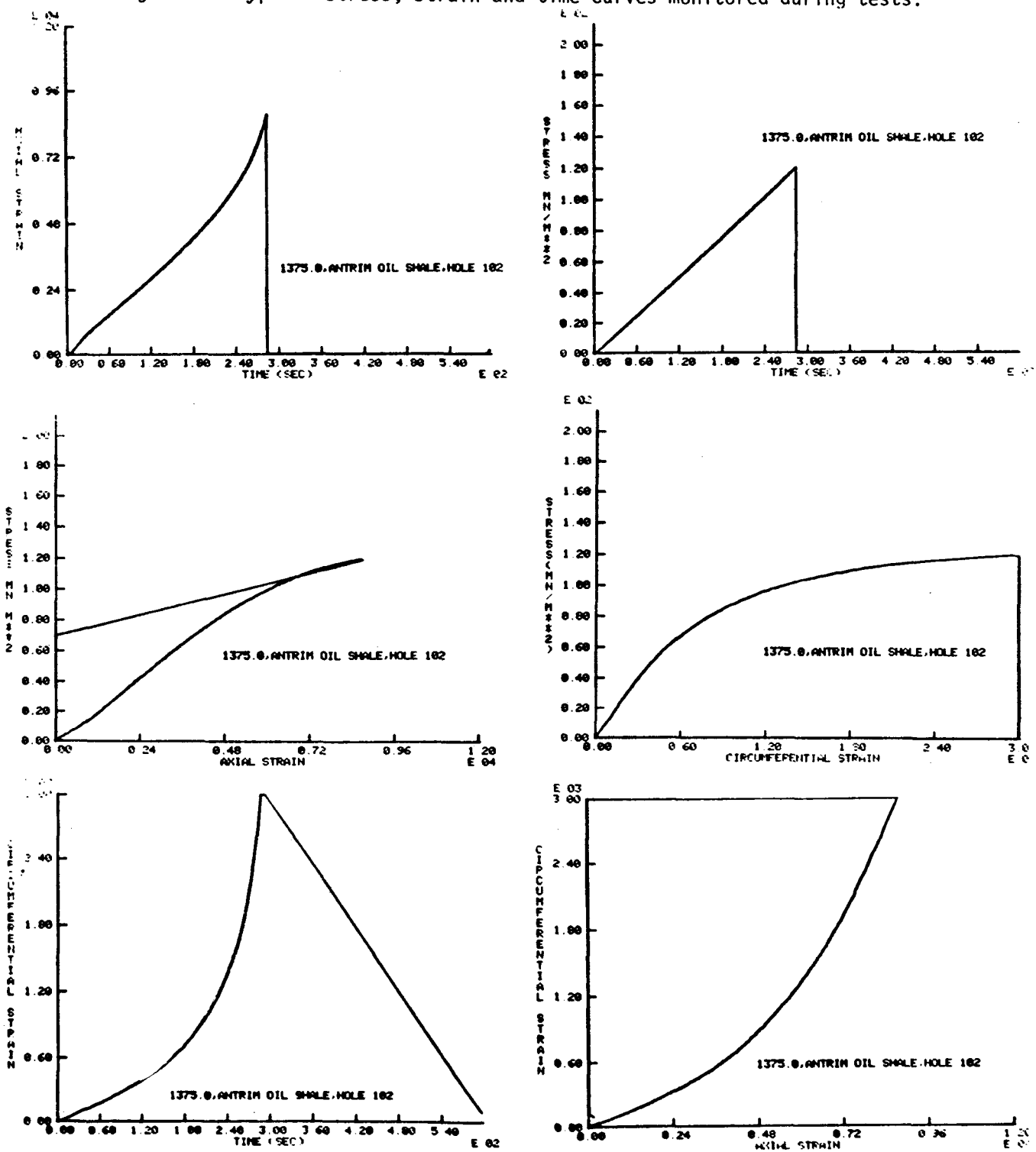
2.1.3 Test Results

A total of 33 specimens were successfully tested. The stress-axial and stress-lateral strain curves were plotted from the digitized data stored in floppy discs. Some typical stress-strain curves are given in Figs. 2a-2d. Others are given in the Appendix.

The compressive strength, Young's modulus, Poisson's ratio and maximum axial strain were calculated from stress-strain curves and tabulated in Tables 1-3. These were also plotted against depth to find the variation with depth (Figs. 3a-5c).

The stress-strain curves can be divided into two groups: (i) low modulus group, and (ii) high modulus group (Fig. 2e). The modulus of

Figure 1. Typical stress, strain and time curves monitored during tests.



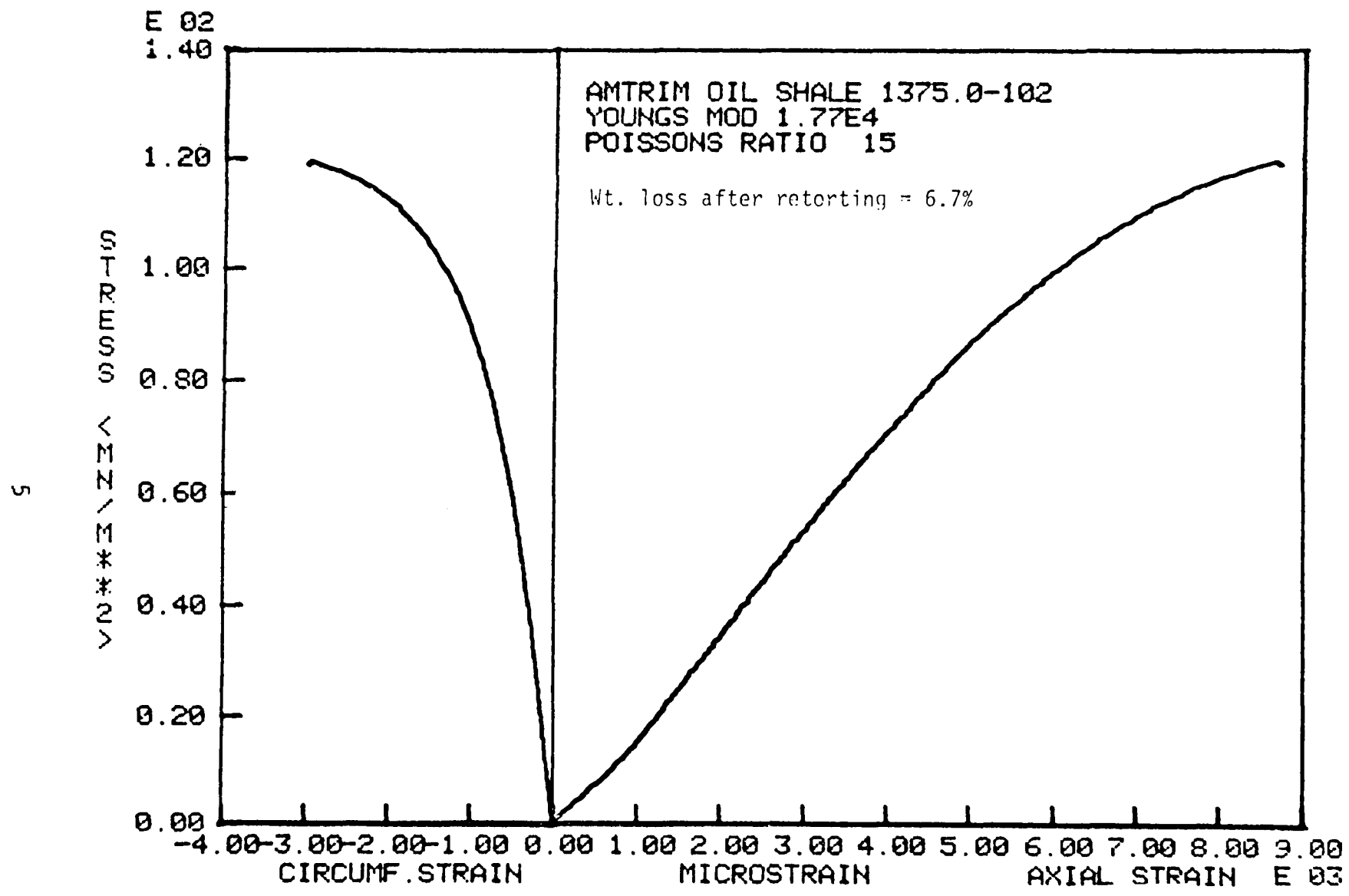


Figure 2a. Typical stress-strain curves of oil shale (Specimen No. 102-1375.0)

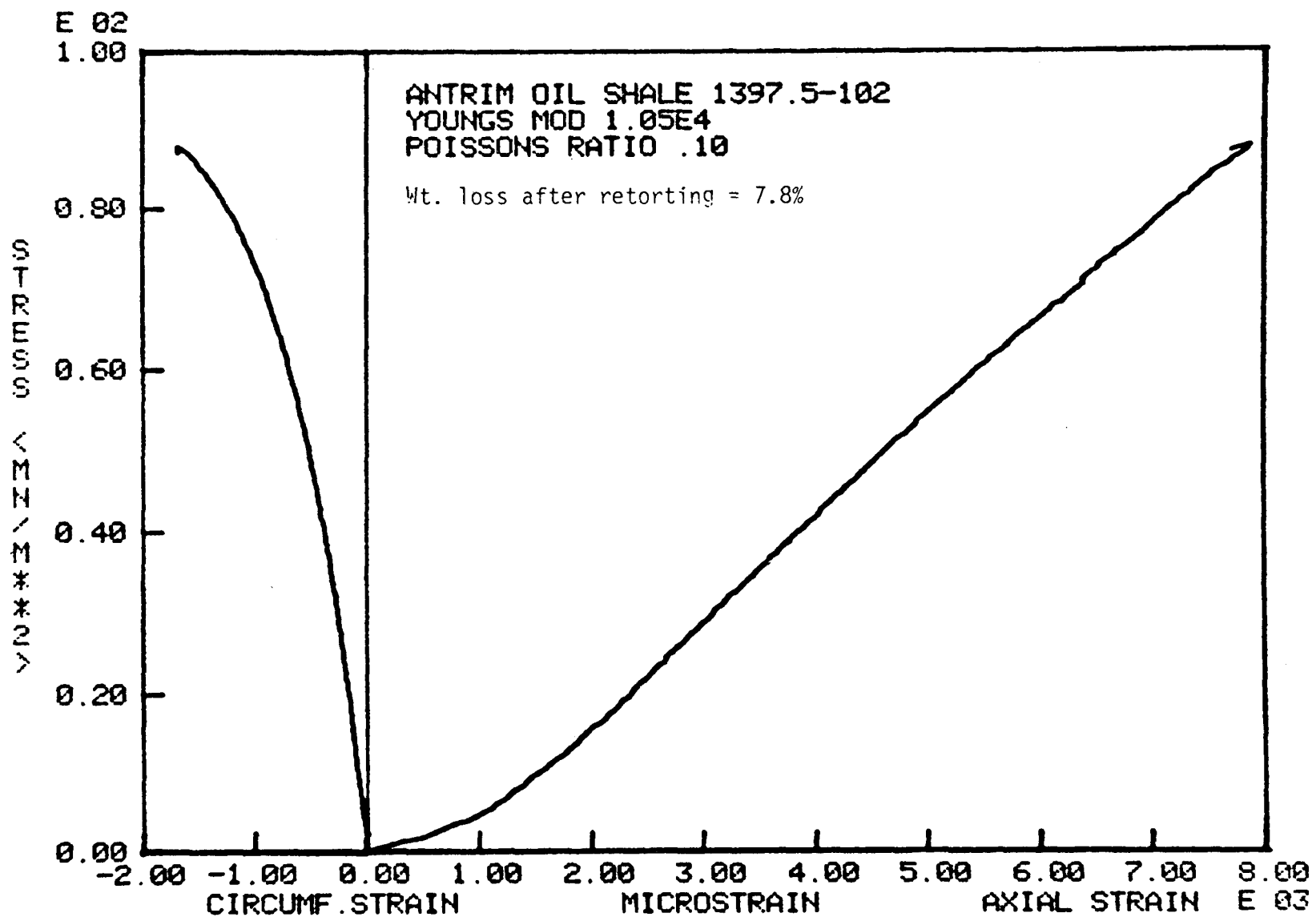


Figure 2b. Typical stress-strain curves of oil shale (Specimen No. 102-1397.5).

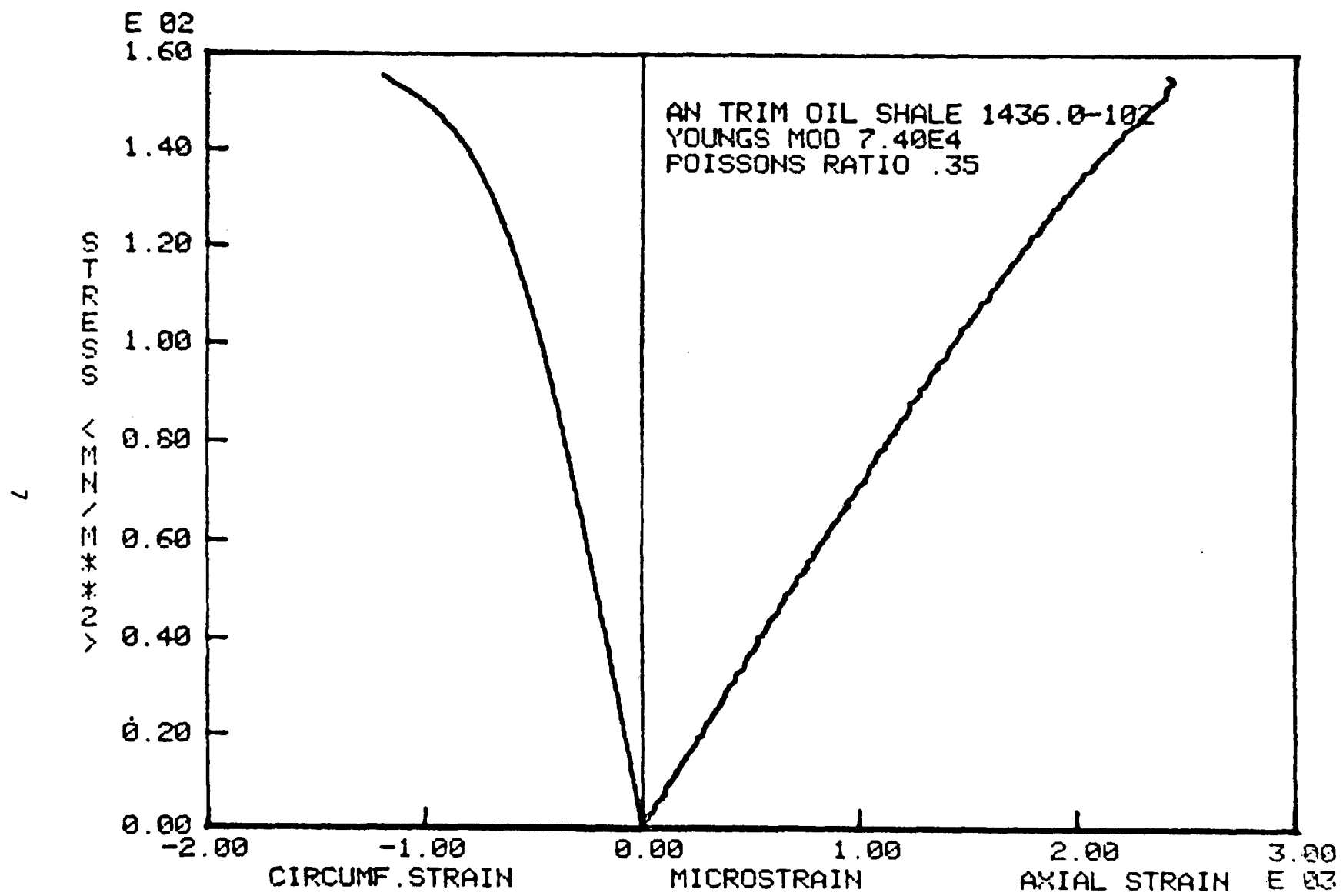


Figure 2c. Typical stress-strain curves of floor rock (Specimen No. 102-1436.0).

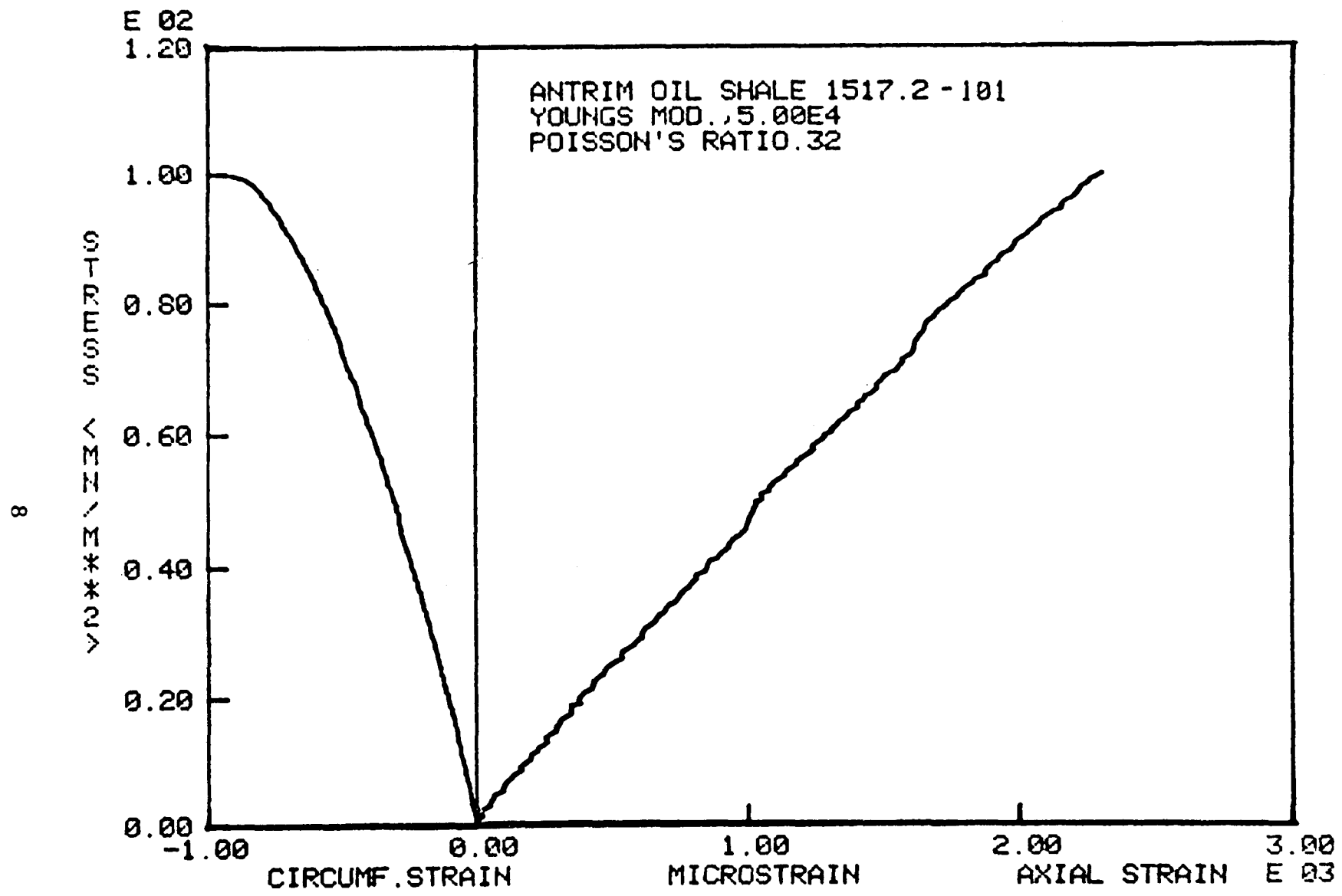


Figure 2d. Typical stress-strain curves of floor rock (Specimen No. 101-1517.2).

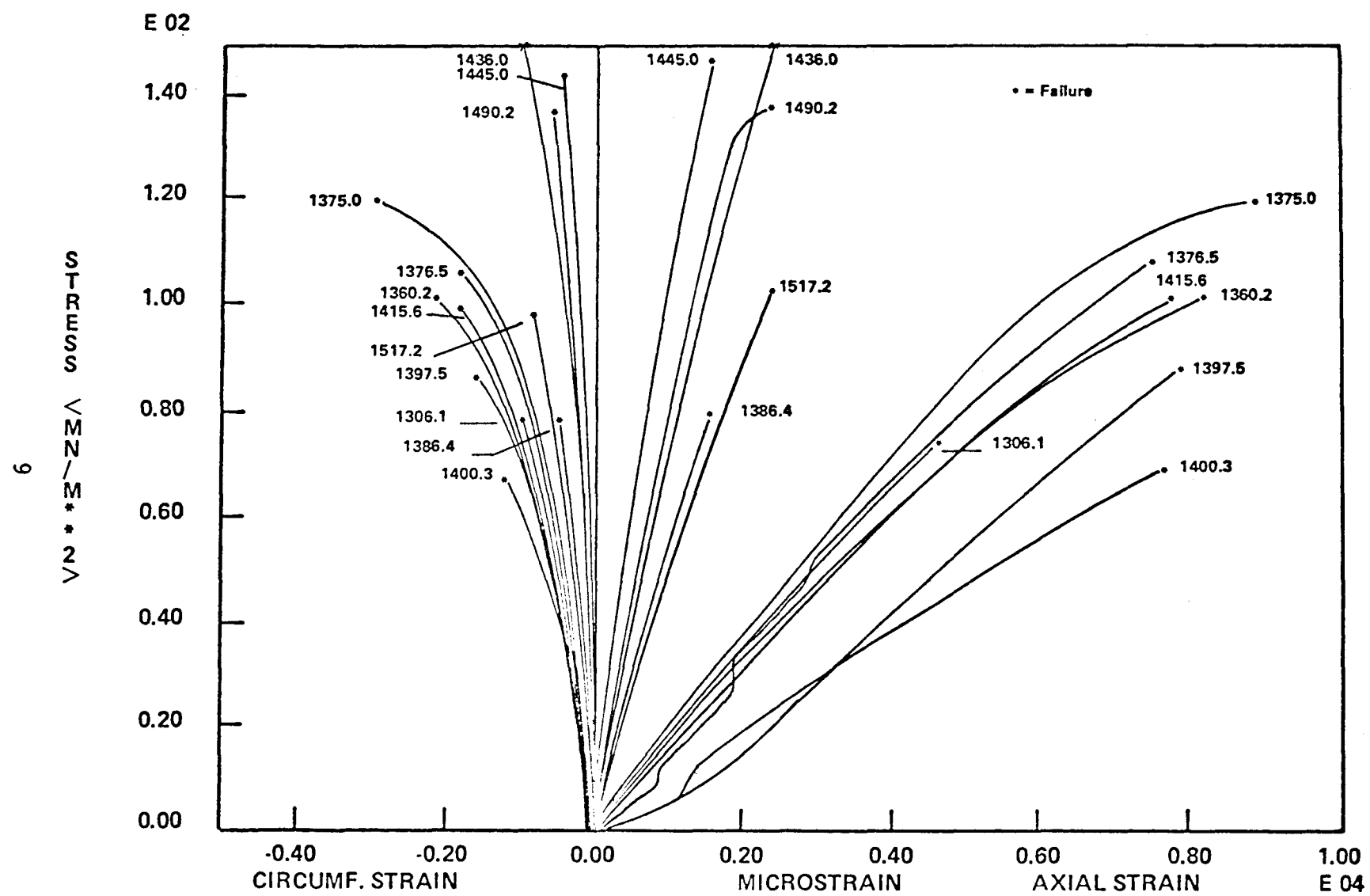


Figure 2e. Stress-strain curves of some selected specimens.

TABLE 1. UNIAXIAL COMPRESSION TEST RESULTS
(Specimens from Well No. Dow/ERDA 100)

Specimen No.	Compressive Strength MPa	Young's Modulus GPa	Poisson's Ratio
100/1346.5	114.0	20.6	0.19
100/1359.5	118.6	14.6	0.19
100/1361.8	78.5	17.7	0.17
100/1374.7	94.7	16.0	0.19
100/1396.6	109.0	50.6	0.24
100/1445.0	131.4	45.7	0.24
100/1477.4	105.8	41.7	0.28

TABLE 2. UNIAXIAL COMPRESSION TEST RESULTS
(Specimens from Well No. Dow/ERDA 101)

Specimen No.	Maximum Axial Strain (10^{-6})	Compressive Strength MPa	Young's Modulus GPa	Poisson's Ratio
101/1326.0	4440	155.9	44.8	0.25
101/1341.1	8760	122.4	18.1	0.17
101/1352.0	8040	100.0	16.0	0.17
101/1360.2	8160	101.4	16.4	0.19
101/1382.3	3000	120.5	45.6	0.22
101/1396.5	6540	87.4	16.2	0.14
101/1400.3	7560	68.2	9.9	0.13
101/1411.8	6720	92.9	14.6	0.13
101/1430.0	2310	131.1	59.1	0.26
101/1440.9	3120	56.4	18.1	0.15
101/1462.8	3060	96.0	34.8	0.24
101/1488.4	1140	72.1	66.8	0.24
101/1490.2	2760	138.5	82.4	0.29
101/1507.2	3780	76.7	21.7	0.08
101/1517.1	2520	102.2	50.0	0.32

TABLE 3. UNIAXIAL COMPRESSION TEST RESULTS
(Specimens from Well No. Dow/ERDA 102)

Specimen No.	Maximum Axial Strain (10^{-6})	Compressive Strength MPa	Young's Modulus GPa	Poisson's Ratio
102/1306.1	5040	80.0	17.7	0.15
102/1375.0	8700	119.4	17.7	0.15
102/1376.5	8760	106.6	15.0	0.13
102/1386.4	1440	78.9	54.7	0.26
102/1397.5	7860	87.4	10.5	0.10
102/1416.6	7800	100.2	15.4	0.16
102/1436.3	3180	161.0	52.6	0.22
102/1438.0	2820	152.5	61.9	0.28
102/1445.0	1920	138.4	96.0	0.31
102/1476.0	2370	155.4	74.0	0.35
102/1496.8	1080	68.2	75.8	0.33

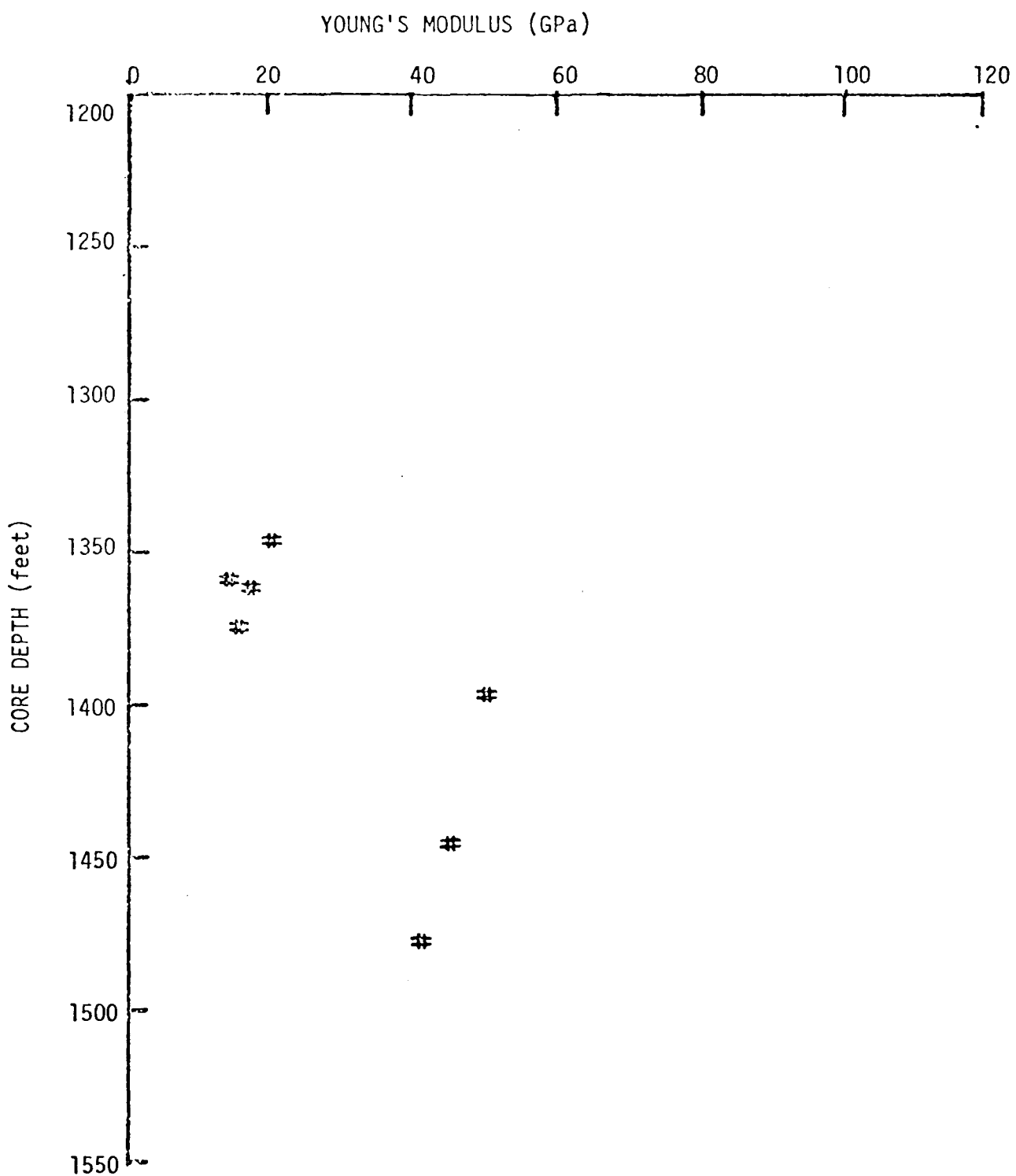


Figure 3a. Variation of static Young's moduli with depth
(Well No. Dow/ERDA 100).

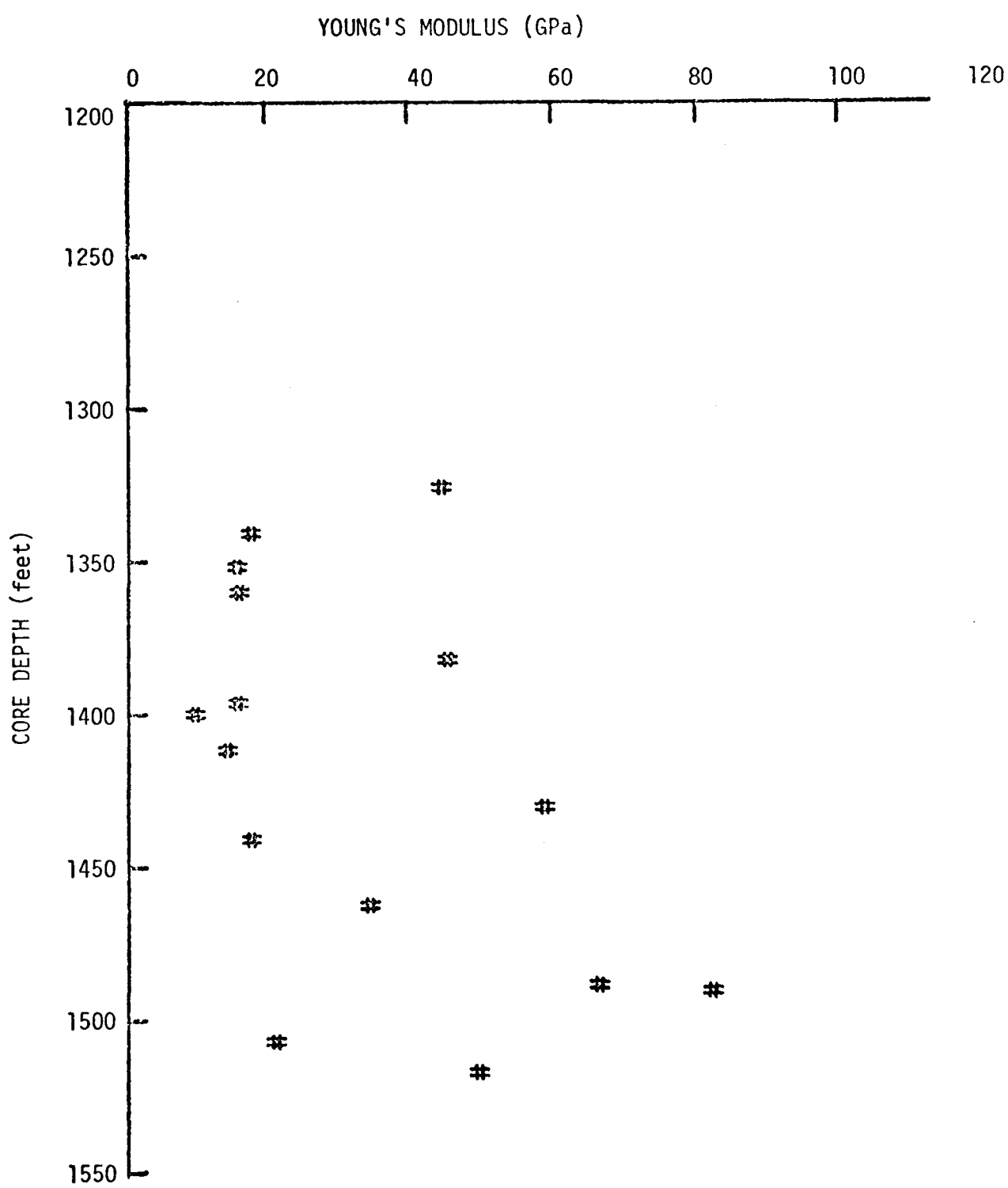


Figure 3b. Variation of static Young's moduli with depth
(Well No. Dow/ERDA 101).

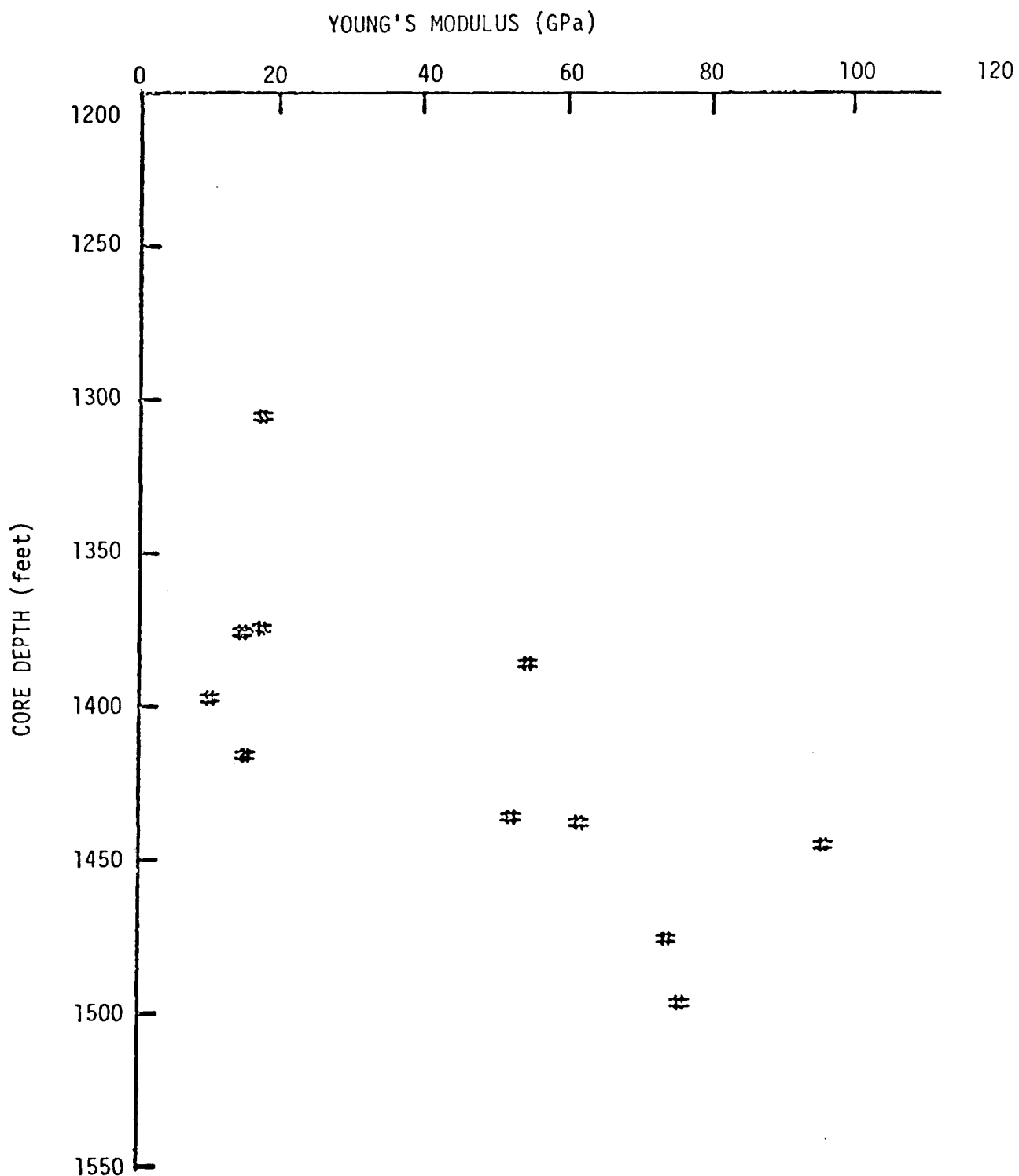


Figure 3c. Variation of static Young's moduli with depth
(Well No. Dow/ERDA 102).

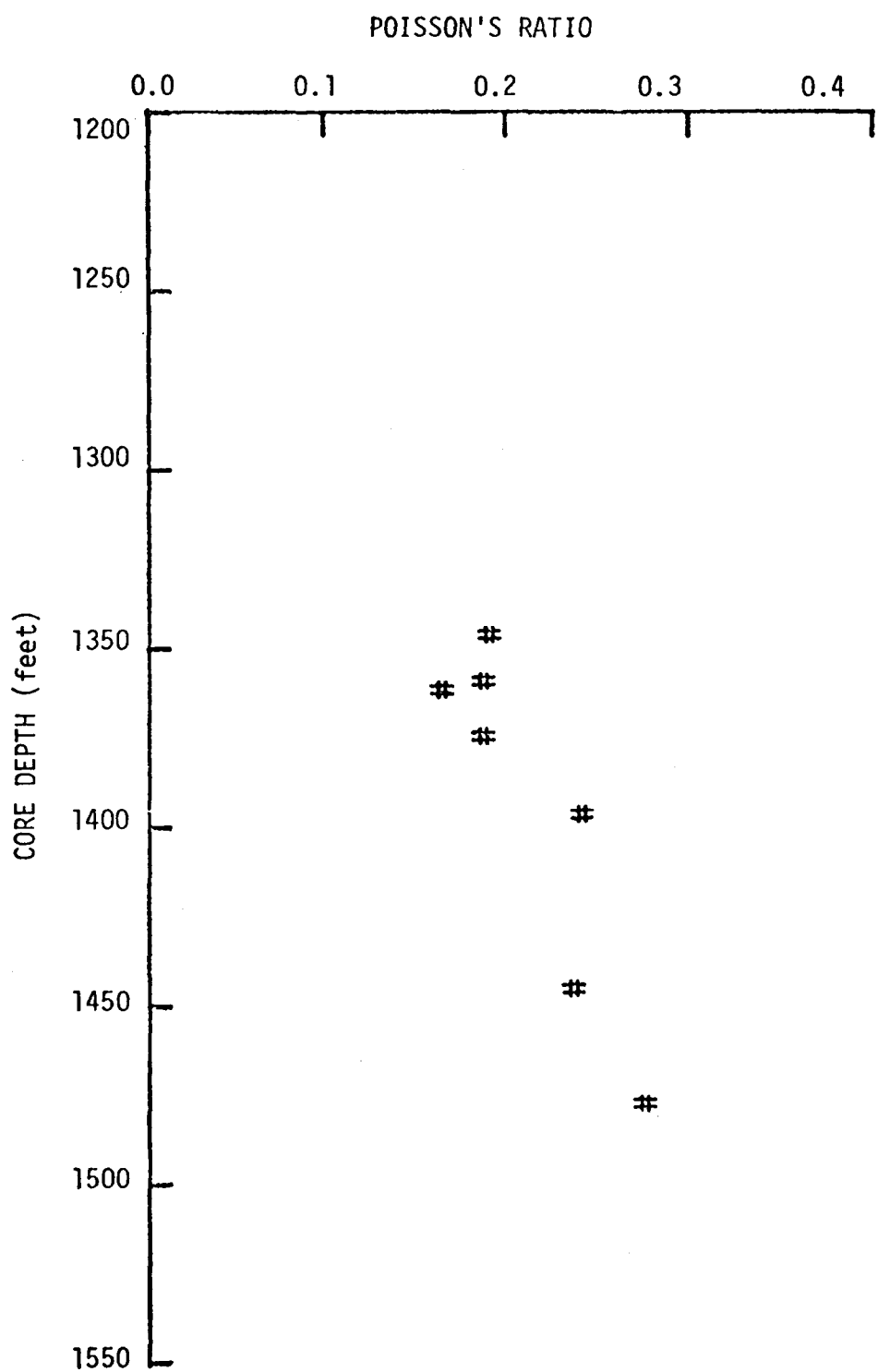
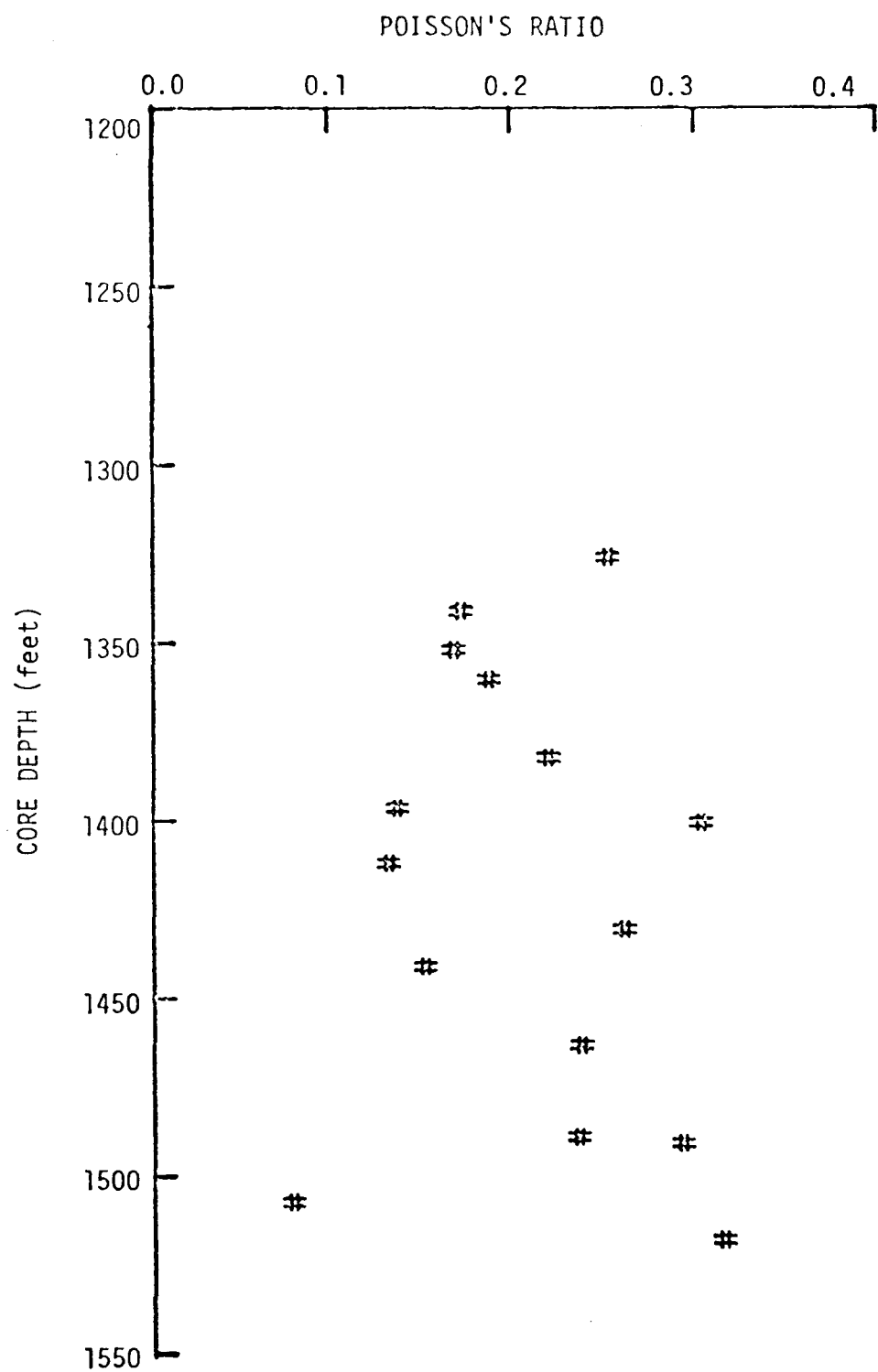


Figure 4a. Variation of static Poisson's ratio with depth
(Well No. Dow/ERDA 100).



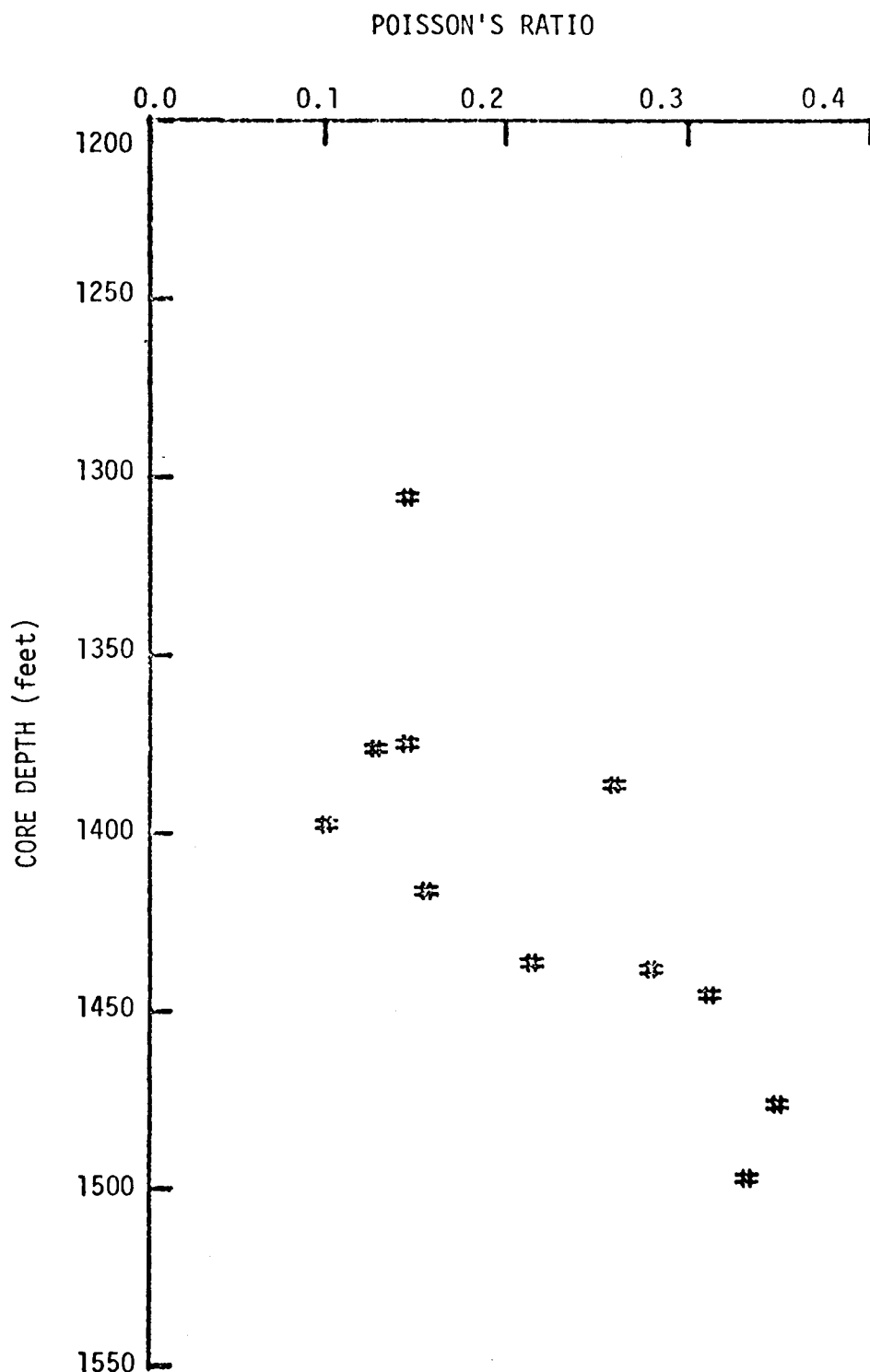


Figure 4c. Variation of static Poisson's ratio with depth
(Well No. Dow/ERDA 102).

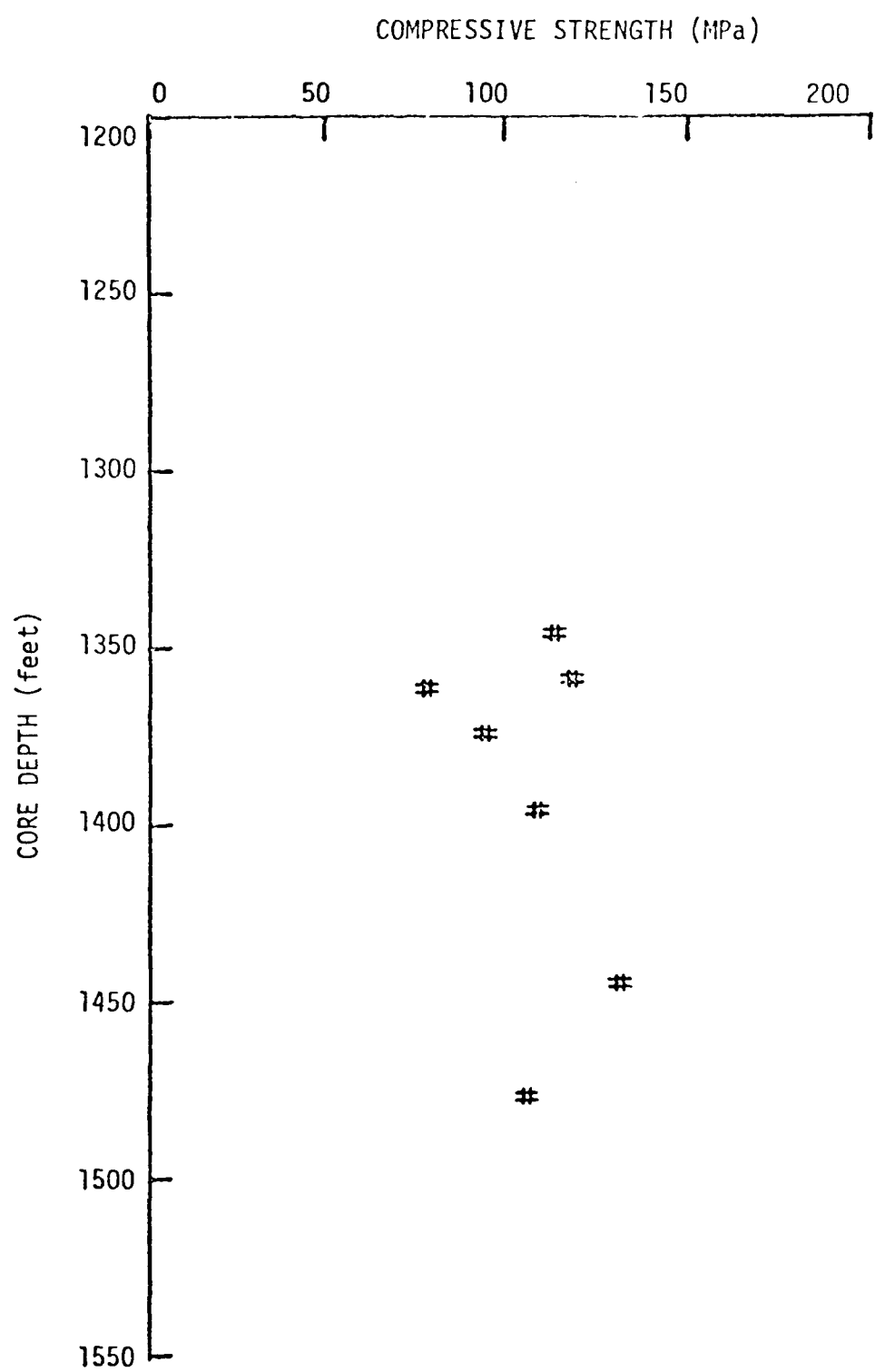


Figure 5a. Variation of uniaxial compressive strength with depth (Well No. Dow/ERDA 100).

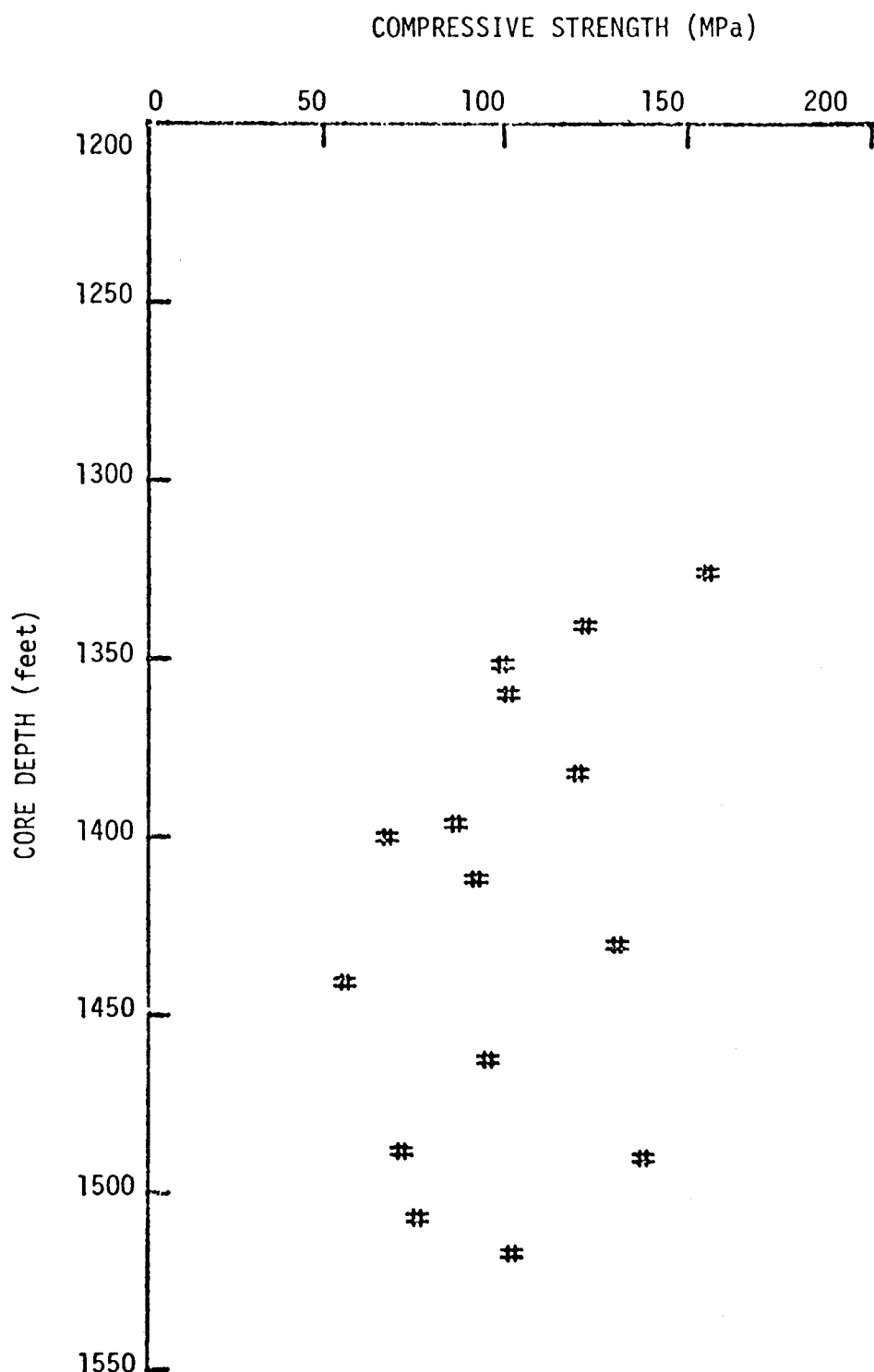


Figure 5b. Variation of uniaxial compressive strength with depth (Well No. Dow/ERDA 101).

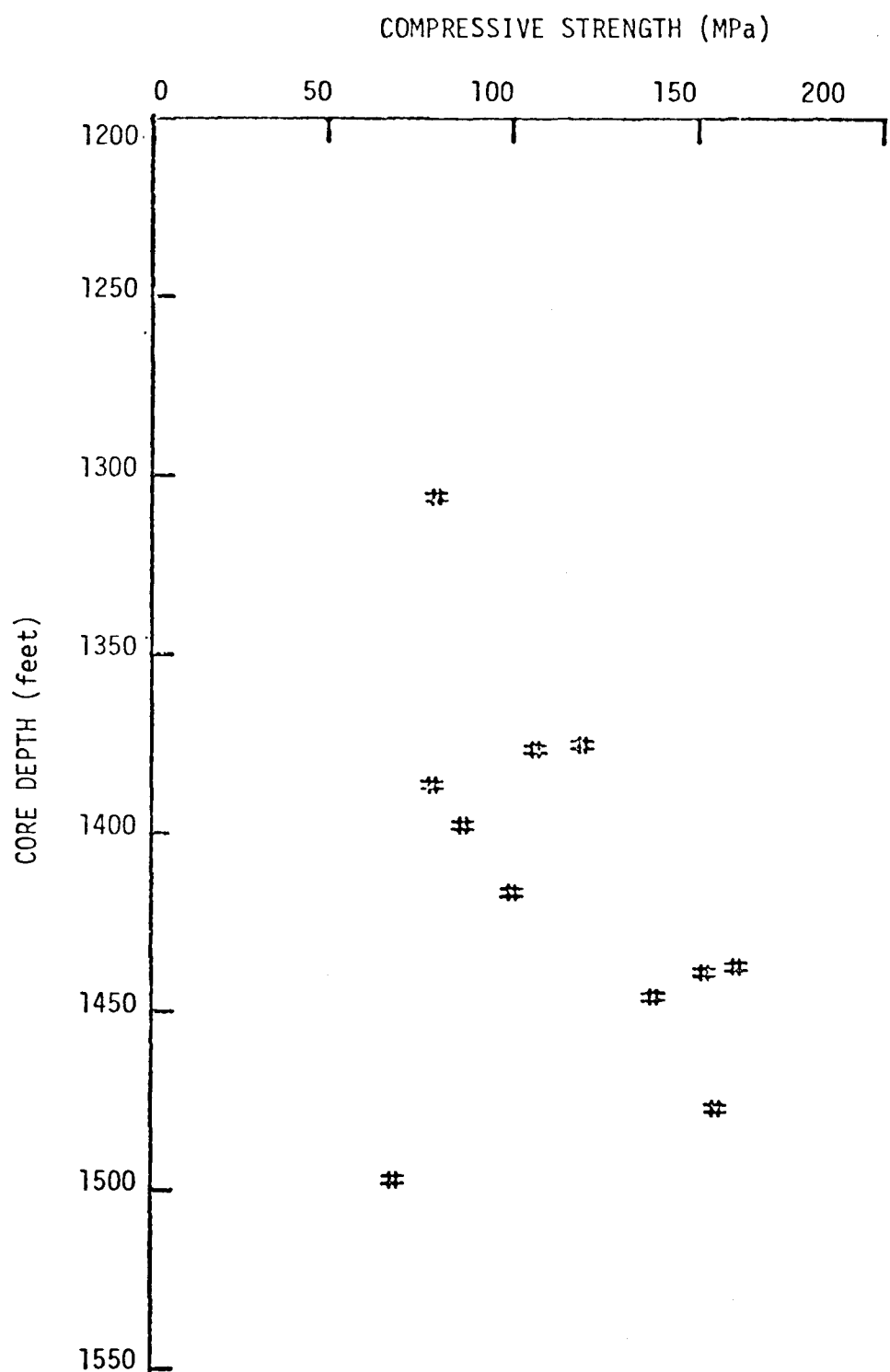


Figure 5c. Variation of uniaxial compressive strength with depth (Well No. Dow/ERDA 102).

the former group ranges from approximately 10 to 20 GPa while the latter ranges from 40 to as high as 96 GPa. The specimens belonging to the latter group were either extremely lean oil shale with high percentage of calcareous material intrusions or floor rock. These rocks showed relatively high Poisson's ratio and low maximum axial strain, typically lower than 0.3%. Figure 2e shows these two contrasting deformation behaviors clearly.

Some selected specimens were retorted after uniaxial compression tests to roughly estimate the kerogen content. Percentage wt. loss was measured after roasting in air at 500°C for about 24 hrs. The results are given in Table 4.

To find the relationships between the kerogen content and the strength and deformation properties obtained, the percentage wt. loss of specimens was plotted against the density, compressive strength, Young's modulus and Poisson's ratio. A decreasing trend in % wt. loss was obtained as the density increases as expected. A best fit linear curve was obtained by linear regression analysis. The slope and the vertical axis intercept are also given in the plot. In the analysis of Young's modulus E , Poisson's ratio ν , compression strength C_o , the data lower than 4% wt. loss were not used because these specimens were highly contaminated with calcareous material and therefore were not considered oil shale. Although scatter is very high yet E and C_o show decreasing trends with increasing % wt. loss (Fig. 7, 8). The Poisson's ratio does not vary significantly (Fig. 9).

TABLE 4. WEIGHT LOSS AFTER ROASTING IN AIR AT 500°C

Specimen No.	% Wt Loss	Specimen No.	% Wt Loss
101/1326.0	3.0	102/1306.1*	8.6
101/1346.5	8.7	102/1375.0	6.7
101/1352.0*	10.2	102/1376.5	7.4
101/1360.2	12.6**	102/1386.4	2.1
101/1382.3	1.4	102/1397.5	7.8
101/1391.1	10.6	102/1416.6	10.0
101/1396.5	6.0		
101/1400.3*	18.5		
101/1411.8	8.1		
101/1425.2*	0.9		

*Roasted in the as-received condition. All other samples jaw-crushed to approximately minus one inch before roasting.

**Sample spilled after roasting; % wt loss will be high if recovery of spilled material was not complete.

NOTE: The data in Table 4 were obtained by Mr. W. A. Hockings of the Institute of Mineral Research, Michigan Technological University.

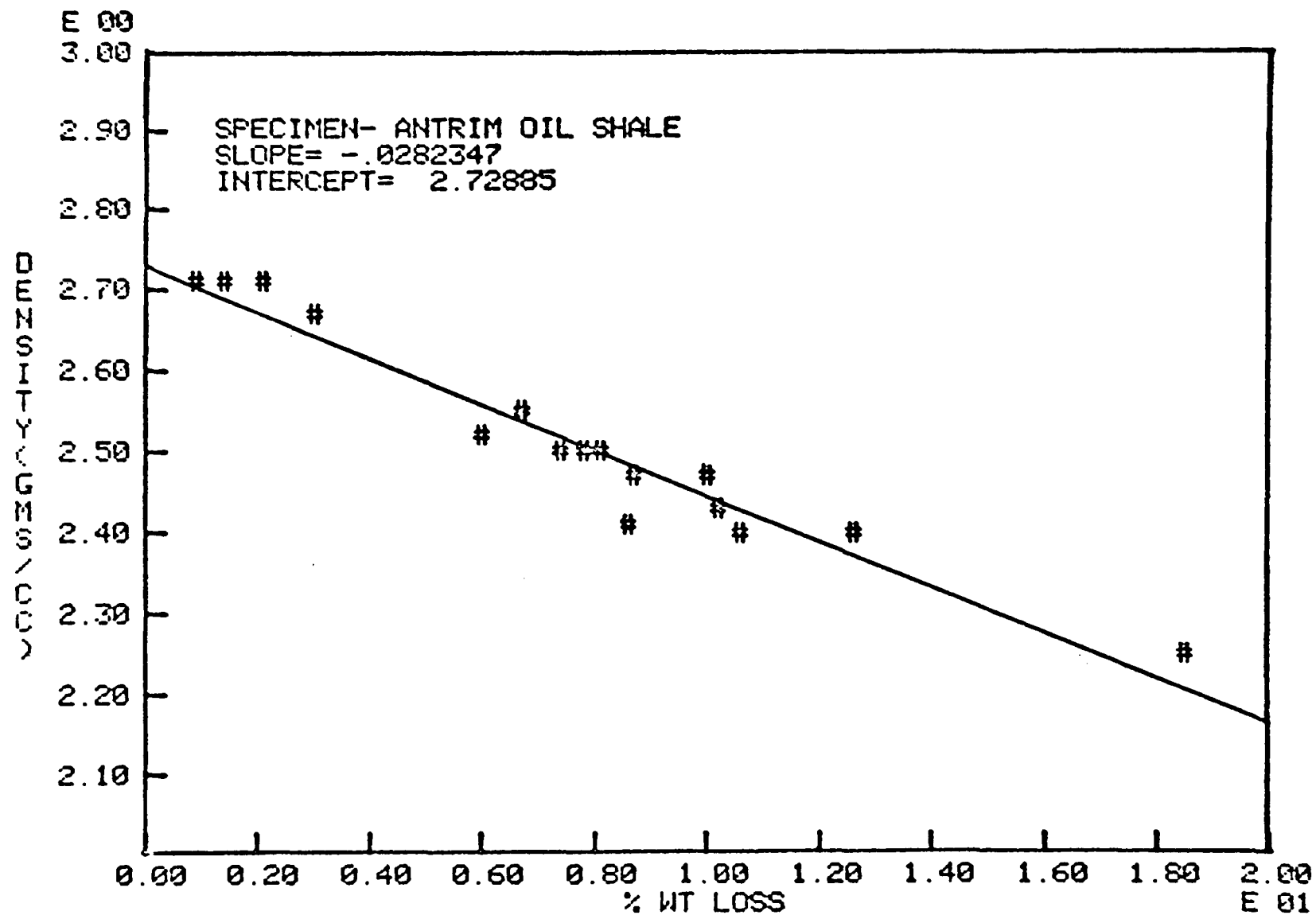


Figure 6. Density vs. % wt. loss.

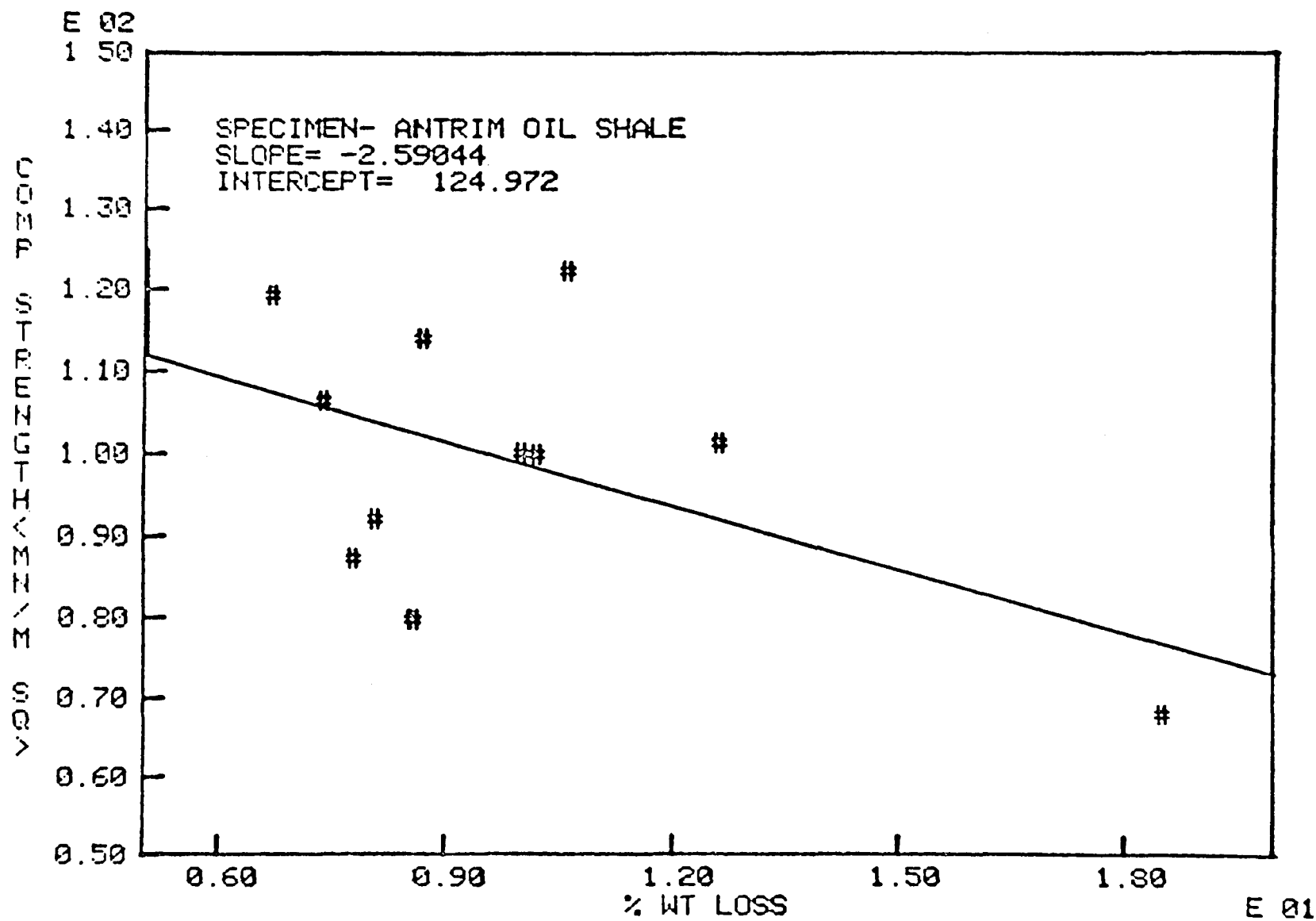


Figure 7. Compressive strength vs. % wt. loss.

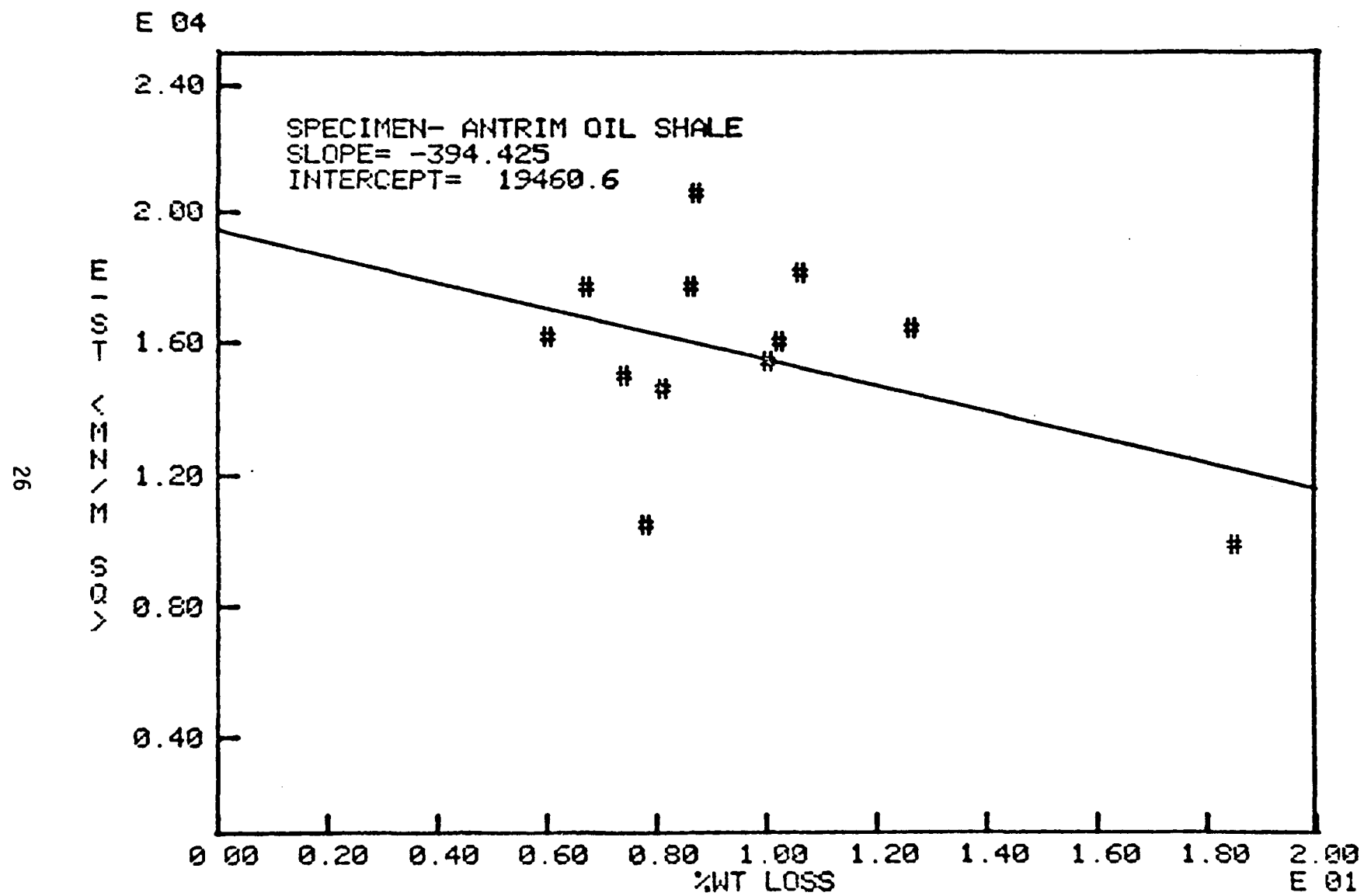


Figure 8. Static Young's modulus vs. % wt. loss.

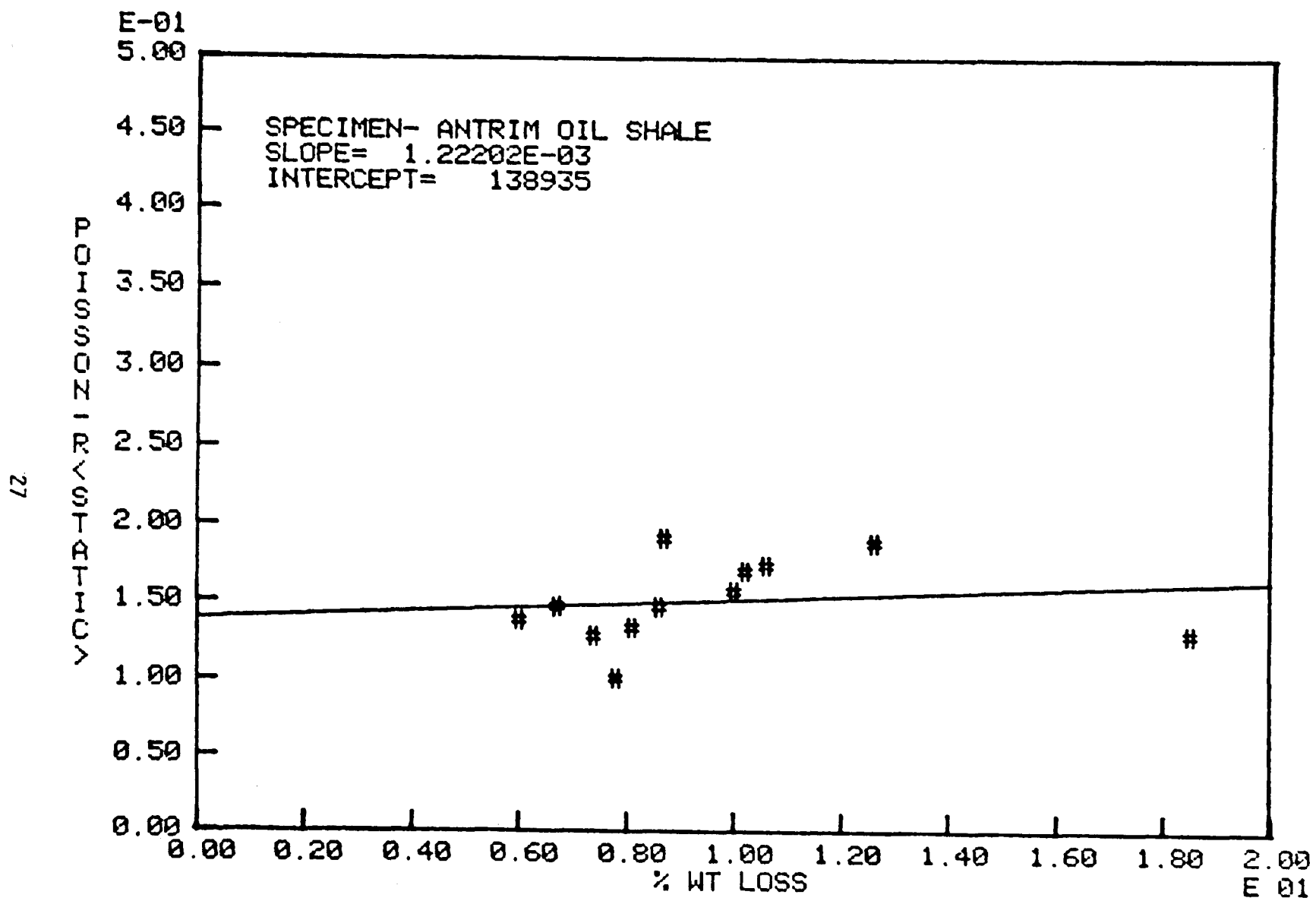


Figure 9. Static Poisson's ratio vs. % wt. loss.

2.2 Ultrasonic Wave Velocity Measurements

2.2.1 Test Procedure

The compressional and shear wave velocities were measured in the axial direction of the core which is approximately perpendicular to the bedding plane.

Terrametrics ultrasonic wave velocity measurement system was used. This system consists of pulse generator, P and S wave crystals, and dual channel oscilloscope. With phenyl salicylate which is normally used for hard rock specimens as coupling medium, a sharp impact was needed to break the bond between the specimen and the crystal head. In some preliminary tests, the impact applied to break this bond resulted in separation of weak bedding planes in oil shale specimens. Therefore high vacuum grease was substituted for phenyl salicylate as a coupling medium in the specimen holding jig designed to ensure proper contact between the crystal heads and the oil shale specimens. Satisfactory results were obtained with this setup.

2.2.2 Test Results

The travel time was measured by first wave arrival technique. Sometimes it was difficult to distinguish the first arrival of shear wave because of the inherent nature of this method. We could identify the shear wave arrival with better confidence by comparing the P and S wave shape pictures obtained by oscilloscope camera.

The test results are presented in Tables 5-7. It was observed that specimens with a greater amount of intrusion of calcareous and kaolinised material showed much higher velocities than pure oil shale specimens. It was found that samples with higher kerogen content showed lower velocity (Fig. 13, 14). The V_p of the specimens with more than 50% intrusions of calcareous material ranged from 5.0 to 6.0 Kms/sec while that of pure oil shale varied from 2.4 to 3.5 Kms/sec which is approximately one-half of the former values.

The dynamic Young's modulus, Poisson's ratio and Shear modulus calculated from V_p and V_s and density were compared with corresponding static properties. The dynamic values were always higher than the static values.

TABLE 5. DYNAMIC ELASTIC CONSTANTS MEASURED BY ULTRASONIC METHOD
(Specimens from Well No. Dow/ERDA 100)

Elevation Interval (ft)	Specimen No.	Density (Mg/m ³)	V _p Km/sec	V _s Km/sec	Young's Modulus GPa	Shear Modulus GPa	Poisson's Ratio	Lithologic Characteristics
1300-10	100/1307.2	2.434	3.212	2.048	23.6	10.2	0.16	
1340-50	100/1346.5	2.475	3.431	2.034	25.1	10.2	0.23	
	100/1349.9	2.602	4.774	2.817	50.8	20.6	0.23	Whitish gray color, contamination of calcareous material
1350-60	100/1350.9	2.636	5.006	2.695	49.5	19.1	0.30	Whitish gray color, contamination of calcareous material
63	100/1356.9	2.410	3.416	2.050	24.6	10.1	0.22	
	100/1359.5	2.384	4.505	2.327	34.0	12.9	0.32	Intrusions of pyrite
1360-70	100/1361.8	2.557	3.365	2.039	25.7	10.6	0.21	
1370-80	100/1374.7	2.427	3.332	2.114	25.2	10.8	0.16	
1390-1400	100/1395.3	2.658	4.340	2.572	43.2	17.5	0.23	Whitish gray color, contamination of calcareous material
	100/1396.6	2.656	5.261	2.813	54.5	21.0	0.30	Whitish gray color, contamination of calcareous material
1440-50	100/1441.7	2.699	5.391	2.723	53.1	19.9	0.33	50% volumetric intrusion of calcareous material
	100/1445.0	2.719	5.404	3.193	68.2	27.7	0.23	Whitish gray color, contamination of calcareous material

TABLE 5 (continued)

Elevation Interval (ft)	Specimen No.	Density (Mg/m ³)	V _p Km/sec	V _s Km/sec	Young's Modulus GPa	Shear Modulus GPa	Poisson's Ratio	Lithologic Characteristics
1450-60	100/1446.2	2.696	5.488	2.858	57.8	22.0	0.31	60% volumetric intrusion of calcareous material
	100/1451.2	2.696	5.614	3.003	63.1	24.3	0.30	50% volumetric intrusion of calcareous material
	100/1451.8	2.770	6.060	3.167	72.8	27.7	0.31	65% volumetric intrusion of calcareous material
1470-80	100/1477.4	2.682	5.129	2.762	52.9	20.4	0.30	Whitish gray color, contamination of calcareous material

TABLE 6. DYNAMIC ELASTIC CONSTANTS MEASURED BY ULTRASONIC METHOD
(Specimens from Well No. Dow/ERDA 101)

Elevation Interval (ft)	Specimen No.	Density (Mg/m ³)	V _p Km/sec	V _s Km/sec	Young's Modulus GPa	Shear Modulus GPa	Poisson's Ratio	Lithologic Characteristics
1320-30	101/1325.1	2.637	4.825	2.814	51.8	20.8	0.24	Heavier with a little contamination of calcareous material
	101/1326.0	2.667	5.160	3.180	64.3	26.9	0.19	Blackish but heavier with little contamination of calcareous material
1340-50	101/1341.1	2.394	3.438	2.190	26.6	11.5	0.16	
	101/1342.0	2.416	3.568	2.170	27.4	11.4	0.21	
1350-60	101/1352.0	2.433	3.286	2.073	24.4	10.4	0.17	
1360-70	101/1360.2	2.400	3.202	2.010	22.7	9.7	0.17	
1380-90	101/1382.3	2.711	5.213	3.128	64.6	26.5	0.22	Contamination of calcareous material
1390-1400	101/1396.5	2.522	3.295	1.977	24.0	9.8	0.22	
1400-10	101/1400.3	2.248	2.925	1.897	18.4	8.1	0.14	
1410-20	101/1411.8	2.500	3.248	2.030	24.3	10.3	0.18	
	101/1412.5	2.588	3.921	2.434	36.3	15.3	0.19	Bands of calcareous material
1420-30	101/1425.2	2.706	5.302	2.964	60.4	23.7	0.27	50% intrusion of calcareous material
	101/1427.8	2.855	6.482	3.411	86.8	33.1	0.31	Considerable intrusions of calcareous material
	101/1430.0	2.716	5.704	3.298	73.7	29.5	0.25	About 70% presence of calcareous material
1440-50	101/1440.9	2.647	3.394	1.885	24.0	9.4	0.28	

TABLE 6 (continued)

Elevation Interval (ft)	Specimen No.	Density (Mg/m ³)	V _p Km/sec	V _s Km/sec	Young's Modulus GPa	Shear Modulus GPa	Poisson's Ratio	Lithologic Characteristics
1460-70	101/1462.8	2.684	4.473	2.508	42.8	16.8	0.27	Intrusions of calcareous material
1480-90	101/1488.4	2.691	5.035	2.756	52.5	20.4	0.29	About 60% intrusion of calcareous material
1490-1500	101/1490.2	2.799	6.256	3.484	86.5	33.9	0.28	Considerable intrusions of calcareous material
1500-10	101/1507.2	2.669	4.484	2.360	38.8	14.8	0.31	Presence of calcareous material
	101/1509.1	2.707	5.767	3.117	67.9	26.2	0.29	60% intrusions of calcareous material, appearance like Westley granite
1510-20	101/1513.5	2.674	5.260	3.048	61.9	24.8	0.25	About 40% intrusions of calcareous material
	101/1517.1	2.663	4.492	2.475	41.8	16.3	0.28	Intrusions of calcareous material

TABLE 7. DYNAMIC ELASTIC CONSTANTS MEASURED BY ULTRASONIC METHOD
(Specimens from Well No. Dow/ERDA 102)

Elevation Interval (ft)	Specimen No.	Density (Mg/m ³)	V _p Km/sec	V _s Km/sec	Young's Modulus GPa	Shear Modulus GPa	Poisson's Ratio	Lithologic Characteristics
1300-10	102/1306.1	2.41	3.279	1.927	22.1	9.0	0.24	w
1370-80	102/1375.0	2.55	3.396	2.264	28.7	13.1	0.10	
	102/1376.5	2.50	2.665	1.738	17.0	7.5	0.13	
1380-90	102/1386.4	2.71	4.565	2.548	44.8	17.6	0.27	
1390-1400	102/1397.5	2.50	3.051	1.564	16.1	6.1	0.32	
1410-20	102/1415.9	2.47	2.422	1.633	14.2	6.6	0.08	
1430-40	102/1436.3	2.78	5.638	2.953	63.5	24.2	0.31	
	102/1438.0	2.71	5.543	3.000	63.0	24.3	0.29	
1440-50	102/1445.0	2.82	6.182	3.342	81.4	31.4	0.29	
1470-80	102/1475.2	2.69	5.762	3.130	68.0	26.3	0.29	
	102/1476.0	2.70	5.894	3.202	71.5	27.7	0.29	
1490-1500	102/1496.8	2.70	5.366	3.086	64.4	25.7	0.25	50% contamination of calcareous material

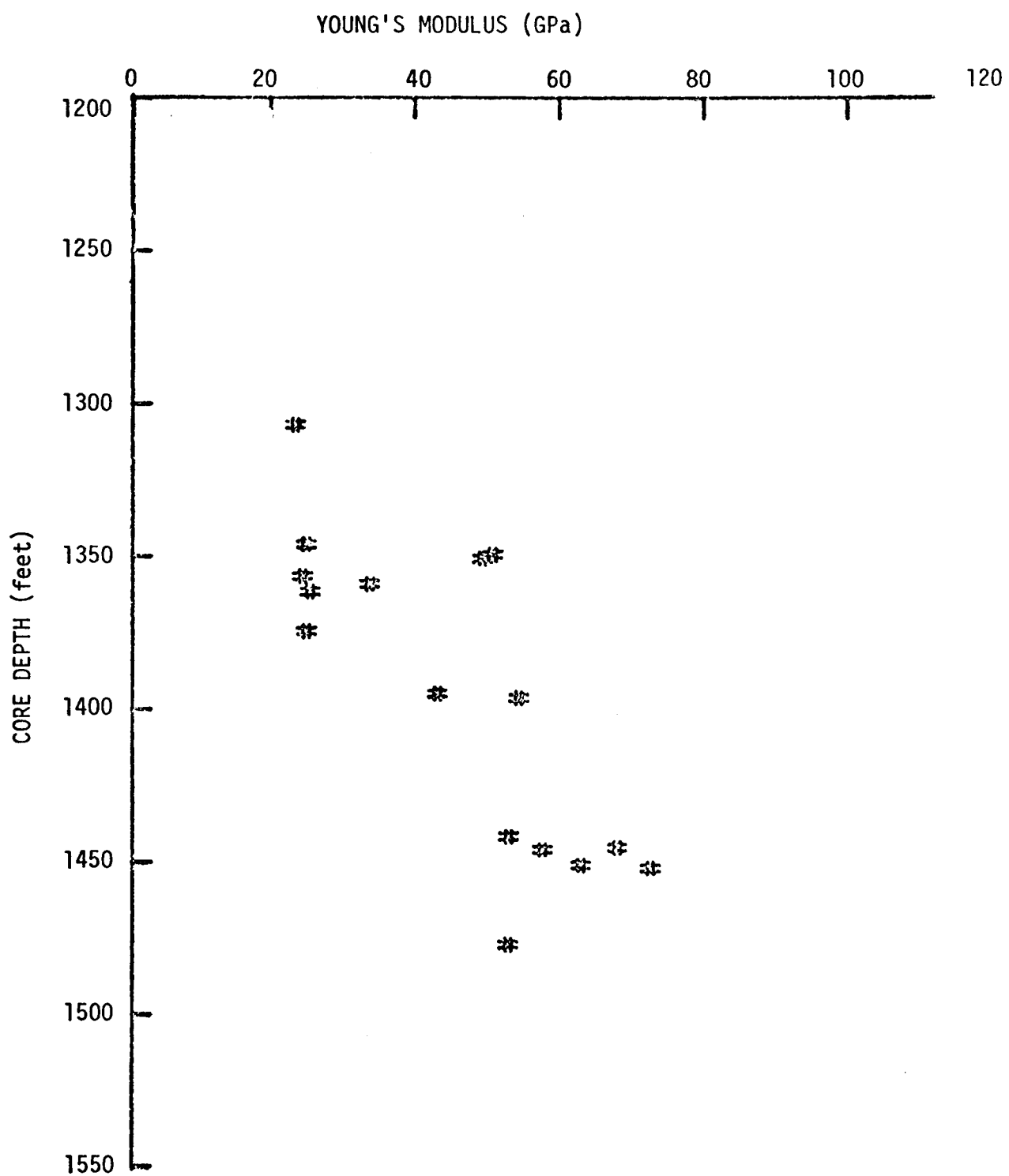


Figure 10a. Variation of dynamic Young's modulus with depth (Well No. Dow/ERDA 100).

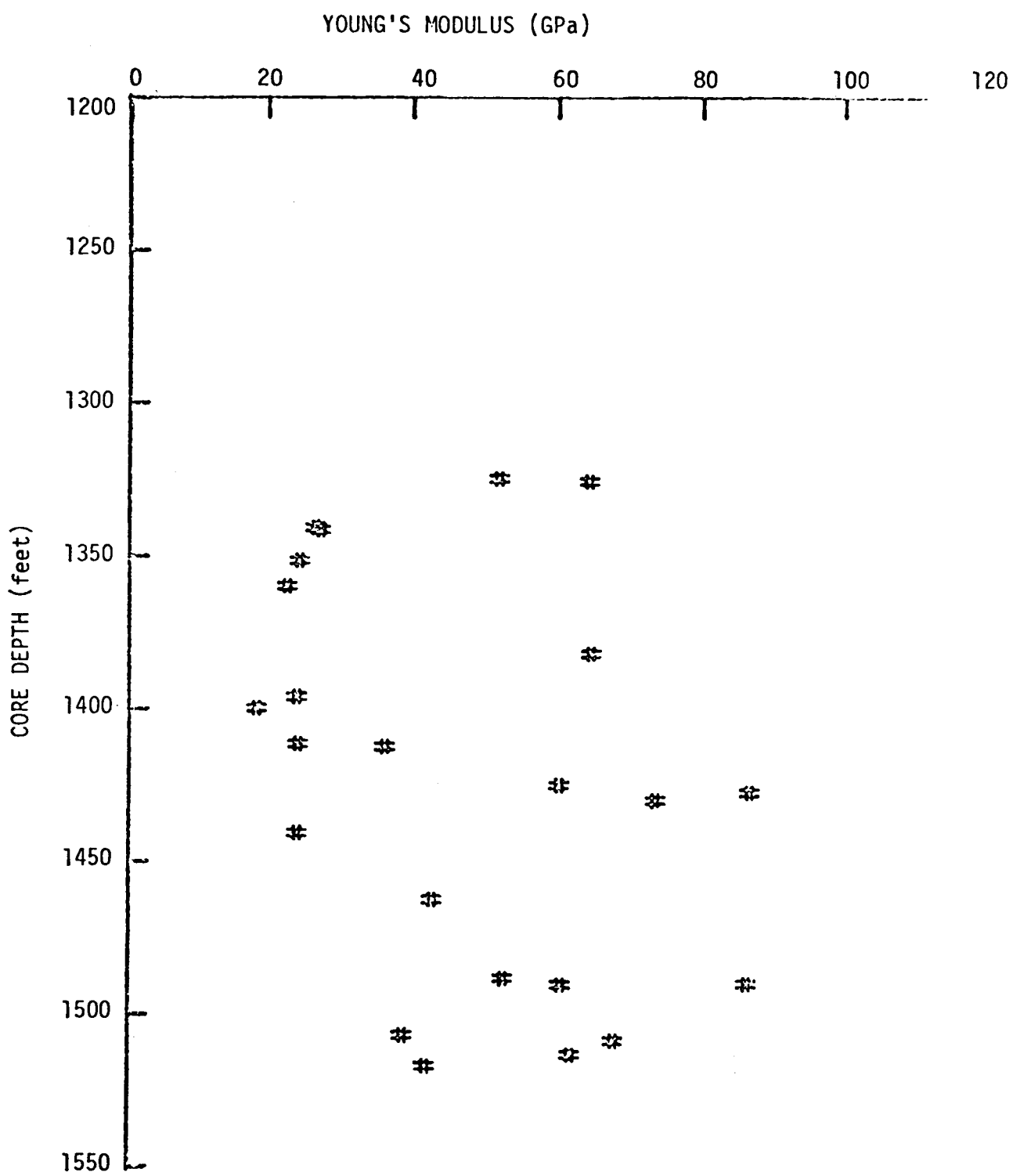


Figure 10b. Variation of dynamic Young's modulus with depth (Well No. Dow/ERDA 101).

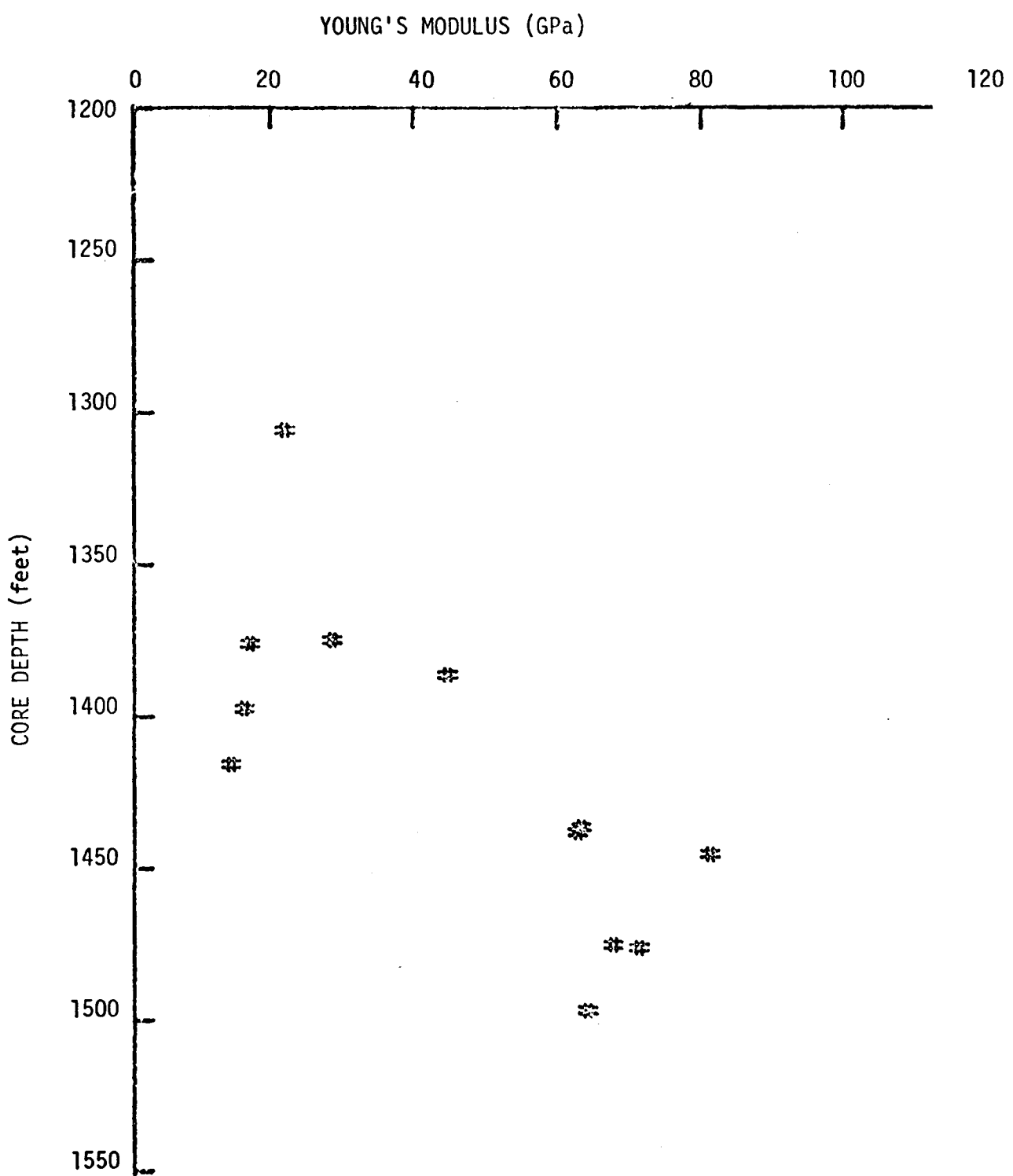


Figure 10c. Variation of dynamic Young's modulus with depth
(Well No. Dow/ERDA 102).

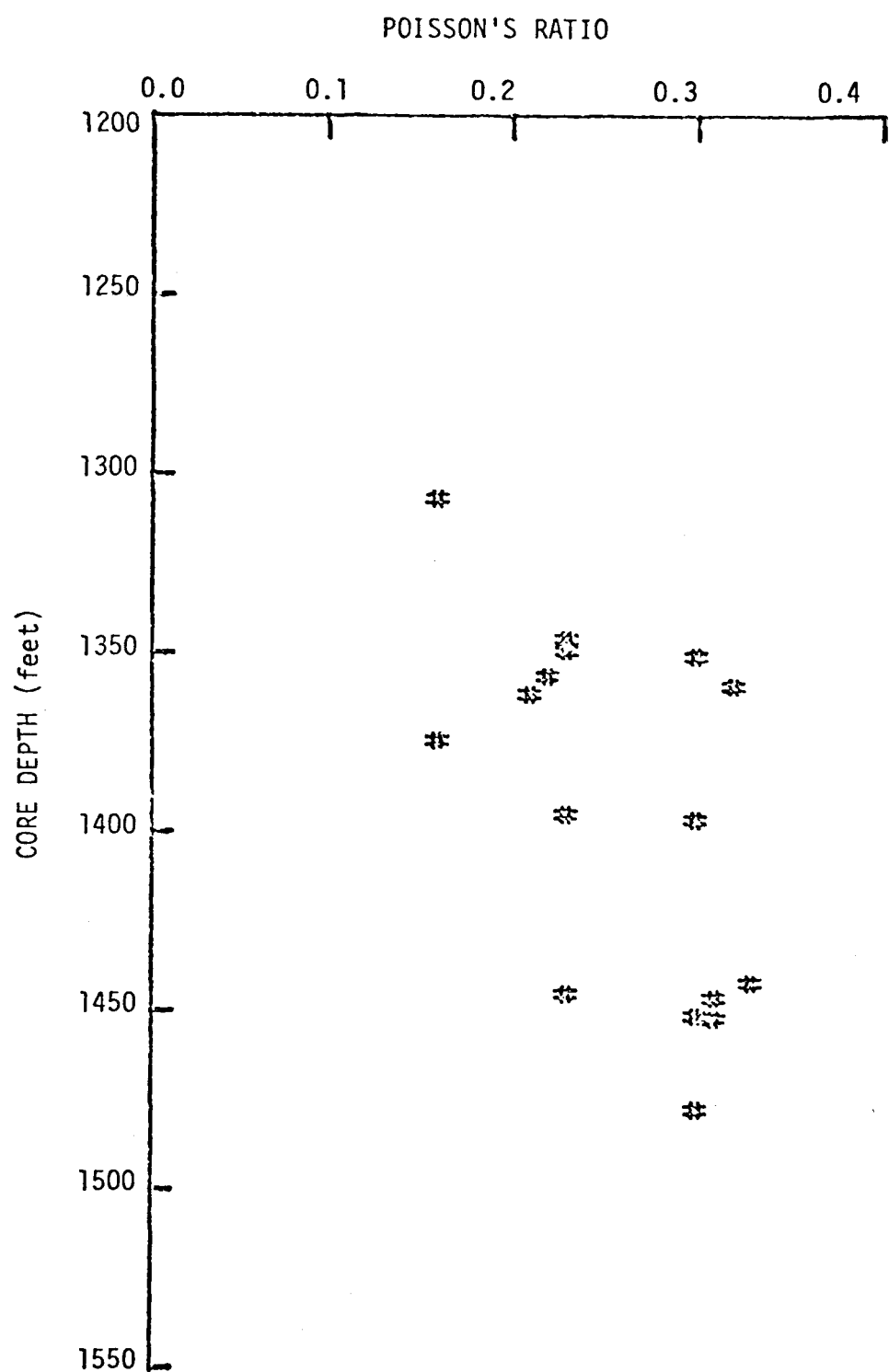


Figure 11a. Variation of dynamic Poisson's ratio with depth
(Well No. Dow/ERDA 100).

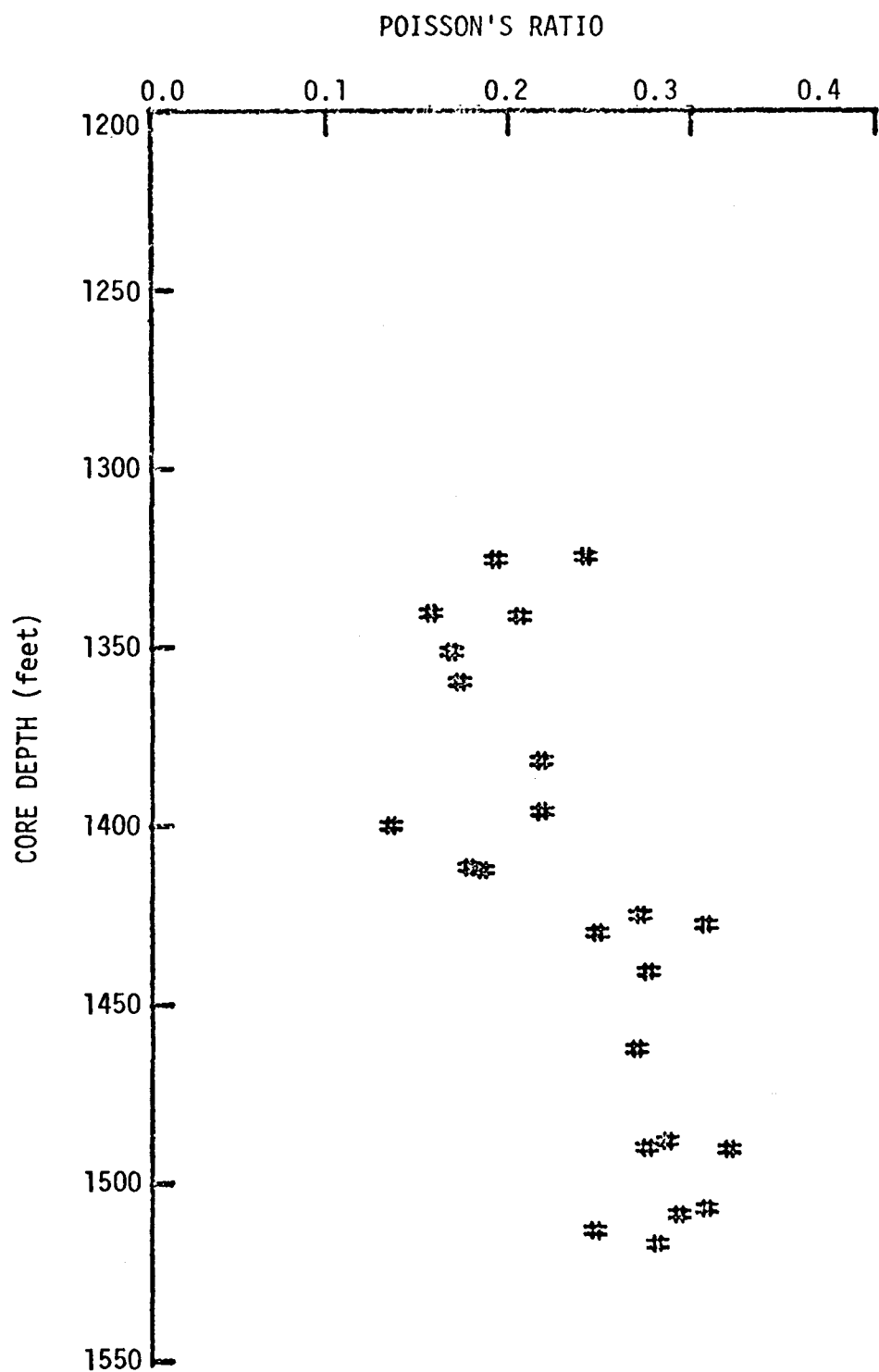


Figure 11b. Variation of dynamic Poisson's ratio with depth (Well No. Dow/ERDA 101).

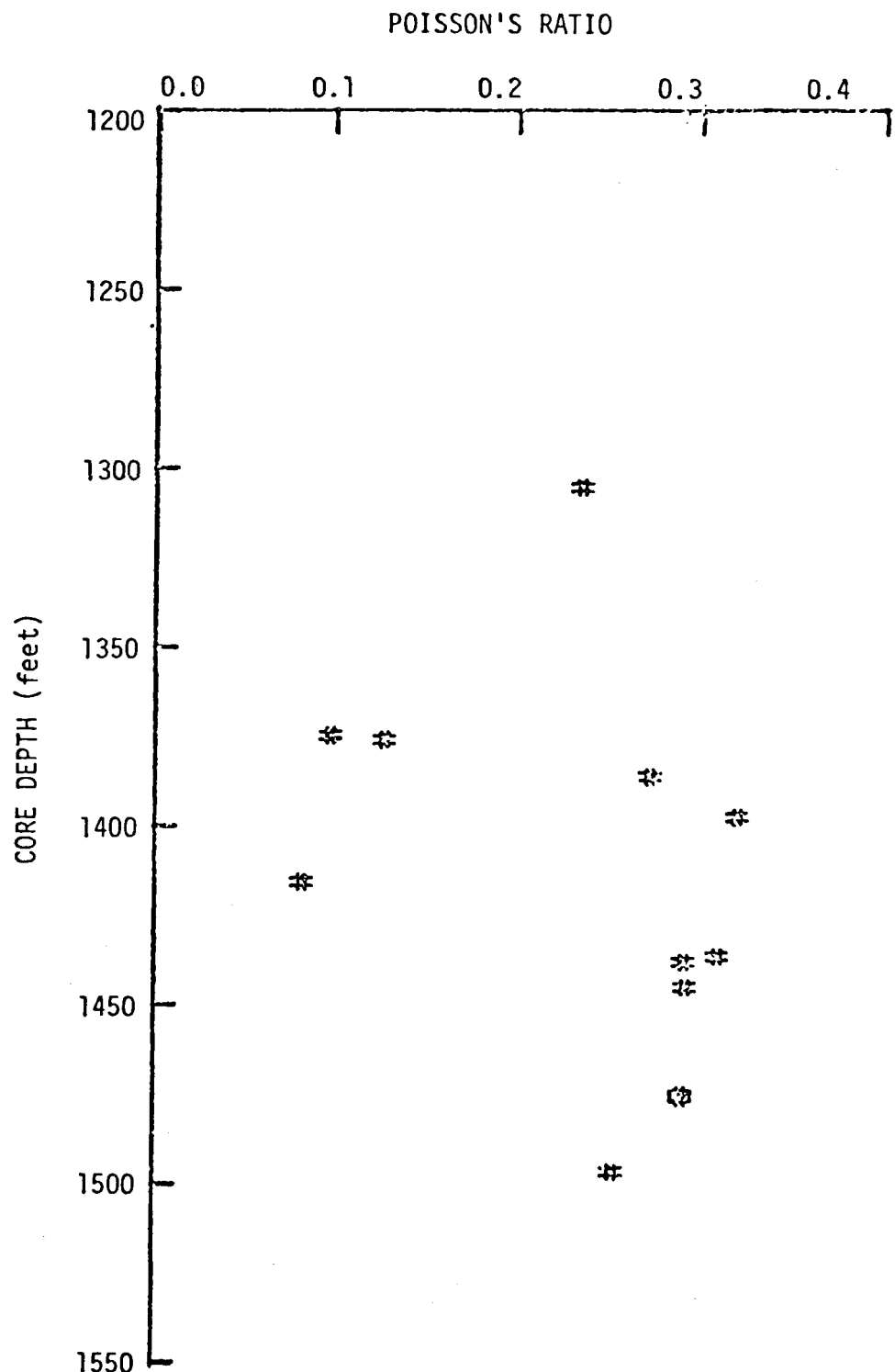


Figure 11c. Variation of dynamic Poisson's ratio with depth
(Well No. Dow/ERDA 102).

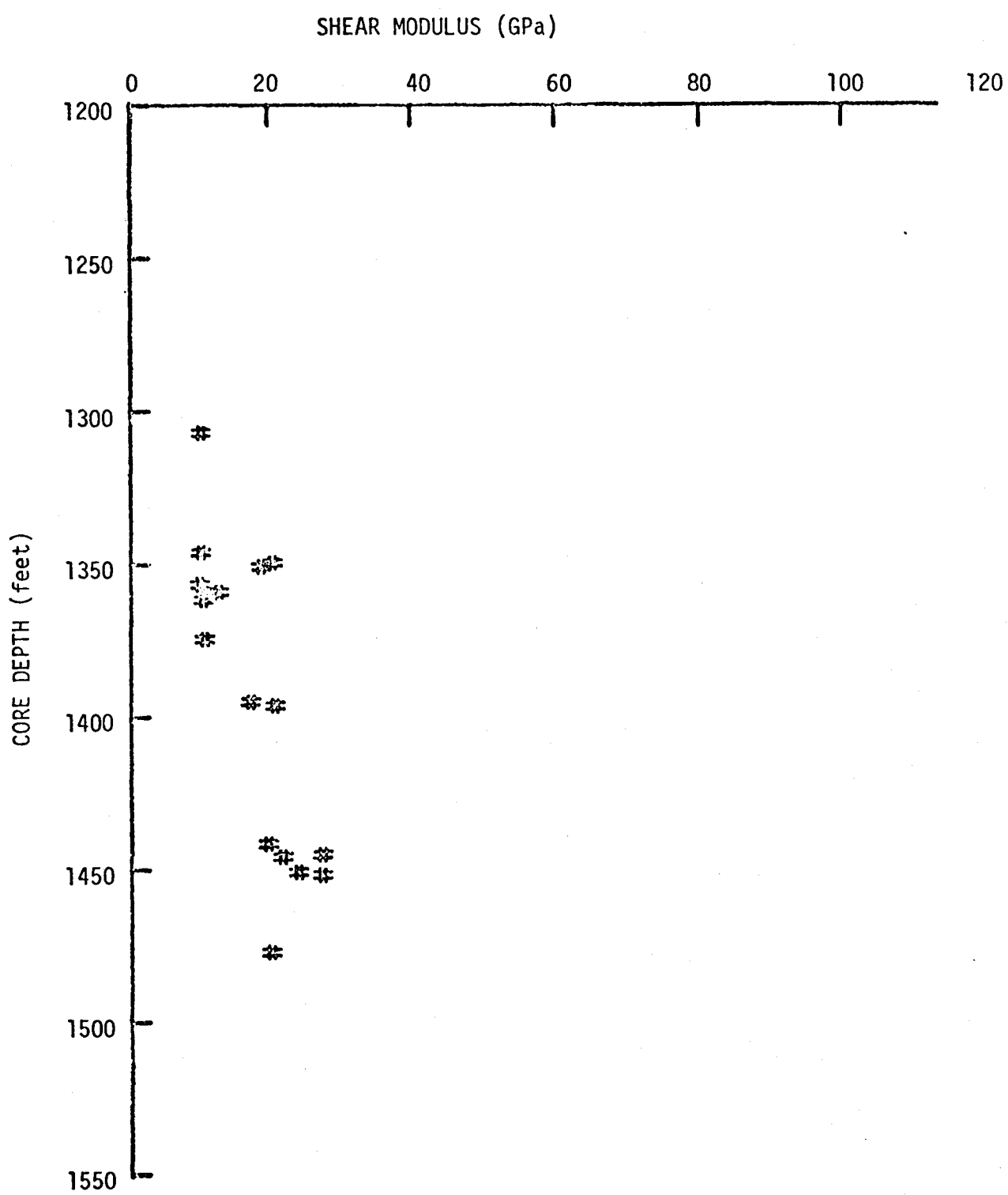


Figure 12a. Variation of shear modulus with depth (Well No. Dow/ERDA 100).

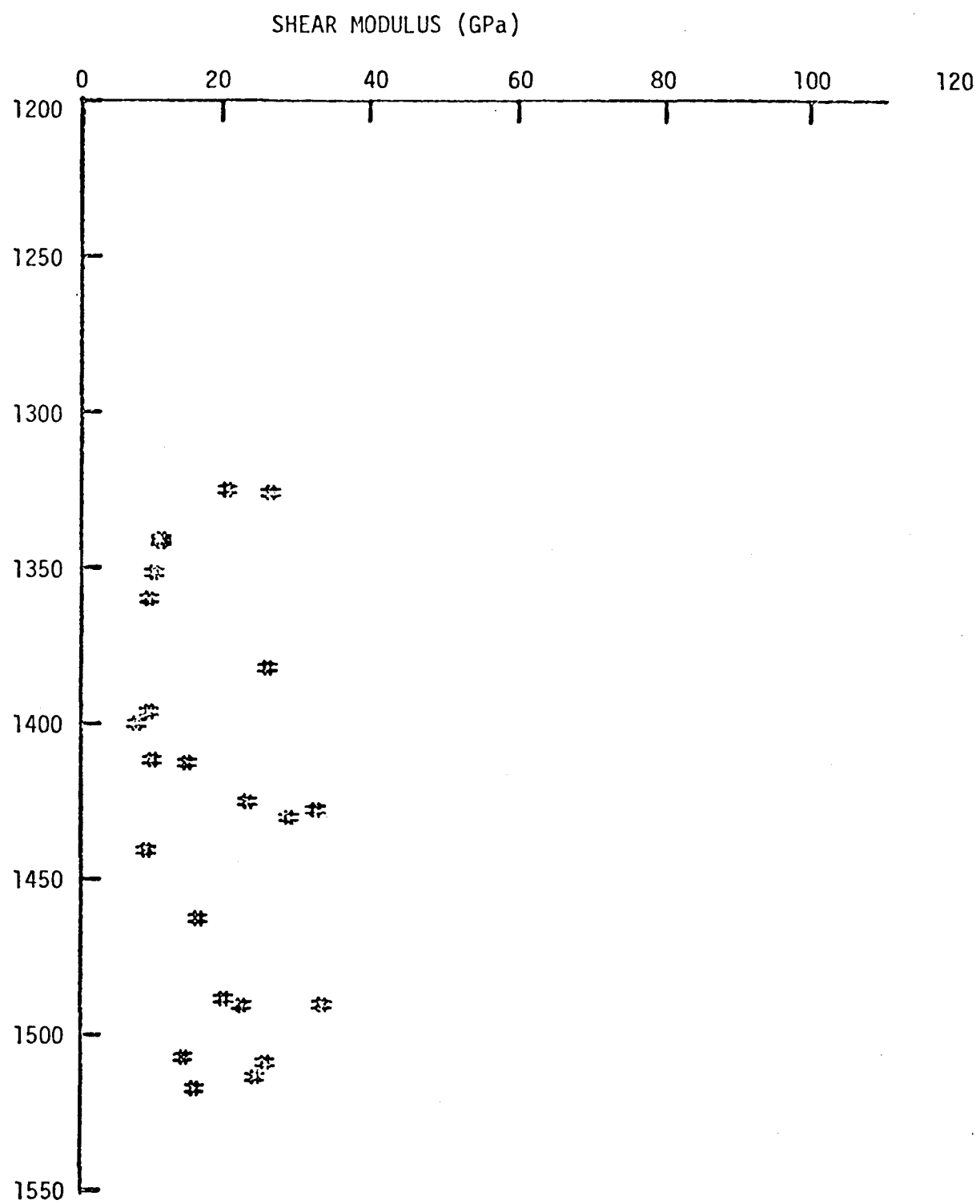


Figure 12b. Variation of shear modulus with depth (Well No. Dow/ERDA 101).

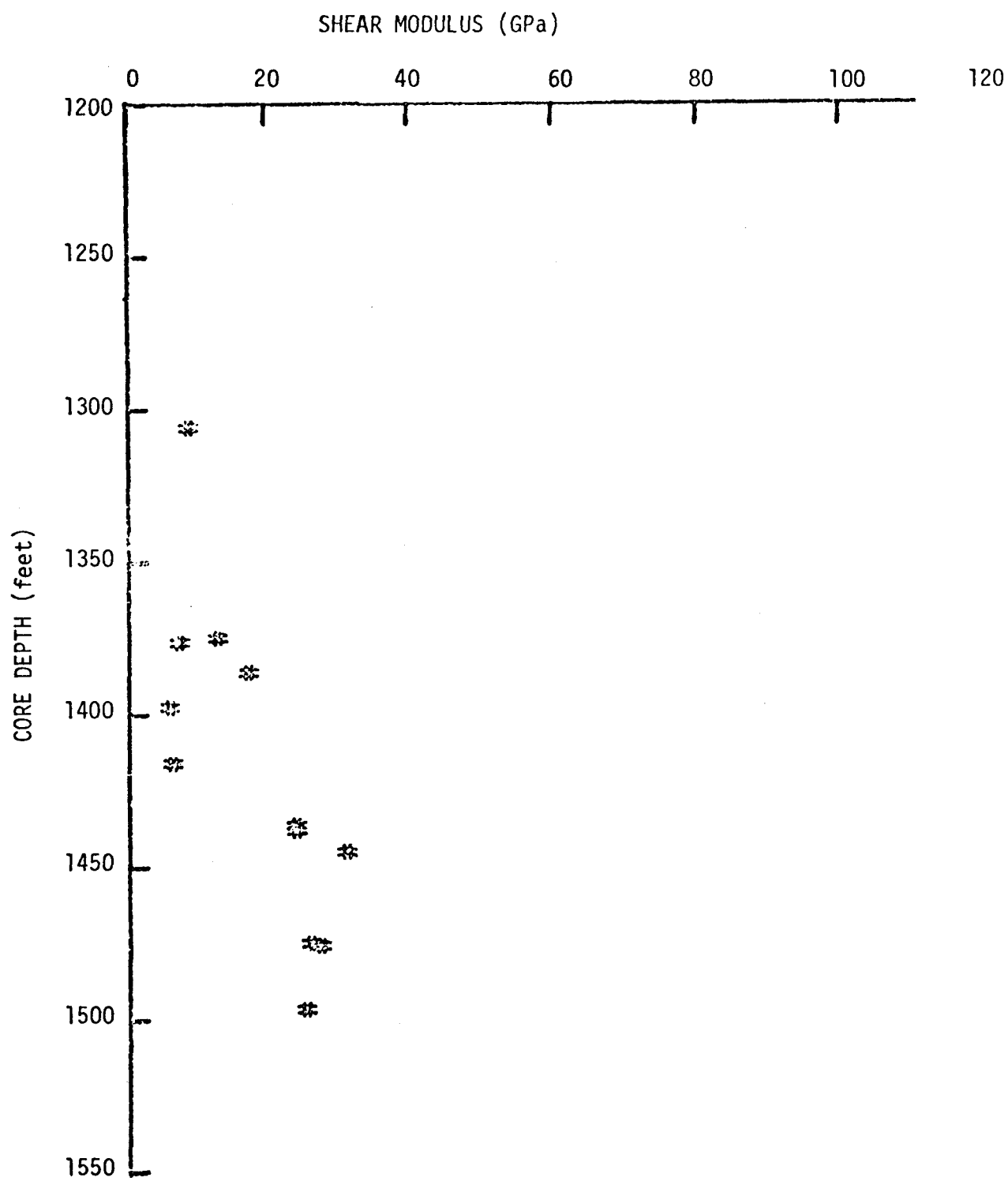


Figure 12c. Variation of shear modulus with depth (Well No. Dow/ERDA 102).

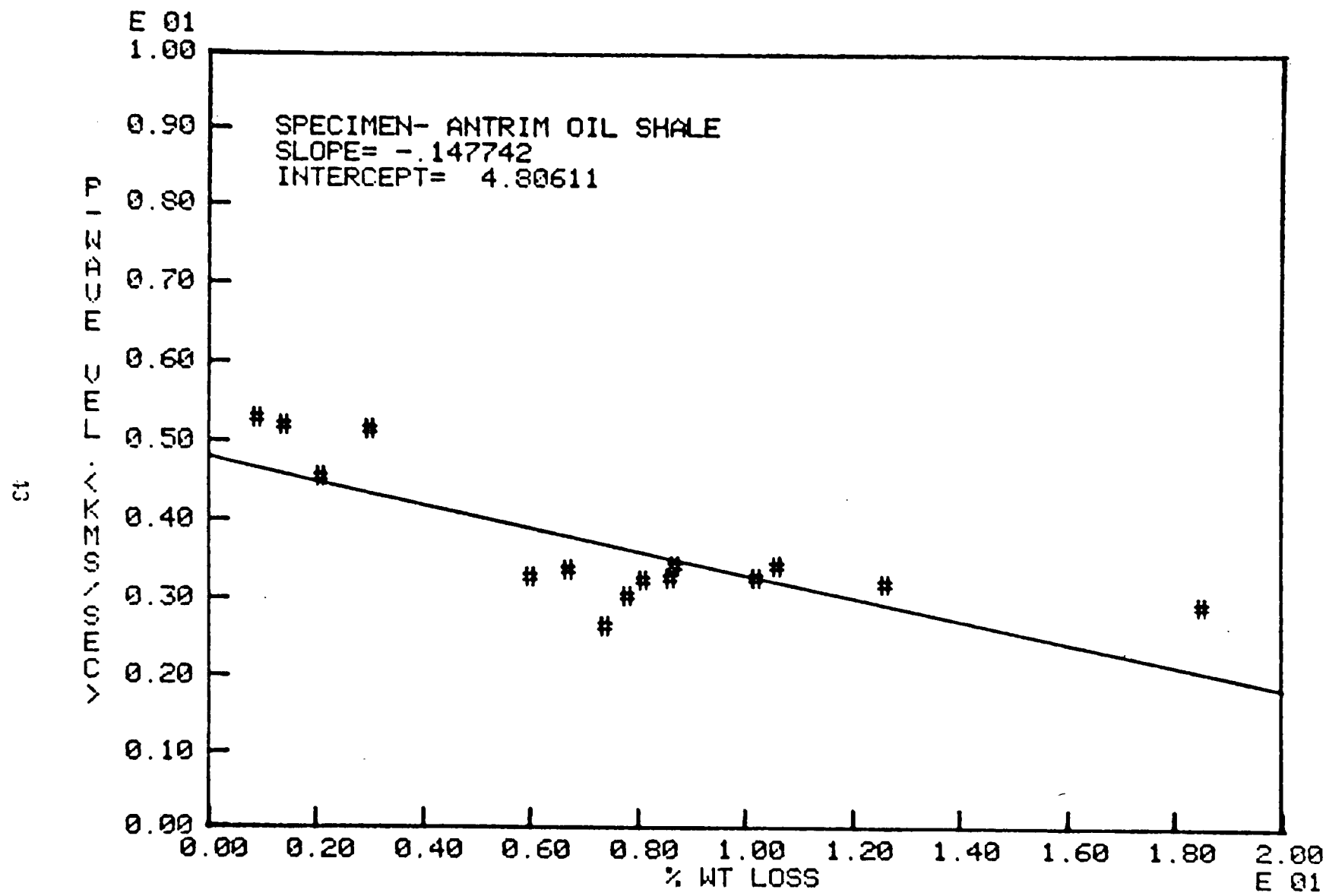


Figure 13. P-wave velocity vs. % wt. loss.

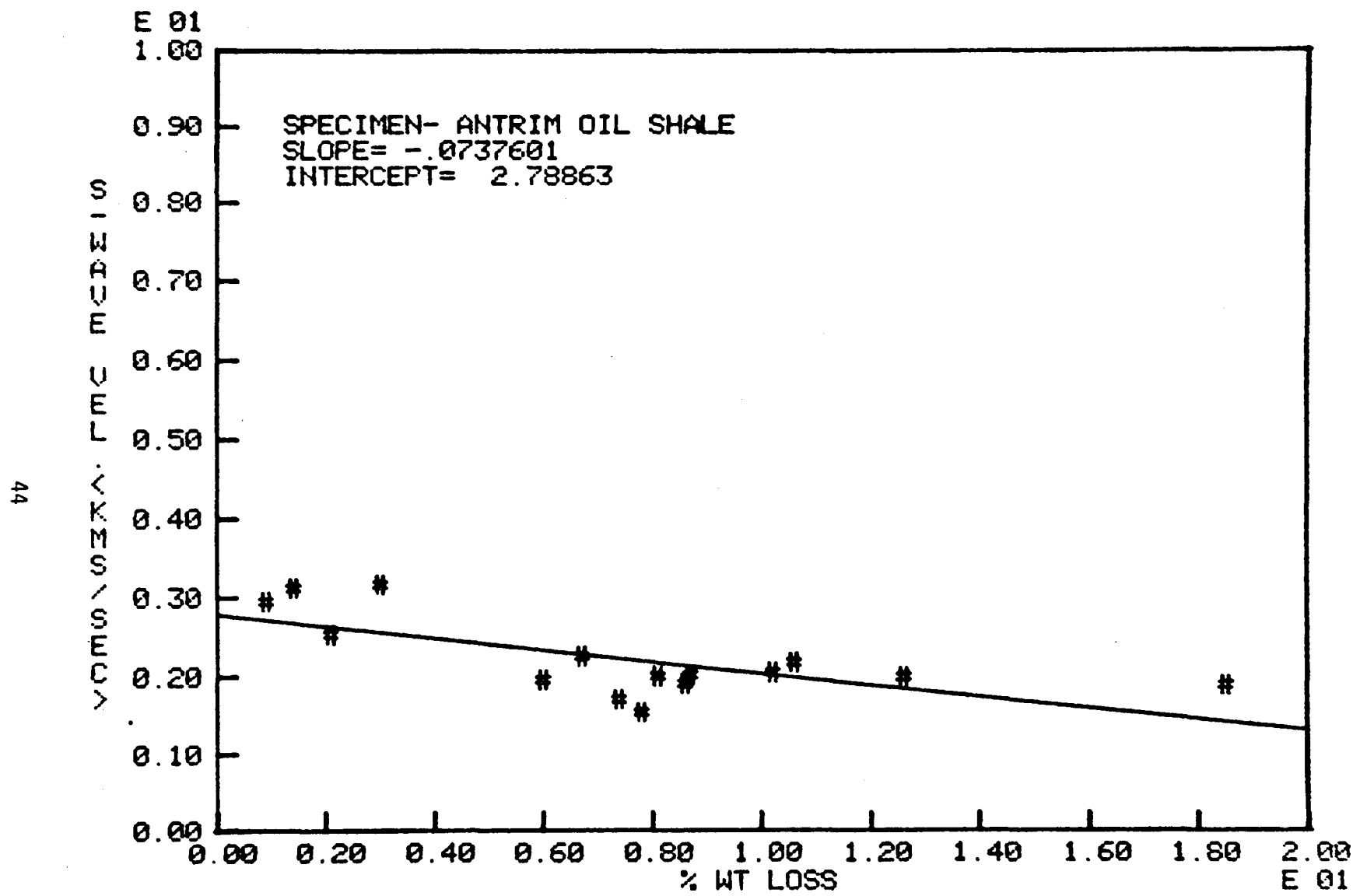


Figure 14. S-wave velocity vs. % wt. loss.

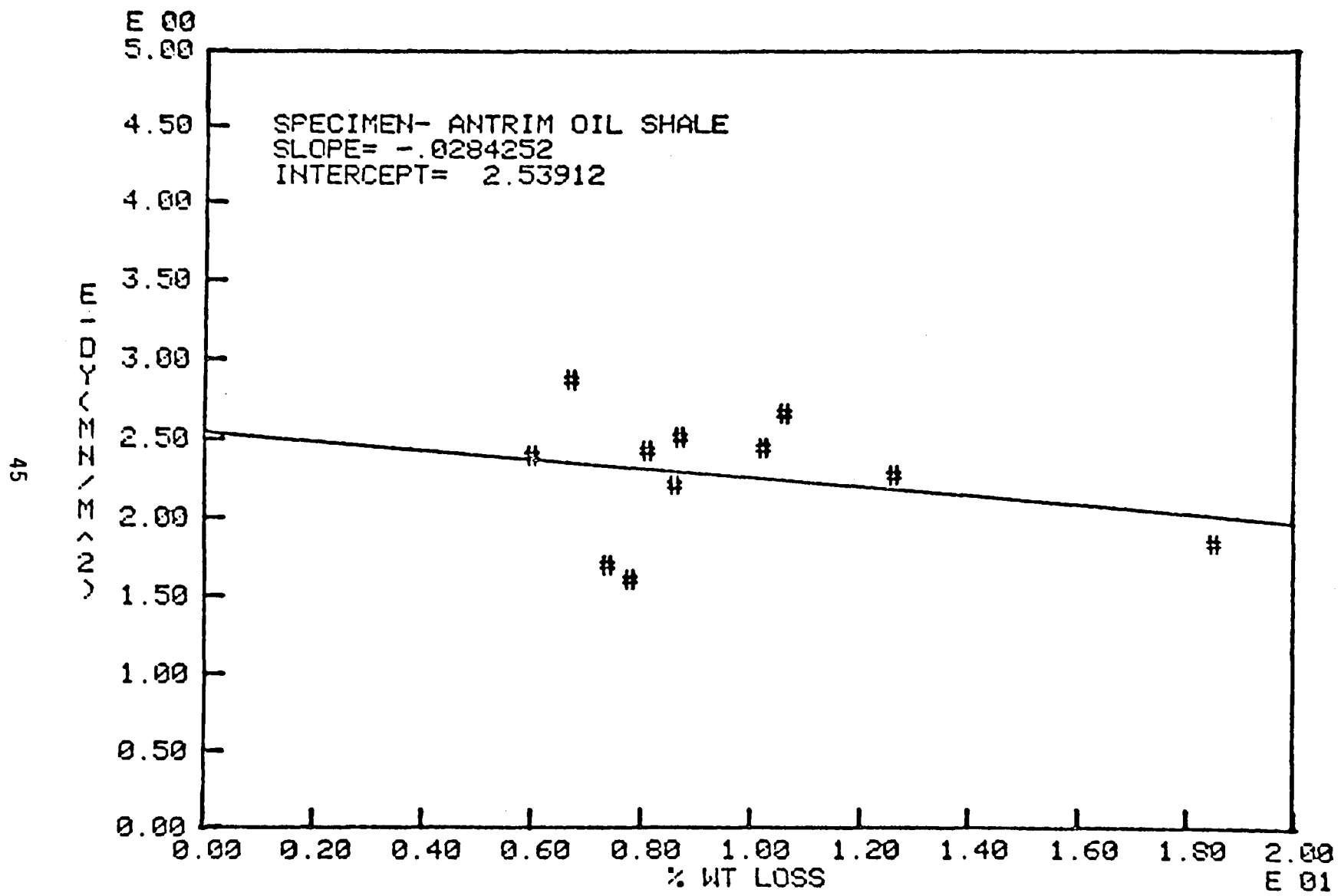


Figure 15. Dynamic Young's modulus vs. % wt. loss.

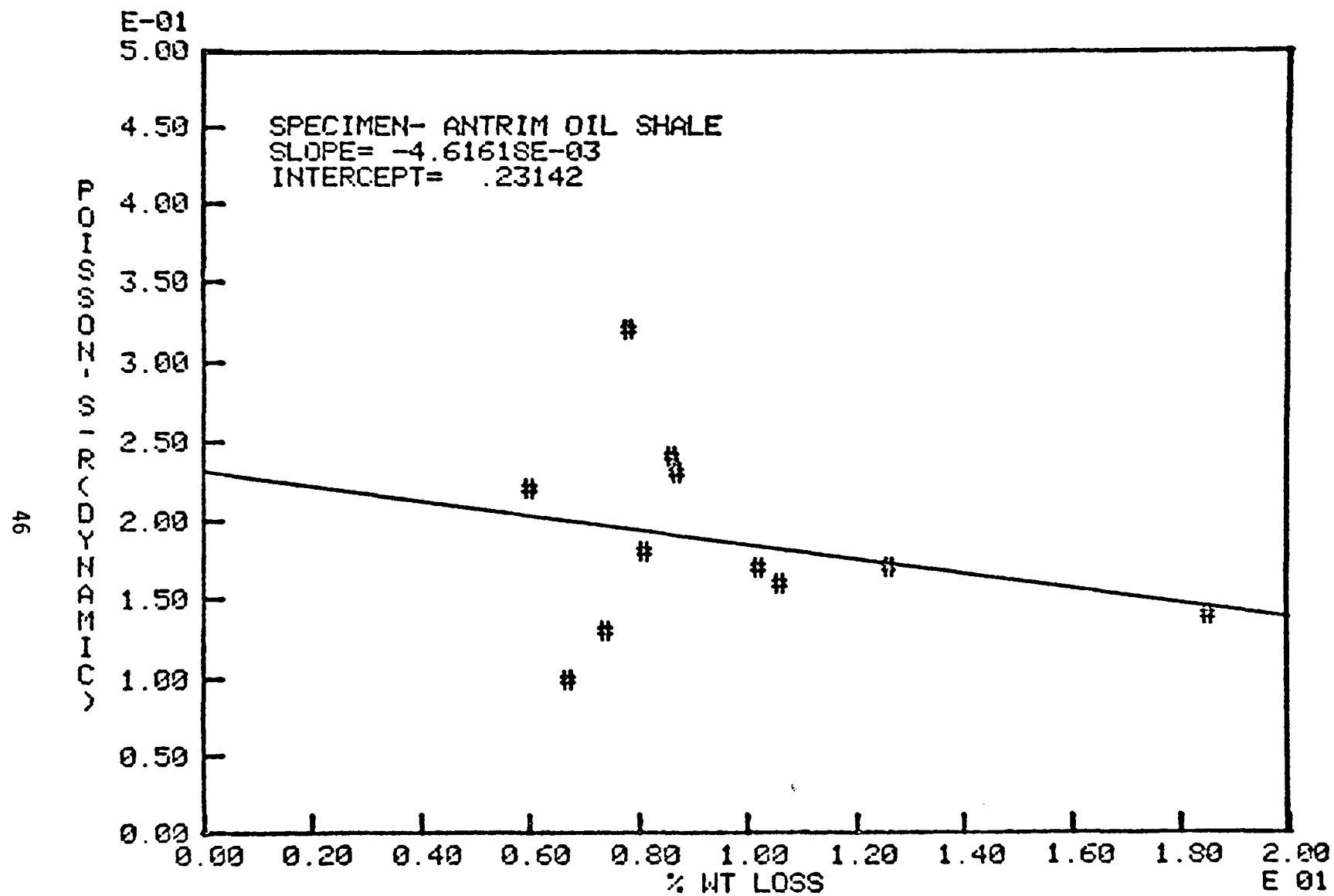


Figure 16. Dynamic Poisson's ratio vs. % wt. loss.

The dynamic Young's modulus and Poisson's ratio were also plotted against % wt. loss similar to the static case (Fig. 15, 16). Results obtained were similar to those for static values.

These results demonstrate that the methods we used produced very reliable results and also that the dynamic method can be substituted for the static method which is more time consuming and cumbersome in specimen preparation.

2.3 Point Load Strength Index

Point load test is known as a simple and quick method of determining strength properties of rock. The method consists of breaking rock by the application of a concentrated point load through a pair of conical load applicators aligned at opposite sides of a test specimen. The strength index value can be used to estimate the tensile or compressive strength. The load at failure obtained thereby, is used to calculate the point load strength index value using the formula, $I_s = \frac{P}{D^2}$, where I_s is the point load strength index, P is load at failure and D is the distance between loading points at failure.

2.3.1 Test Procedure

The suggested method by the International Society of Rock Mechanics² was used as a guideline. Cylindrical samples were prepared to meet the length diameter ratio in accordance with ISRM method and were subjected to test using a portable point load tester. Preliminary results indicated that failure did not occur in a plane connecting loading points and instead chipping occurred usually at one loading point, when the load is applied in axial direction, i.e. the perpendicular direction to bedding. The length/diameter ratio had to be reduced to approximately 1/2 to obtain tensile mode failures connecting loading points. Even with length/diameter ratio 1/2, chipping took place occasionally. The data were discarded in such cases. Loading in the parallel direction to bedding resulted in separation of bedding plane without any appreciable amount of loading. Test in this direction was discontinued.

Then NX (2 1/8" diameter) approximately .75" thick disc-shaped specimens were prepared at each 10 ft interval. All specimens were tested to obtain statistically meaningful index values.

2.3.2 Test Results

Test results for point load are tabulated in Tables 8-10. The mean index values were also plotted against depth to find the variation with depth (Figures 17-19). The variation of density is also plotted for comparison (Figures 20-22). An interesting point is that the average strength index for hole 102 appears to be higher than for hole 100 or 101, although no substantial differences were noticed in the density.

2.4 Scleroscope Hardness

Shore scleroscope hardness tester Model D was used to measure the surface hardness of the specimen. The tester consists of a frame in which a diamond-tipped hammer is dropped from a fixed height onto the specimen's surface, positioned on the base of the instrument. The measurement of hardness number is based on the principle that the harder the material the higher the rebound of the hammer.

A series of preliminary tests were conducted to find if the condition of surface influences the reading. Diamond saw cut and polished discs were prepared and tested. Test results showed that there was no significant difference between the scleroscope hardness number of polished and diamond saw cut specimens. Therefore in order to save the time consumed in polishing, it was decided to use diamond saw cut specimens.

2.4.1 Test Procedure

The circular disc of Antrim oil shale is placed upright on the base of the instrument and the hammer is dropped. The height of rebound of the hammer is read from the dial indicator of the instrument. Five drops are made along an arbitrary diametral line of the circular disc of oil shale. The disc is then rotated 90° on its longitudinal axis and five

TABLE 8. POINT LOAD TEST RESULTS
(Specimens from Well No. Dow/ERDA 100)

Elevation Interval (ft)	Specimen No.	Density (Mg/m ³)	I _s * MPa	I _s _{mean} MPa
1210-20	100/1212.8/a	2.28	14.0	13.4
	100/1212.8/b	2.29	12.8	
1220-30	100/1222.7/a	2.32	8.6	8.6
1230-40	100/1236.3/a	2.32	12.7	15.1
	100/1236.5/a	2.32	20.6	
	100/1236.5/b	2.31	16.2	
	100/1236.5/c	2.31	11.0	
1240-50	100/1245.9/b	2.28	12.5	11.4
	100/1245.9/c	2.30	10.2	
1250-60	100/1258.8/a	2.37	18.9	17.6
	100/1259.1/a	2.43	16.2	
1260-70	100/1265.5/b	2.45	11.4	14.8
	100/1265.5/c	2.44	18.2	
1270-80	100/1280.0/a	2.43	12.4	12.4
1280-90	100/1285.0/a	2.46	14.1	14.2
	100/1285.0/b	2.49	14.2	
1300-10	100/1300.3/a	2.46	16.5	14.6
	100/1300.3/b	2.48	14.0	
	100/1309.0/b	2.37	13.4	
1310-20	100/1315.4/c	2.45	13.0	13.0
1320-30	100/1321.2/a	2.47	16.2	15.8
	100/1321.2/b	2.41	15.3	
1330-40	100/1335.4/b	2.43	13.8	26.4
	100/1335.4/c	2.41	17.9	
	100/1338.8/a	2.40	21.1	
1340-50	100/1340.3/a	2.41	16.0	16.0
1350-60	100/1351.7/a	2.58	14.5	16.7
	100/1351.7/b	2.56	17.0	
	100/1358.8/b	2.41	18.5	
1360-70	100/1368.7/a	2.42	18.1	18.1
1370-80	100/1370.4/b	2.38	14.8	13.1
	100/1370.4/d	2.39	11.4	
1380-90	100/1380.6/a	2.49	15.2	16.3
	100/1380.6/b	2.52	17.4	

TABLE 8 (continued)

Elevation Interval (ft)	Specimen No.	Density (Mg/m ³)	Is* MPa	Is _{mean} MPa
1400-10	100/1409.3/b	2.32	12.3	14.6
	100/1409.3/c	2.35	16.9	
1410-20	100/1417.9/a	2.21	15.5	14.8
	100/1417.9/b	2.23	14.0	
1420-30	100/1426.4/a	2.49	11.5	12.4
	100/1426.4/b	2.56	13.2	
1440-50	100/1441.1/b	2.64	19.5	18.7
	100/1441.1/d	2.66	17.9	
1460-70	100/1463.4/a	2.66	17.5	18.4
	100/1463.4/b	2.68	19.2	

$$*Is = \frac{P}{D^2}$$

where: Is = point load strength index

P = load at failure

D = distance between loading points at failure

TABLE 9. POINT LOAD TEST RESULTS
(Specimens from Well No. Dow/ERDA 101)

Elevation Interval (ft)	Specimen No.	Density (Mg/m ³)	I _s * MPa	I _s _{mean} MPa
1220-30	101/1220.5/c	2.32	15.0	13.6
	101/1220.5/d	2.33	12.2	
1230-40	101/1234.5/a	2.34	16.6	15.4
	101/1234.5/c	2.33	14.1	
1270-80	101/1273.6/b	2.43	10.3	10.3
1280-90	101/1281.1/b	2.42	12.8	14.1
	101/1281.1/c	2.42	15.3	
1290-00	101/1297.9/a	2.46	18.2	17.6
	101/1297.9/d	2.47	17.0	
1300-10	101/1309.8/a	2.39	12.8	12.8
1310-20	101/1316.0/b	2.38	14.3	14.3
1320-30	101/1326.6/d	2.69	23.9	20.5
	101/1326.6/c	2.62	17.1	
1330-40	101/1332.8/a	2.46	14.8	15.5
	101/1332.8/c	2.44	16.2	
1340-50	101/1341.6/d	2.39	21.3	17.4
	101/1341.6/a	2.36	13.6	
1350-60	101/1353.0/b	2.47	14.6	15.6
	101/1353.0/c	2.06	16.5	
1360-70	101/1361.8/c	2.47	14.9	14.9
1370-80	101/1373.3/a	2.60	10.1	10.1
1380-90	101/1382.8/a	2.60	13.4	10.8
	101/1382.8/c	2.62	8.3	
1390-00	101/1399.7/a	2.31	21.6	18.8
	101/1399.7/b	2.16	16.0	
1400-10	101/1403.5/c	2.16	16.2	16.2
1410-20	101/1410.8/b	2.35	10.2	12.4
	101/1410.8/d	2.47	14.6	
1420-30	101/1426.0/b	2.65	13.4	18.0
	101/1426.0/a	2.71	22.5	
1430-40	101/1431.6/b	2.68	23.7	23.7
1450-60	101/1453.5/a	2.64	10.9	14.0
	101/1453.5/c	2.62	17.0	

TABLE 9 (continued)

Elevation Interval (ft)	Specimen No.	Density (Mg/m ³)	Is* MPa	Is _{mean} MPa
1460-70	101/1460.6/a	2.65	7.5	13.0
	101/1460.6/b	2.66	18.4	
1470-80	101/1469.9/a	2.68	20.4	17.8
	101/1469.9/b	2.61	15.3	
1480-90	101/1488.3/e	2.71	18.4	21.0
	101/1488.3/c	2.72	23.5	
1490-00	101/1491.2/a	2.72	20.5	20.2
	101/1491.2/b	2.71	19.9	
1510-20	101/1513.0/a	2.65	17.6	23.5
	101/1513.0/b	2.74	29.4	

TABLE 10. POINT LOAD TEST RESULTS
(Specimens from Well No. Dow/ERDA 102)

Elevation Interval (ft)	Specimen No.	Density (Mg/m ³)	I _s * MPa	I _s _{mean} MPa
1200-10	102/1205.9/a	2.27	6.5	10.4
	102/1205.9/b	2.34	14.3	
1250-60	102/1255.2/b	2.32	19.5	19.8
	102/1255.2/c	2.33	20.0	
1280-90	102/1281.6/a	2.45	24.5	19.7
	102/1284.3/a	2.48	21.6	
	102/1284.3/c	2.48	13.1	
1290-1300	102/1293.5/b	2.43	23.4	26.6
	102/1293.5/c	2.40	22.2	
	102/1295.4/a	2.42	35.9	
	102/1295.4/c	2.40	25.1	
1300-10	102/1305.1/a	2.56	16.2	16.2
1310-20	102/1318.8/a	2.33	32.1	30.7
	102/1318.8/b	2.33	29.3	
1320-30	102/1328.9/b	2.35	19.0	20.6
	102/1328.9/c	2.34	22.1	
1330-40	102/1337.1/a	2.59	25.7	23.4
	102/1337.1/b	2.41	21.0	
1340-50	102/1345.5/c	2.61	24.7	23.4
	102/1345.5/d	2.40	22.0	
1360-70	102/1364.6/a	2.48	26.5	25.3
	102/1364.6/d	2.48	24.0	
1370-80	102/1375.9/b	2.45	20.3	20.9
	102/1375.9/c	2.44	21.5	
1380-90	102/1385.0/a	2.53	17.7	17.7
1390-1400	102/1396.0/a	2.44	18.9	15.1
	102/1396.0/c	2.53	14.2	
1400-10	102/1409.0/c	2.29	21.2	23.1
	102/1409.0/d	2.29	25.0	
1410-20	102/1415.2/b	2.60	17.5	17.3
	102/1415.2/c	2.57	17.1	
1430-40	102/1437.1/b	2.69	18.8	19.2
	102/1437.1/d	2.69	19.6	
1440-50	102/1444.5/a	2.83	48.4	40.6
	102/1444.5/c	2.84	32.2	

TABLE 10 (continued)

Elevation Interval (ft)	Specimen No.	Density (Mg/m ³)	Is* MPa	Is _{mean} MPa
1450-60	102/1450.3/b	2.61	16.0	16.5
	102/1450.3/c	2.64	16.9	
1470-80	102/1474.6/a	2.49	30.5	29.6
	102/1474.6/b	2.70	28.7	
1490-1500	102/1495.4/a	2.56	21.2	20.0
	102/1495.4/c	2.50	10.6	
	102/1495.5/a	2.68	31.9	
	102/1495.5/d	2.64	16.3	

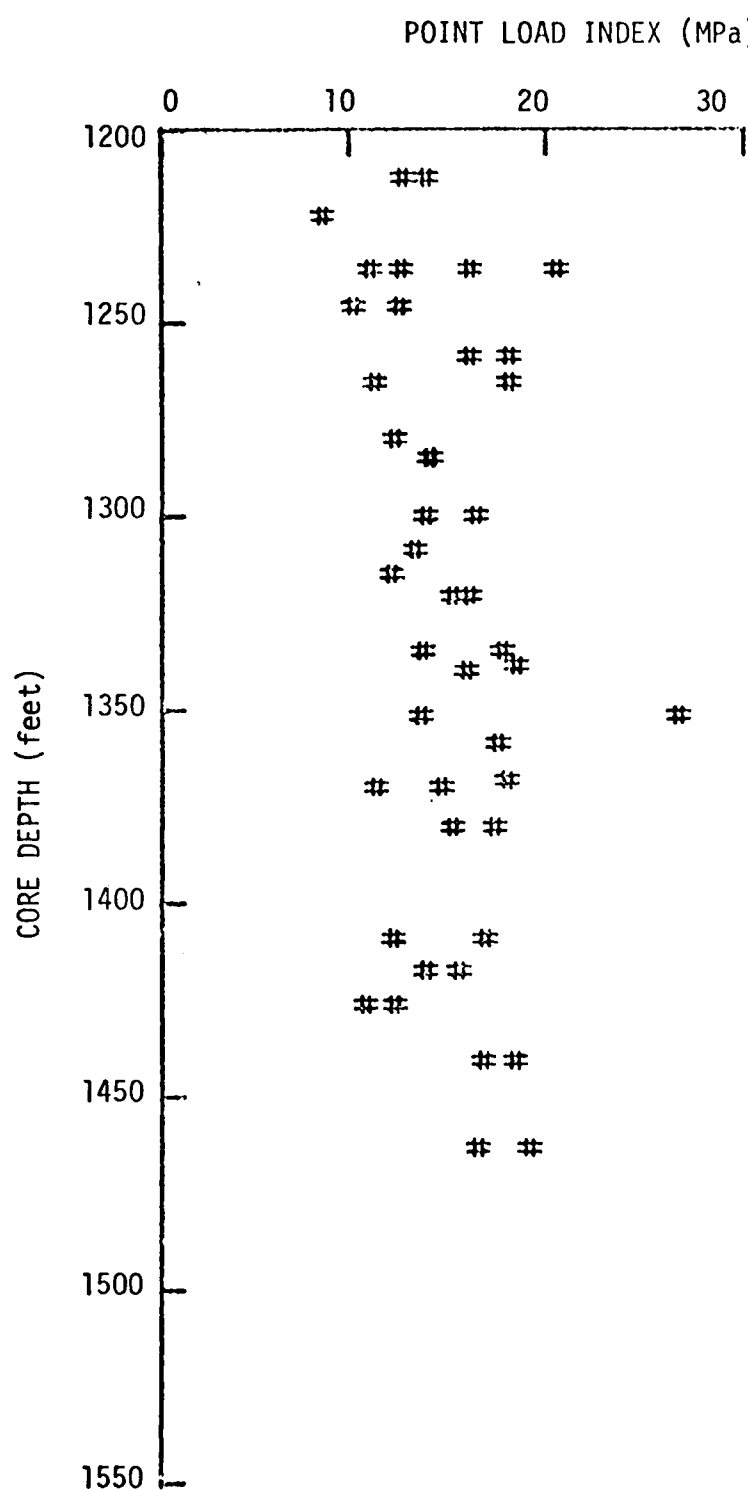


Figure 17. Variation of point load strength index with depth (Well No. Dow/ERDA 100).

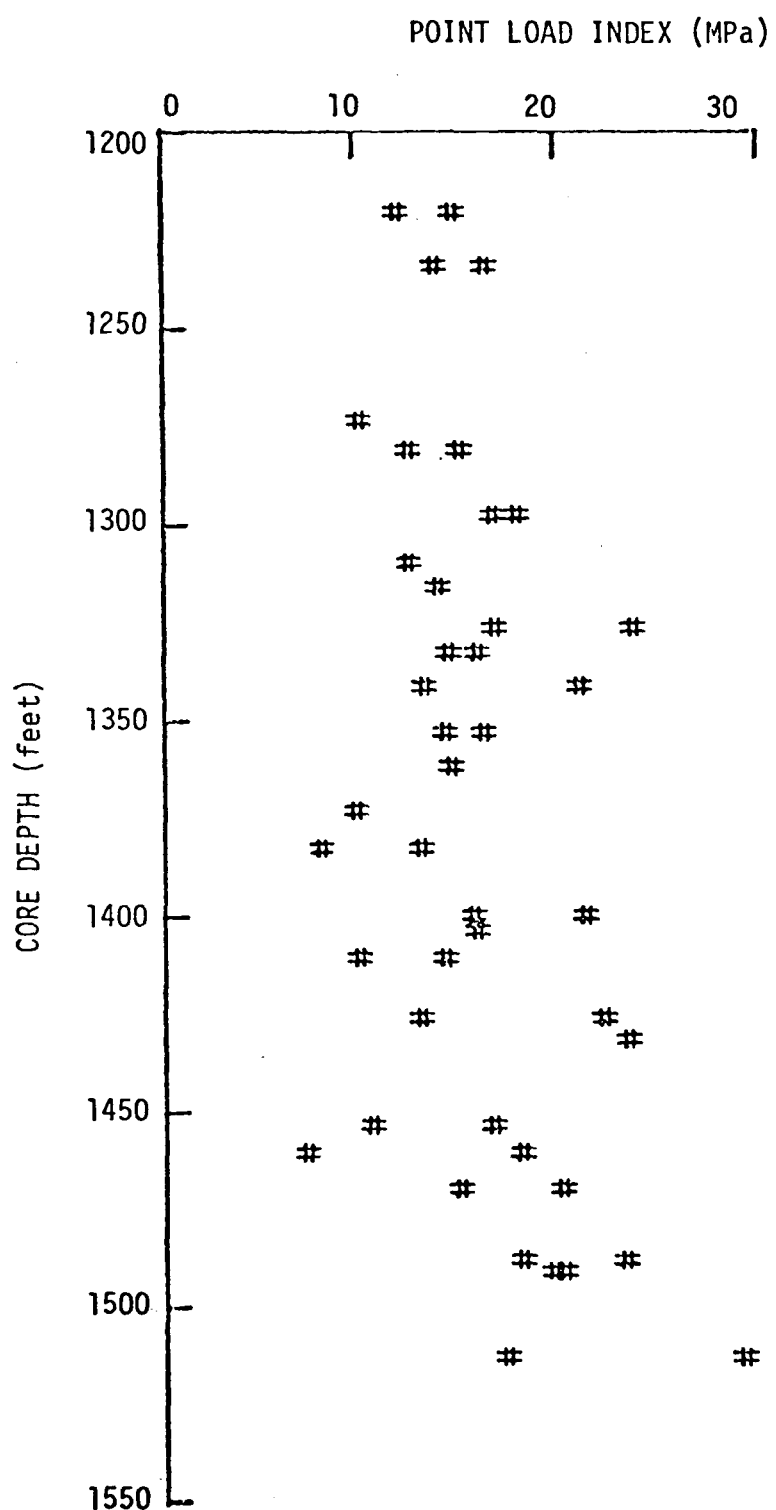


Figure 18. Variation of point load strength index with depth (Well No. Dow/ERDA 101).

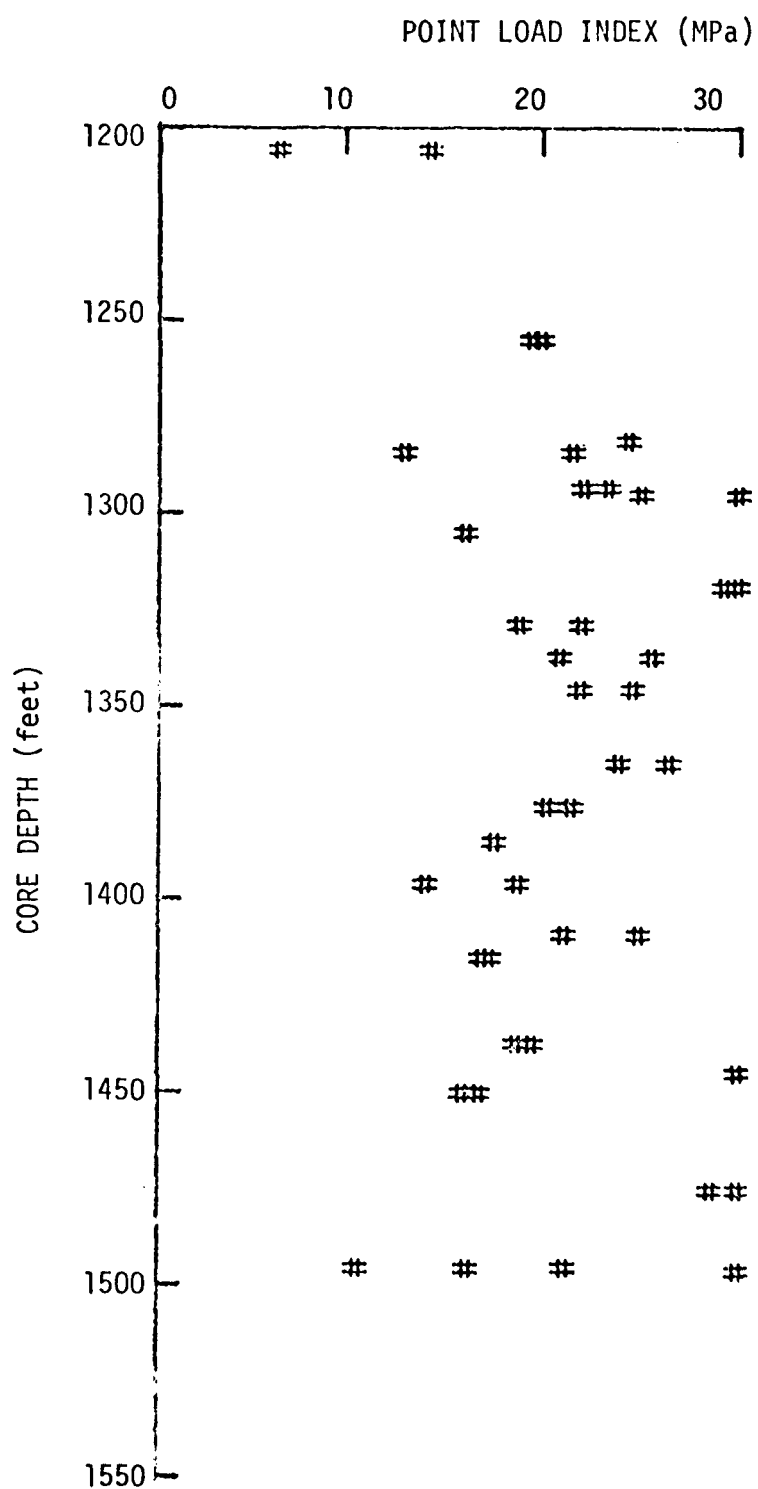


Figure 19. Variation of point load strength index with depth (Well No. Dow/ERDA 102).

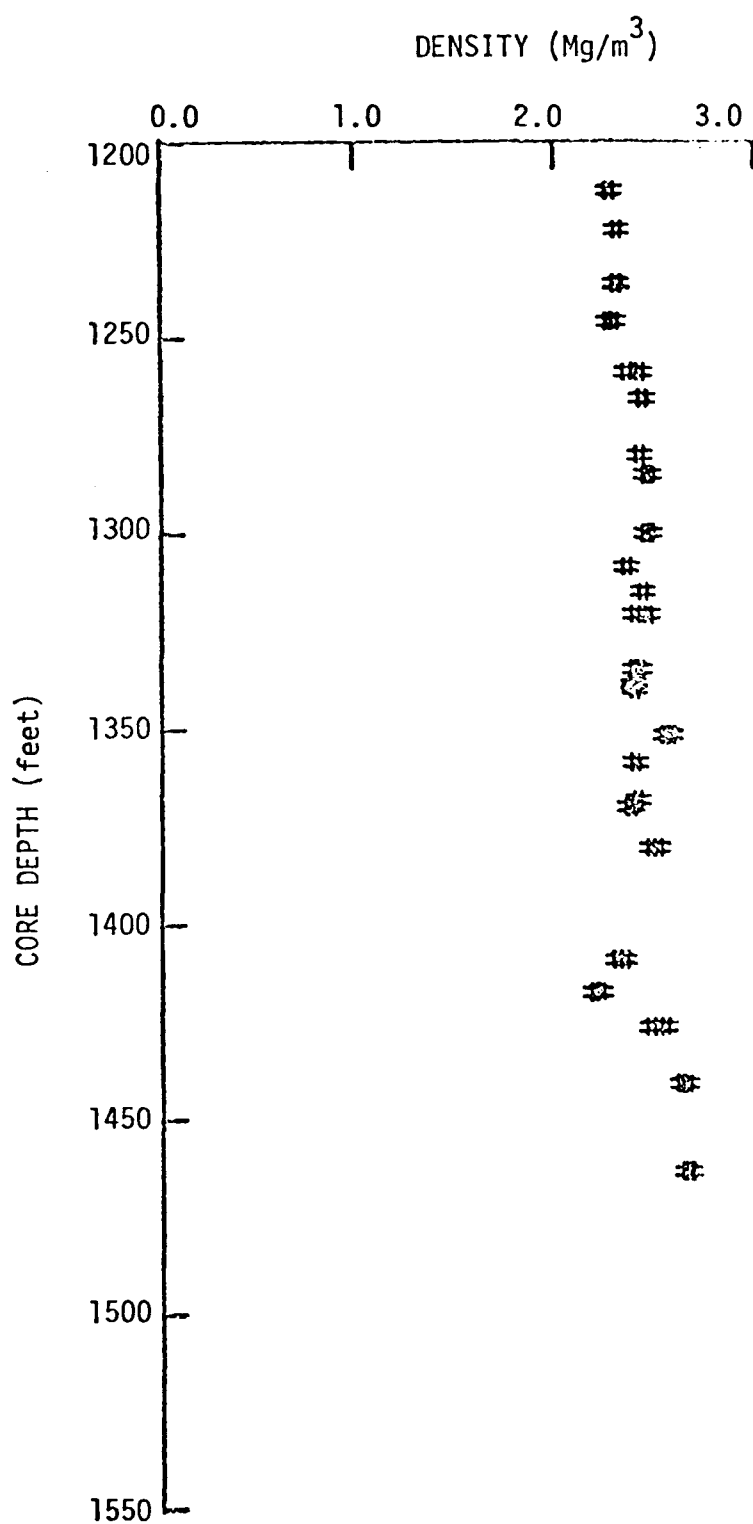


Figure 20. Variation of density with depth (Well No. Dow/ERDA 100).

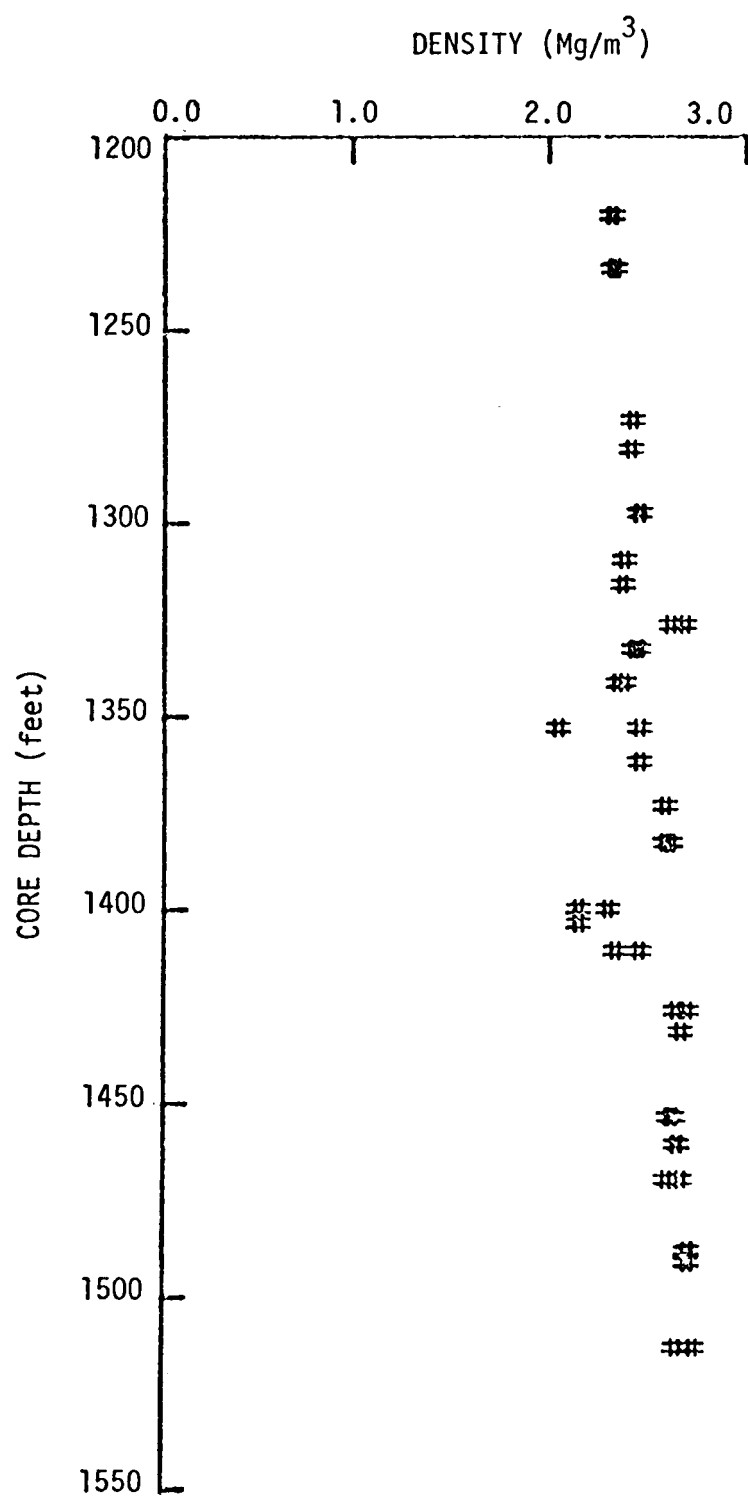


Figure 21. Variation of density with depth (Well No. Dow/ERDA 101).

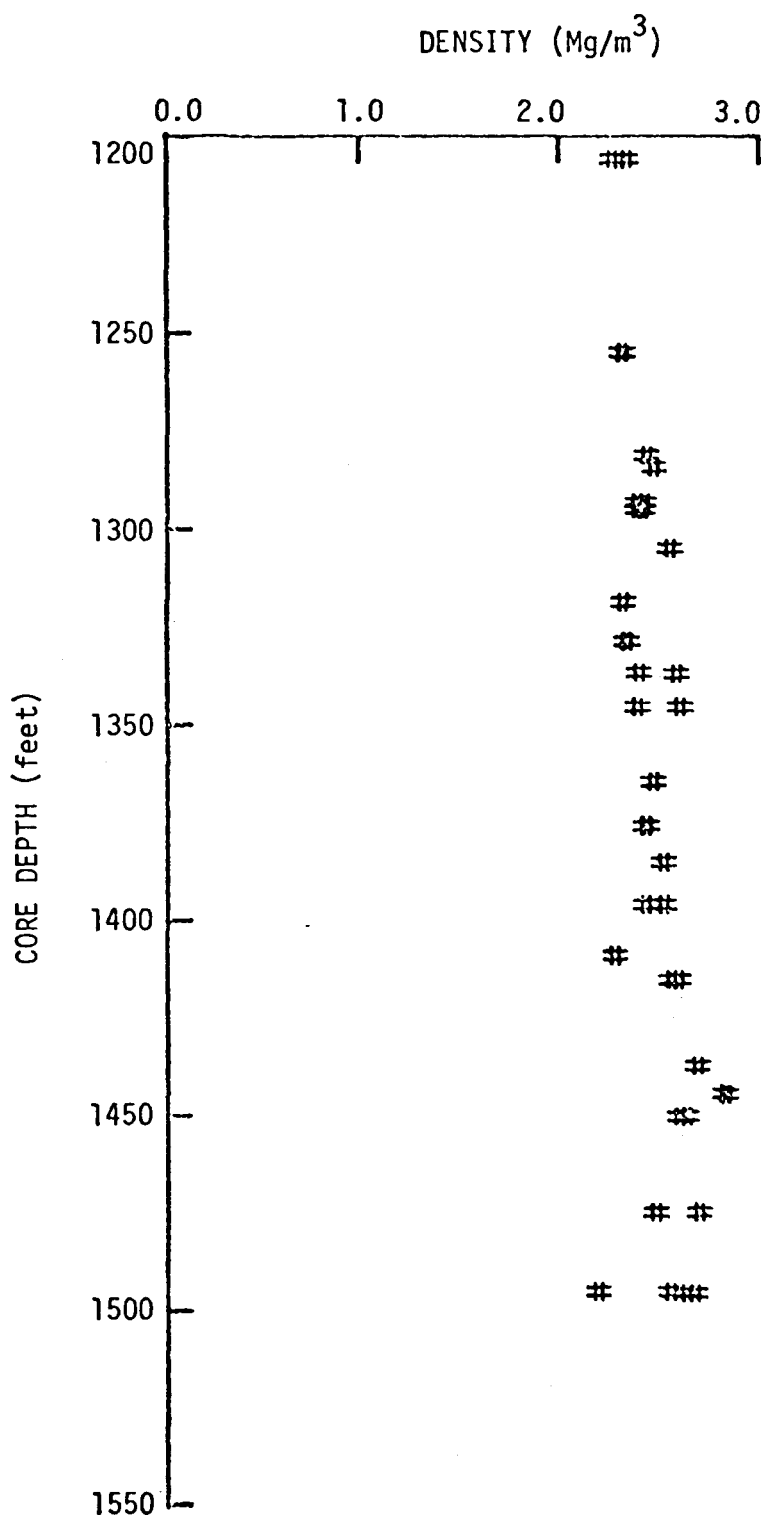


Figure 22. Variation of density with depth (Well No. Dow/ERDA 102).

more drops are made. The same procedure is used at the opposite end of the specimen to give a total of 20 readings for each specimen. The average value of 20 readings is taken as the scleroscope hardness for the specimen under test.

2.4.2 Test Results

Test results are presented in Tables 11-13. The scleroscope hardness numbers were plotted against depth (Fig. 23-25).

The scleroscope hardness data were also plotted against point load strength index (Fig. 26-28). Best fit lines are given in these figures. The plots show that the point load strength index increases as the scleroscope hardness increases. This analysis indicates the strength property measured by the point load test is somewhat related to the deformation property measured by the scleroscope test although both methods provide relative measures in a qualitative manner.

3.0 SUMMARY

The strength and deformation properties measured by destructive and nondestructive methods described in the preceding chapter yielded very comprehensive information regarding the basic mechanical properties of Antrim shale formation.

The variation of the properties with depth showed a general tendency that the kerogen bearing shale has low strength, Young's modulus, Poisson's ratio in comparison with the floor rocks. Only limited information was obtained for the cap rocks due to the high fracture frequency in the cores. The visual observation of cores, point load strength and scleroscope hardness data indicate that the cap rock is incompetent, in general.

The rich oil shale cores tended to break more easily along the bedding planes than the cap and floor rock, the lean oil shale or the oil shale with intrusion of calcareous materials. Very few specimens representing rich oil shale survived after the various treatments experienced during the lithologic logging, transportation from one lab to

TABLE 11. SCLEROSCOPE HARDNESS TEST RESULTS
(Specimens from Well No. Dow/ERDA 100)

Elevation Interval (ft)	Specimen No.	Scleroscope Hardness (average value)*	Standard Deviation	% S.D.
1200-10	100/1207.1/a	21.9	0.9	4.1
1210-20	100/1212.8/a	21.6	1.4	6.5
1220-30	100/1222.7/a	18.6	0.9	4.8
1230-40	100/1239.0	23.5	0.8	3.4
1240-50	100/1245.9/a	23.8	0.9	3.8
1250-60	100/1259.1/a	20.6	0.9	4.4
1260-70	100/1265.5/b	19.1	1.1	5.7
1270-80	100/1280.0/a	19.8	0.8	4.0
1280-90	100/1285.0/a	19.4	1.4	7.2
1290-1300	100/1300.0	20.9	0.8	3.8
1300-10	100/1304.6	20.1	2.1	10.4
1310-20	100/1315.4/b	28.3	2.9	10.2
1320-30	100/1324.8/a	25.2	3.2	12.7
1330-40	100/1335.4/b	36.6	2.0	5.5
1340-50	100/1342.1/a	26.7	3.2	12.0
1350-60	100/1351.7/a	38.1	1.6	4.2
1360-70	100/1368.7/a	18.9	1.1	5.8
1370-80	100/1370.4/b	21.7	1.2	5.5
1380-90	100/1380.6/a	22.3	1.5	6.7
1390-1400	100/1395.9/a	32.2	1.8	5.6
1400-10	100/1405.3/a	19.7	2.3	11.7
1410-20	100/1413.3/a	20.7	2.6	12.6
1420-30	100/1424.0/a	21.5	3.4	15.8
1430-40	100/1439.7/a	39.7	3.7	9.3
1440-50	100/1441.1/a	43.2	1.6	3.7
1450-60	100/1454.7	15.7	1.0	6.4
1460-70	100/1463.4/c	44.7	1.0	2.2
1470-80	100/1474.6	19.7	2.7	13.7

*Average value of 20 readings.

TABLE 12. SCLEROSCOPE HARDNESS TEST RESULTS
(Specimens from Well No. Dow/ERDA 101)

Elevation Interval (ft)	Specimen No.	Scleroscope Hardness (average value)*	Standard Deviation	% S.D.
1220-30	101/1220.5/a	21.9	1.2	5.5
	101/1220.5/b	21.9	1.3	5.9
	101/1220.5/c	22.2	1.3	5.8
	101/1220.5/d	22.4	1.4	6.2
1230-40	101/1234.5/a	26.1	2.5	9.6
	101/1234.5/b	24.0	1.1	4.6
	101/1234.5/c	27.4	1.8	6.6
	101/1234.5/d	23.7	1.5	6.3
1240-50	101/1240.0/a	21.3	1.0	4.7
	101/1240.0/b	21.8	1.1	5.0
	101/1240.0/c	21.7	1.0	4.6
1270-80	101/1273.6/a	20.8	1.2	5.8
	101/1273.6/b	21.3	1.3	6.1
	101/1273.6/c	22.0	1.1	5.0
	101/1273.6/d	21.3	1.2	5.6
1280-90	101/1281.1/a	21.6	1.3	6.0
	101/1281.1/b	22.5	1.1	4.9
	101/1281.1/c	20.9	0.9	4.3
	101/1281.1/d	22.0	1.2	5.4
1290-1300	101/1297.9/a	31.1	1.5	4.8
	101/1297.9/b	33.4	1.6	4.8
	101/1297.9/c	32.8	1.4	4.3
	101/1297.9/d	33.2	1.5	4.5
1300-10	101/1309.8/a	24.2	1.2	5.0
	101/1309.8/b	30.3	4.0	13.2
	101/1309.8/c	24.8	3.5	14.1
	101/1309.8/d	24.3	1.3	5.3
1310-20	101/1316.0/a	27.1	1.6	5.9
	101/1316.0/b	25.6	1.5	5.9
	101/1316.0/c	26.2	2.0	7.6
	101/1316.0/d	24.4	2.0	8.2
1320-30	101/1326.6/a	44.5	2.2	4.9
	101/1326.6/b	43.4	2.0	4.6
	101/1326.6/c	43.8	1.7	3.9
	101/1326.6/d	44.4	2.5	5.6
1330-40	101/1332.8/a	29.8	1.9	6.4
	101/1332.8/b	28.8	2.0	7.0
	101/1332.8/c	28.7	3.4	11.8
	101/1332.8/d	26.5	1.8	6.8

TABLE 12 (continued)

Elevation Interval (ft)	Specimen No.	Scleroscope Hardness (average value)*	Standard Deviation	% S.D.
1340-50	101/1341.6/a	41.7	2.9	6.9
	101/1341.6/b	41.8	1.7	4.1
	101/1341.6/c	30.7	9.7	31.6
	101/1341.6/d	37.3	9.0	24.1
1350-60	101/1353.0/a	20.0	1.4	7.0
	101/1353.0/b	19.3	2.0	10.4
	101/1353.0/c	20.5	1.6	7.8
	101/1353.0/d	21.0	1.2	5.7
1360-70	101/1361.8/a	21.4	1.1	5.1
	101/1361.8/b	22.2	1.2	5.4
	101/1361.8/c	21.9	1.1	5.0
	101/1361.8/d	21.8	0.9	4.1
1370-80	101/1373.3/a	15.9	1.6	10.1
	101/1373.3/b	16.2	1.2	7.4
1380-90	101/1382.8/a	16.3	1.0	6.1
	101/1382.8/b	35.3	11.5	32.6
	101/1382.8/c	16.5	1.0	6.1
	101/1382.8/d	18.0	1.4	7.8
1390-1400	101/1399.7/a	22.8	1.2	5.3
	101/1399.7/b	28.6	4.3	15.0
	101/1399.7/c	29.1	2.9	10.0
	101/1399.7/d	31.1	8.3	26.7
1400-10	101/1403.5/a	25.8	2.8	10.8
	101/1403.5/b	33.7	7.6	22.5
	101/1403.5/c	36.9	1.8	4.9
	101/1403.5/d	24.4	1.7	7.0
1410-20	101/1410.8/a	18.8	2.4	12.8
	101/1410.8/b	21.1	1.0	4.7
	101/1410.8/c	19.7	1.8	9.1
	101/1410.8/d	21.8	1.4	6.4
1420-30	101/1426.0/a	33.0	7.9	23.9
	101/1426.0/b	34.8	9.8	28.2
	101/1426.0/c	47.5	2.2	4.6
	101/1426.0/d	43.5	6.7	15.4
1430-40	101/1431.6/a	43.9	2.9	6.6
	101/1431.6/b	41.6	6.0	14.4
	101/1431.6/c	39.7	6.5	16.4
	101/1431.6/d	47.7	2.3	4.8
1440-50	101/1449.5/a	17.3	1.5	8.7
	101/1449.5/b	17.6	1.6	9.1

TABLE 12 (continued)

Elevation Interval (ft)	Specimen No.	Scleroscope Hardness (average value)*	Standard Deviation	% S.D.
1450-60	101/1453.5/a	20.1	1.6	8.0
	101/1453.5/b	17.7	1.5	8.5
	101/1453.5/c	16.3	1.1	6.7
	101/1453.5/d	17.6	1.3	7.4
1460-69	101/1460.0/a	39.6	1.7	4.3
	101/1460.0/b	38.9	1.4	3.6
	101/1460.6/a	19.8	1.2	6.1
	101/1460.6/b	16.9	1.3	7.7
1469-80	101/1469.9/a	31.4	5.0	15.9
	101/1469.9/b	21.7	6.2	28.6
1480-90	101/1488.3/a	37.9	6.7	17.7
	101/1488.3/b	39.3	5.8	14.8
	101/1488.3/c	40.5	3.0	7.4
	101/1488.3/d	41.7	2.3	5.5
	101/1488.3/e	42.3	1.9	4.5
1490-1500	101/1491.2/a	44.6	2.2	4.9
	101/1491.2/b	46.2	1.7	3.7
1510-20	101/1513.0/a	20.4	2.0	9.8
	101/1513.0/b	20.4	1.6	7.8

TABLE 13. SCLEROSCOPE HARDNESS TEST RESULTS
(Specimens from Well No. Dow/ERDA 102)

Elevation Interval (ft)	Specimen No.	Scleroscope Hardness (average value)*	Standard Deviation	% S.D.
1200-10	102/1205.9/a	30.7	2.1	6.9
	102/1205.9/b	28.2	2.5	8.8
	102/1205.9/c	24.5	1.6	6.4
1240-50	102/1244.1/a	34.4	1.3	3.8
1250-60	102/1255.2/a	34.2	1.3	3.8
	102/1255.2/b	35.6	1.4	4.0
	102/1255.2/c	35.2	1.4	4.0
1280-90	102/1281.6/a	35.6	1.1	3.1
	102/1281.6/b	35.2	1.4	3.9
	102/1281.6/c	33.1	2.3	7.1
	102/1281.6/d	24.6	1.4	5.8
	102/1284.3/a	31.4	5.5	17.6
	102/1284.3/c	31.6	8.0	25.2
	102/1284.3/d	31.5	3.6	11.5
1290-1300	102/1293.5/a	24.7	1.7	6.8
	102/1293.5/b	24.4	2.0	8.2
	102/1293.5/c	24.6	2.1	8.4
	102/1293.4/a	28.1	5.1	18.2
	102/1295.4/b	24.5	3.9	16.1
	102/1295.4/c	24.2	2.3	9.7
	102/1295.4/d	26.5	3.2	11.9
1300-10	102/1305.1/a	22.3	1.8	8.2
1310-20	102/1318.8/a	33.3	3.6	11.0
	102/1318.8/b	33.6	3.9	11.6
	102/1318.8/c	33.6	3.4	10.0
	102/1318.8/d	32.1	4.6	14.5
1320-30	102/1328.9/a	36.7	2.3	6.4
	102/1328.9/b	36.2	1.3	3.6
	102/1328.9/c	36.4	1.9	5.1
	102/1328.9/d	36.3	2.8	7.7
1330-40	102/1337.1/a	29.2	2.6	8.8
	102/1337.1/b	37.1	2.7	7.3
	102/1337.1/c	35.9	2.2	6.1
	102/1337.1/d	37.9	2.3	6.0
1340-50	102/1345.5/a	37.5	1.4	3.7
	102/1345.5/b	38.2	1.1	3.0
	102/1345.5/c	38.3	1.6	4.3
	102/1345.5/d	38.4	1.4	3.7

TABLE 13 (continued)

Elevation Interval (ft)	Specimen No.	Scleroscope Hardness (average value)*	Standard Deviation	% S.D.
1360-70	102/1364.6/a	22.3	1.2	5.4
	102/1364.6/b	22.8	1.7	7.3
	102/1364.6/c	22.3	1.4	6.5
	102/1364.6/d	22.9	1.5	6.5
1370-80	102/1375.9/a	20.5	2.1	10.2
	102/1375.9/b	26.4	5.2	19.5
	102/1375.9/c	25.3	4.3	17.2
1380-90	102/1385.0/a	20.3	1.2	5.7
	102/1385.0/b	22.5	1.7	7.4
	102/1385.0/c	20.5	2.0	9.8
1400-10	102/1409.0/a	37.5	1.7	4.6
	102/1409.0/b	35.6	2.9	8.2
	102/1409.0/c	28.5	2.2	7.6
	102/1409.0/d	33.7	3.6	10.6
1410-20	102/1415.2/a	22.3	2.1	9.3
	102/1415.2/b	23.0	1.9	8.3
	102/1415.2/c	21.9	1.5	7.1
1430-40	102/1437.1/a	44.1	4.3	9.7
	102/1437.1/b	41.7	3.7	8.9
	102/1437.1/c	41.7	3.9	9.3
	102/1437.1/d	36.5	6.7	18.4
1440-50	102/1444.5/a	56.3	6.2	11.0
	102/1444.5/b	54.9	6.1	11.1
	102/1444.5/c	61.6	6.7	10.9
1450-60	102/1450.3/a	23.9	2.1	8.7
	102/1450.3/b	20.4	2.6	12.9
	102/1450.3/c	21.6	2.4	11.0
1470-80	102/1474.6/a	47.1	1.5	3.1
	102/1474.6/b	47.8	1.9	4.0
	102/1474.6/c	46.2	1.5	3.3
	102/1474.6/d	46.6	1.8	4.0
1490-1500	102/1495.4/a	23.0	1.7	7.4
	102/1495.4/b	23.8	1.9	7.9
	102/1495.4/c	23.9	2.2	9.3
	102/1495.5/a	40.8	2.9	7.2
	102/1495.5/b	22.1	3.3	15.0
	102/1495.5/c	29.4	5.0	16.9
	102/1495.5/d	30.4	6.6	21.6

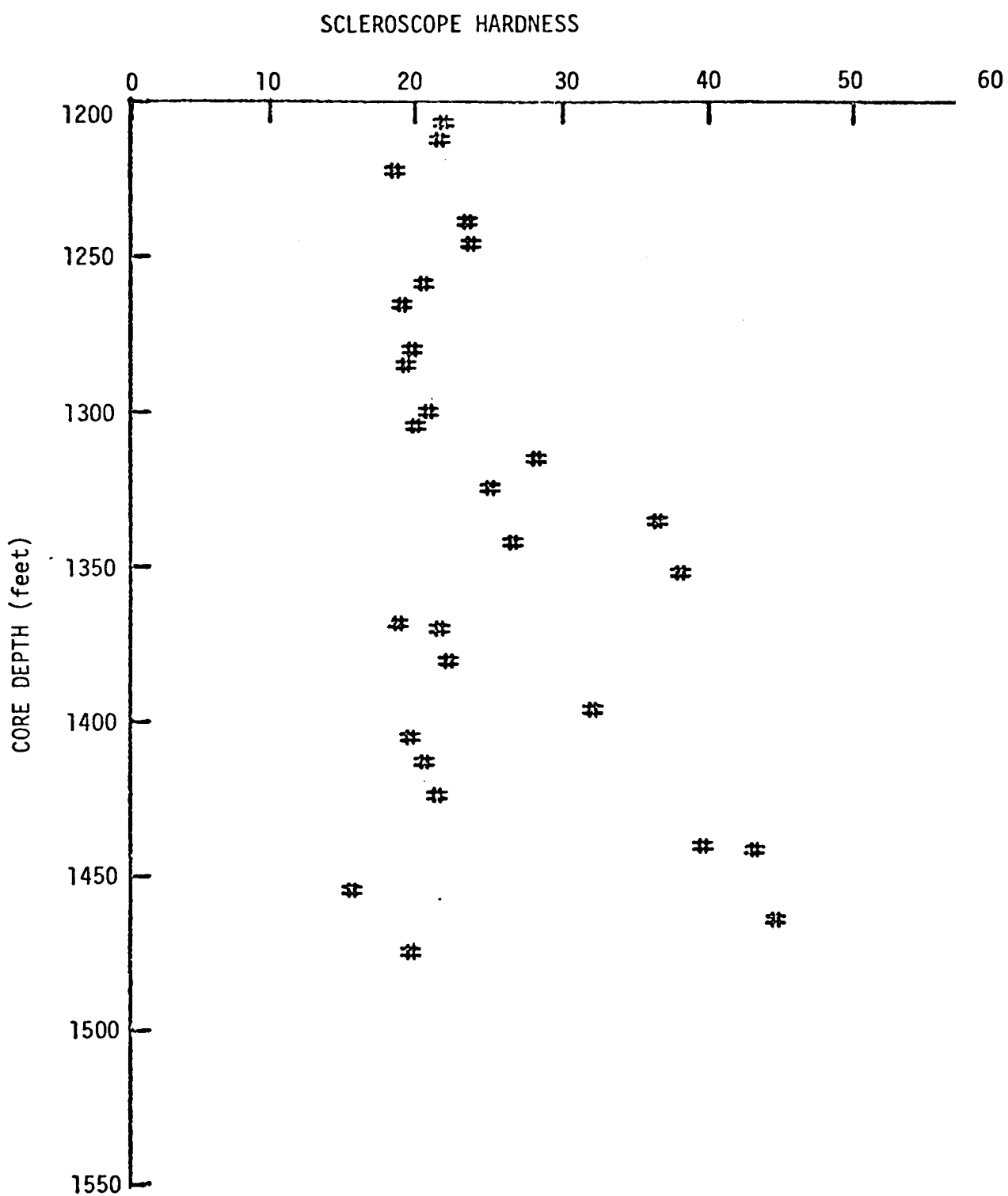


Figure 23. Variation of scleroscope hardness with depth (Well No. Dow/ERDA 100).

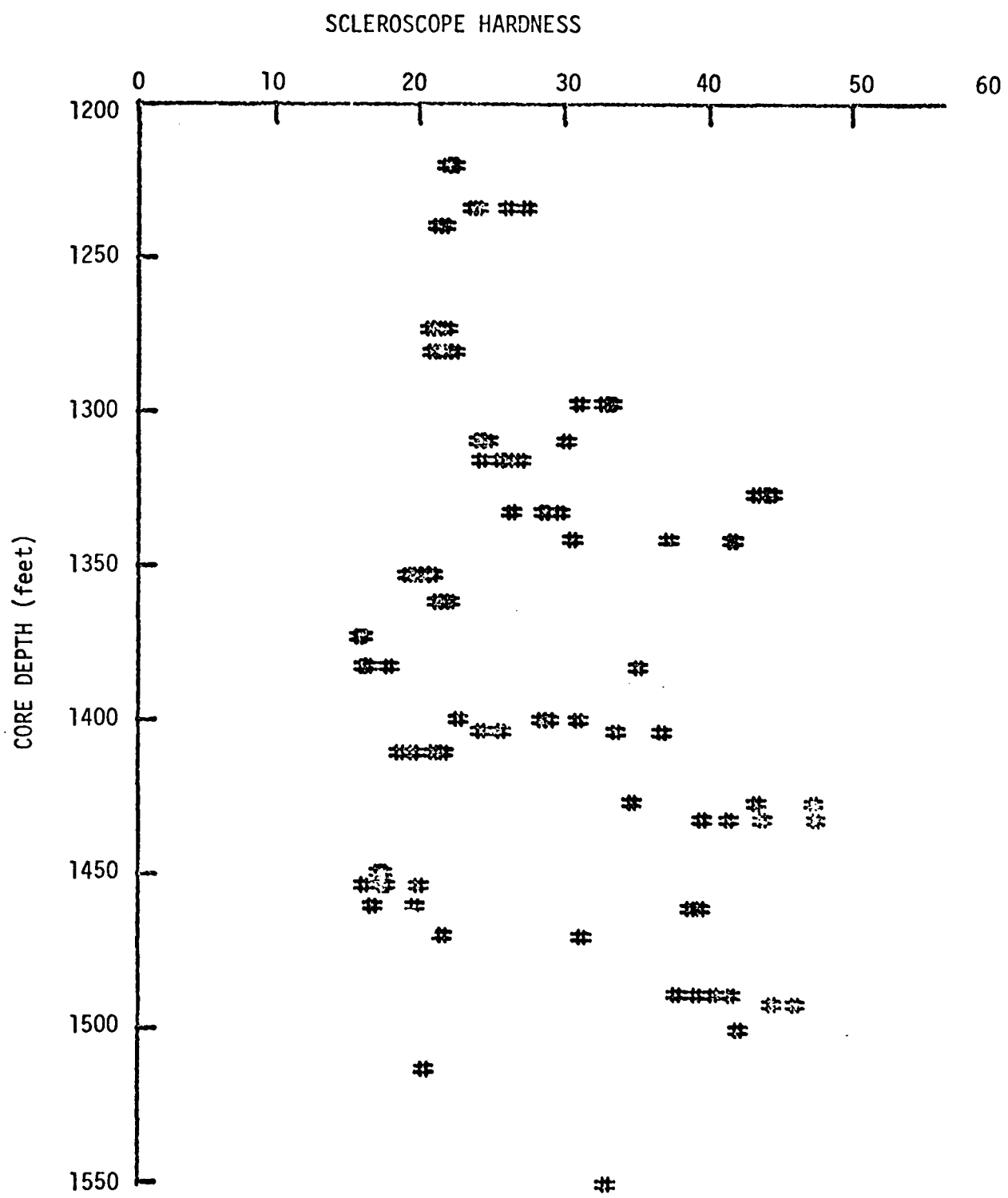


Figure 24. Variation of scleroscope hardness with depth (Well No. Dow/ERDA 101).

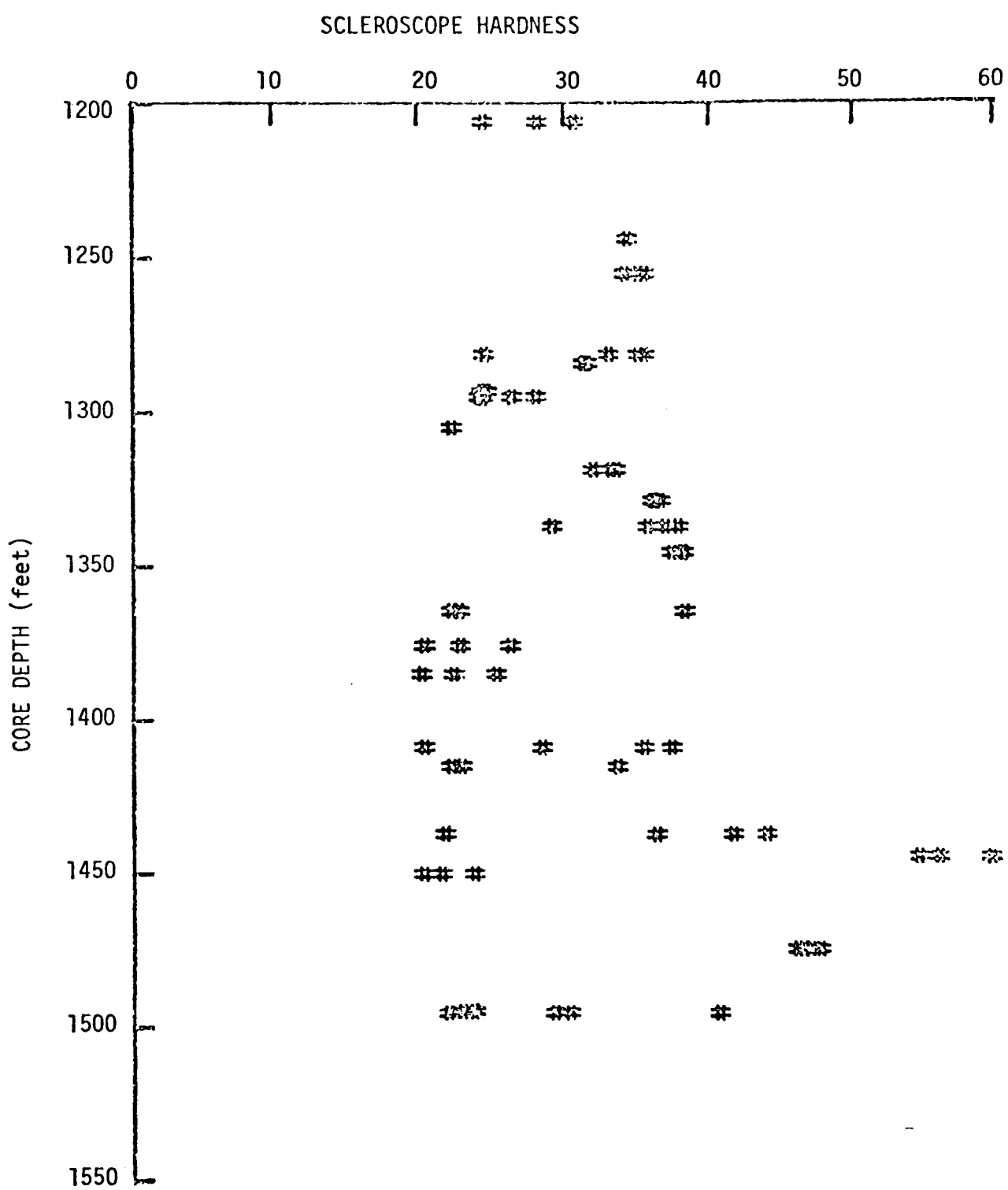


Figure 25. Variation of scleroscope hardness with depth (Well No. Dow/ERDA 102).

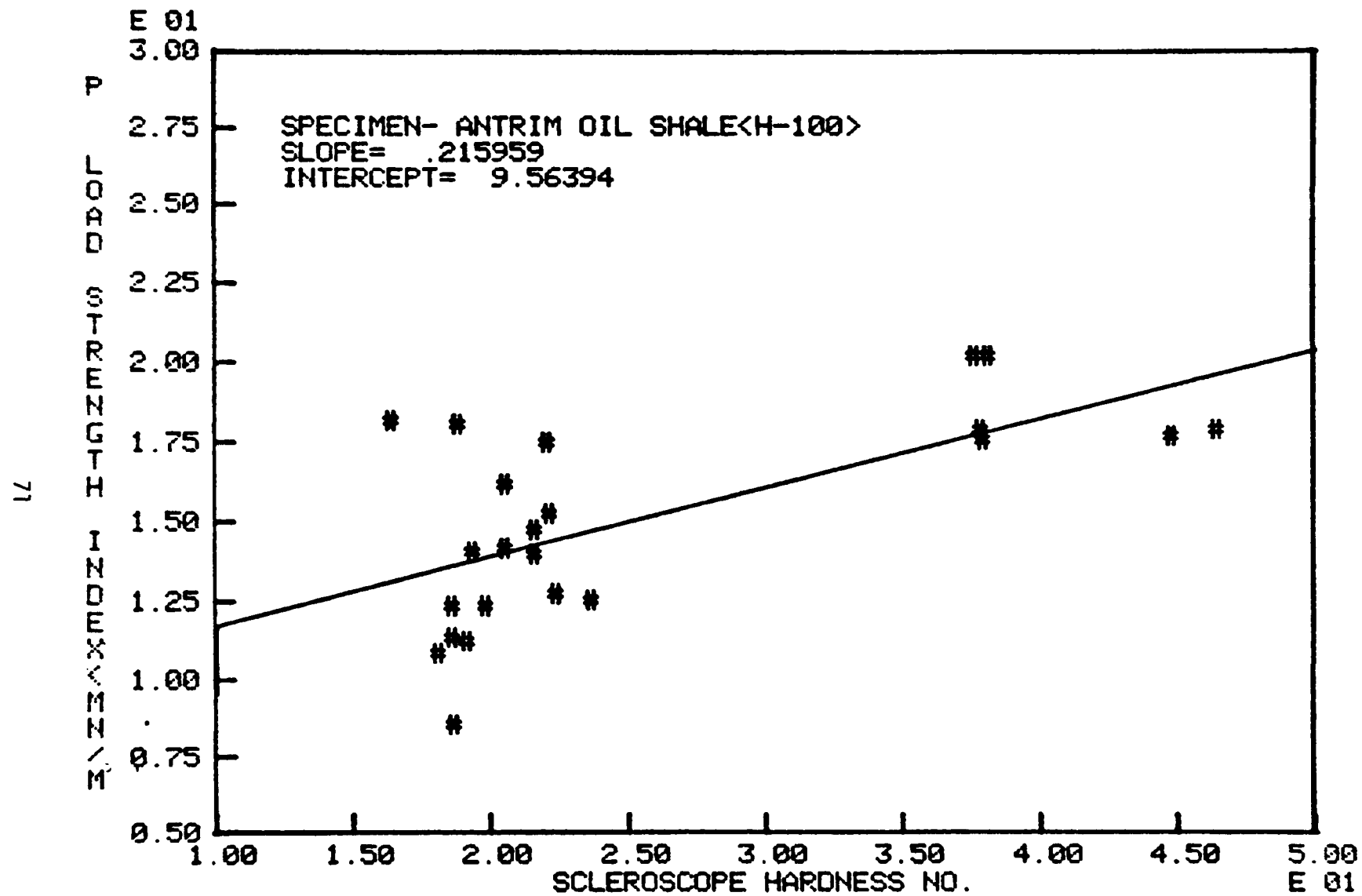


Figure 20. Point load strength index vs. scleroscope hardness no. (Hell No. Dow/ERDA 100).

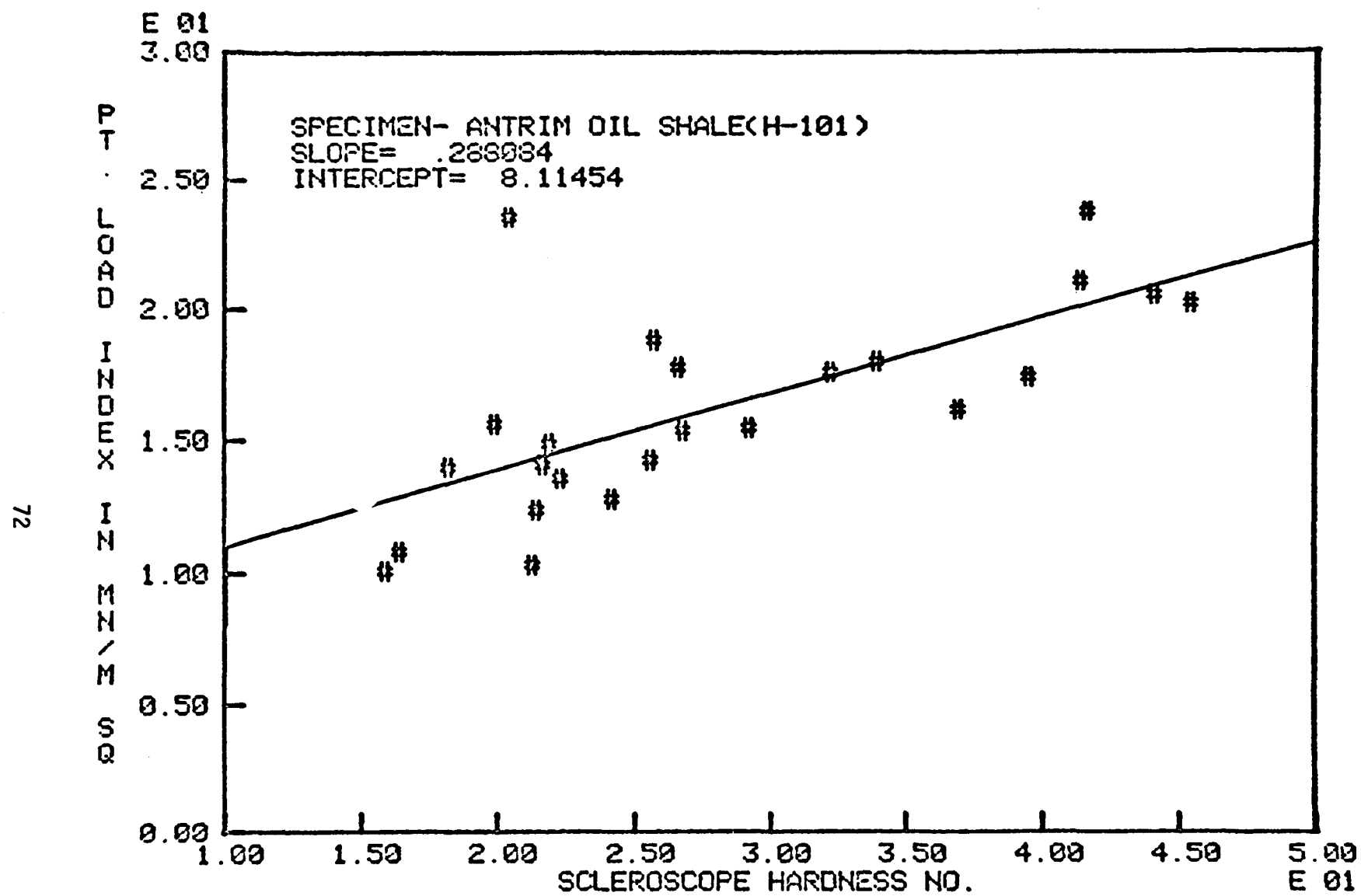


Figure 27. Point load strength index vs. scleroscope hardness no. (Well No. Dow/ERDA 101).

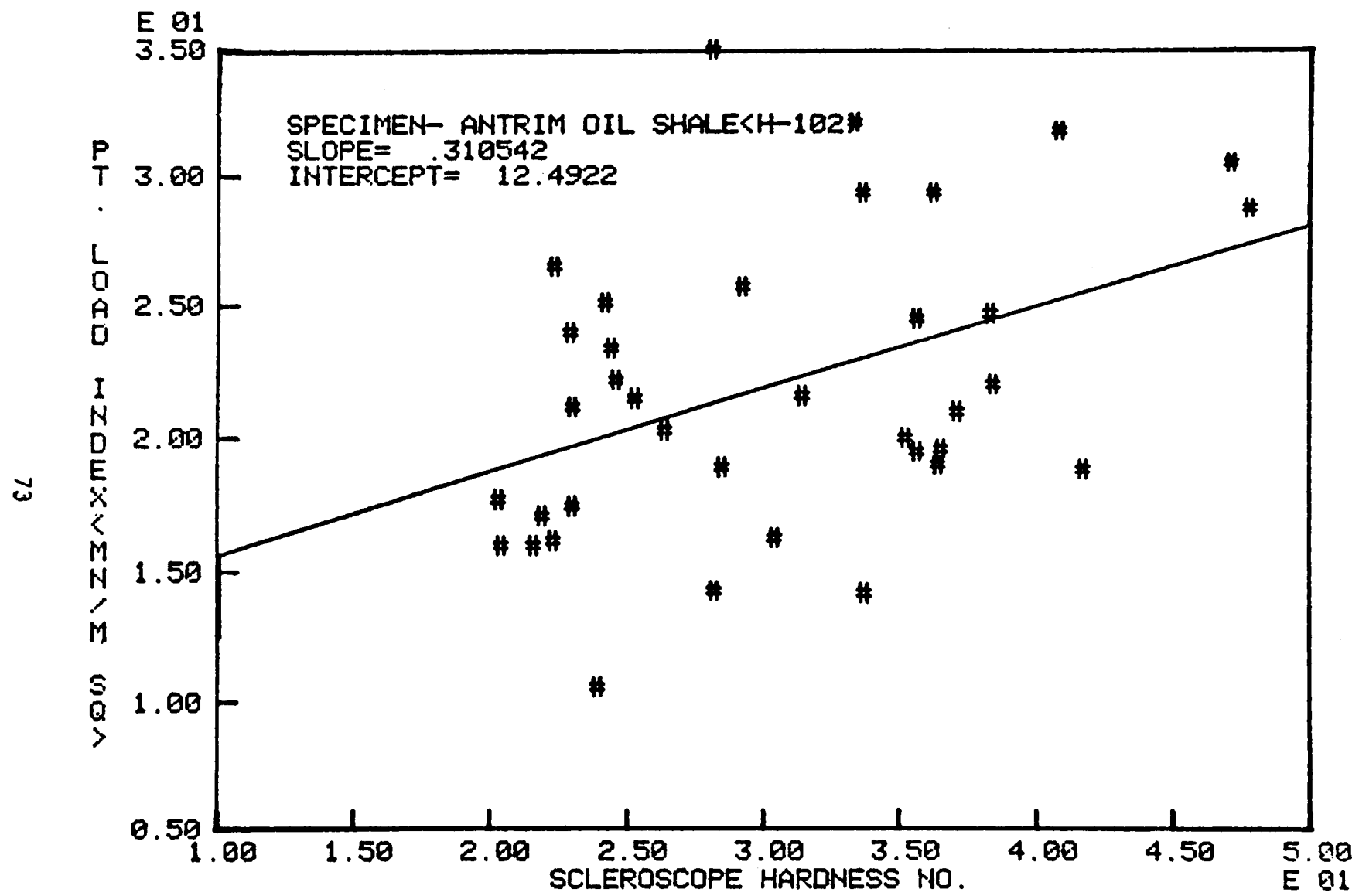


Figure 29. Point load strength index vs. scleroscone hardness no. (Well No. Dow/ERDA 102).

another and the final specimen preparation procedures including coring, cutting and surface grinding.

The kerogen contents in the Antrim oil shale were found to be related to the deformation and strength properties as in the Western oil shales⁴ which are significantly richer in kerogen. The Young's modulus and compressive strength decrease with increased kerogen content whereas the Poisson's ratio does not vary substantially with kerogen content.

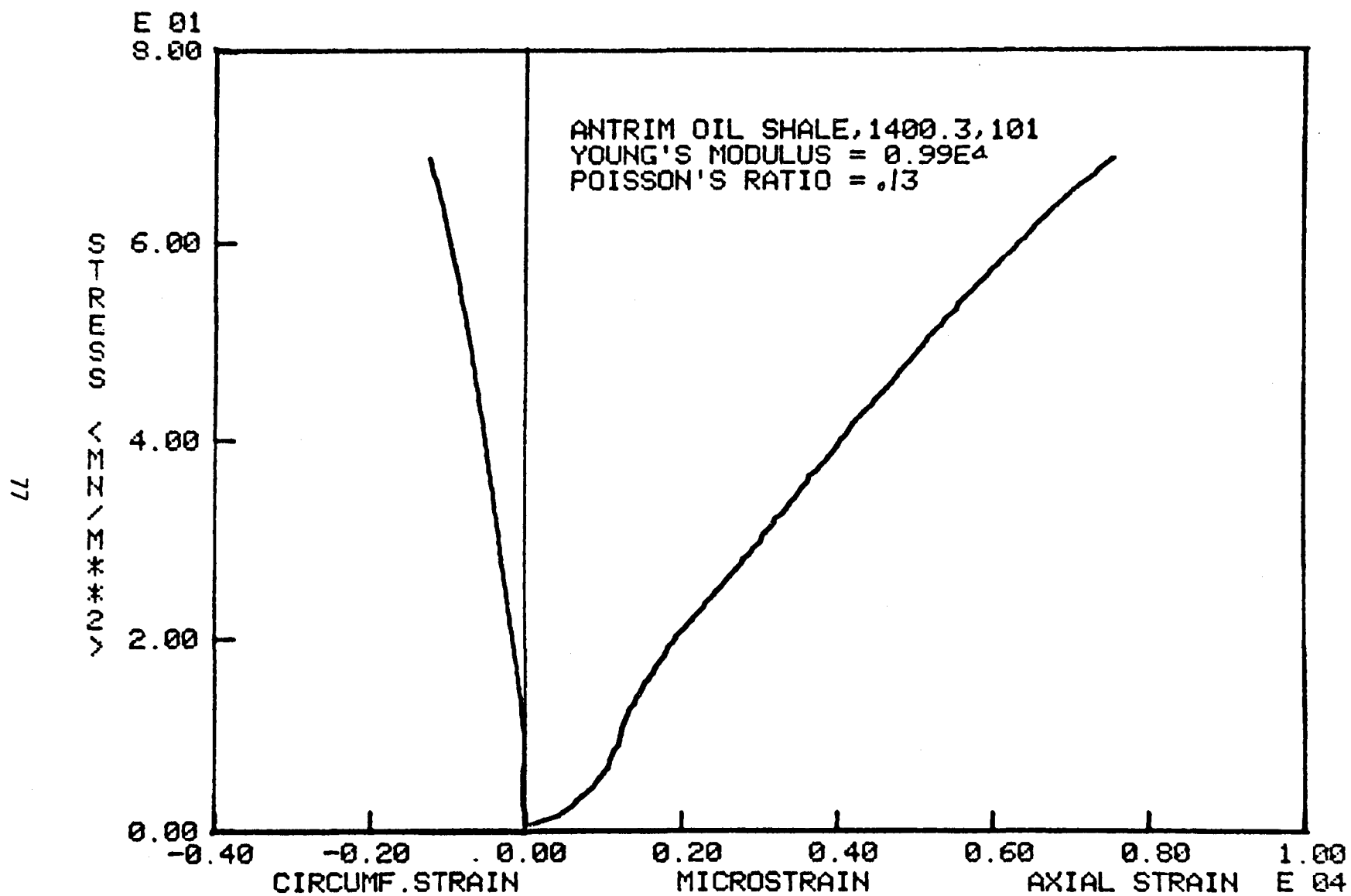
A distinct characteristic of Antrim shale is the extreme weakness of the bedding planes which caused great difficulties in specimen preparation. This property, however, could be utilized constructively to facilitate the horizontal fracturing through separation of bedding planes in in-situ fracturing operations.

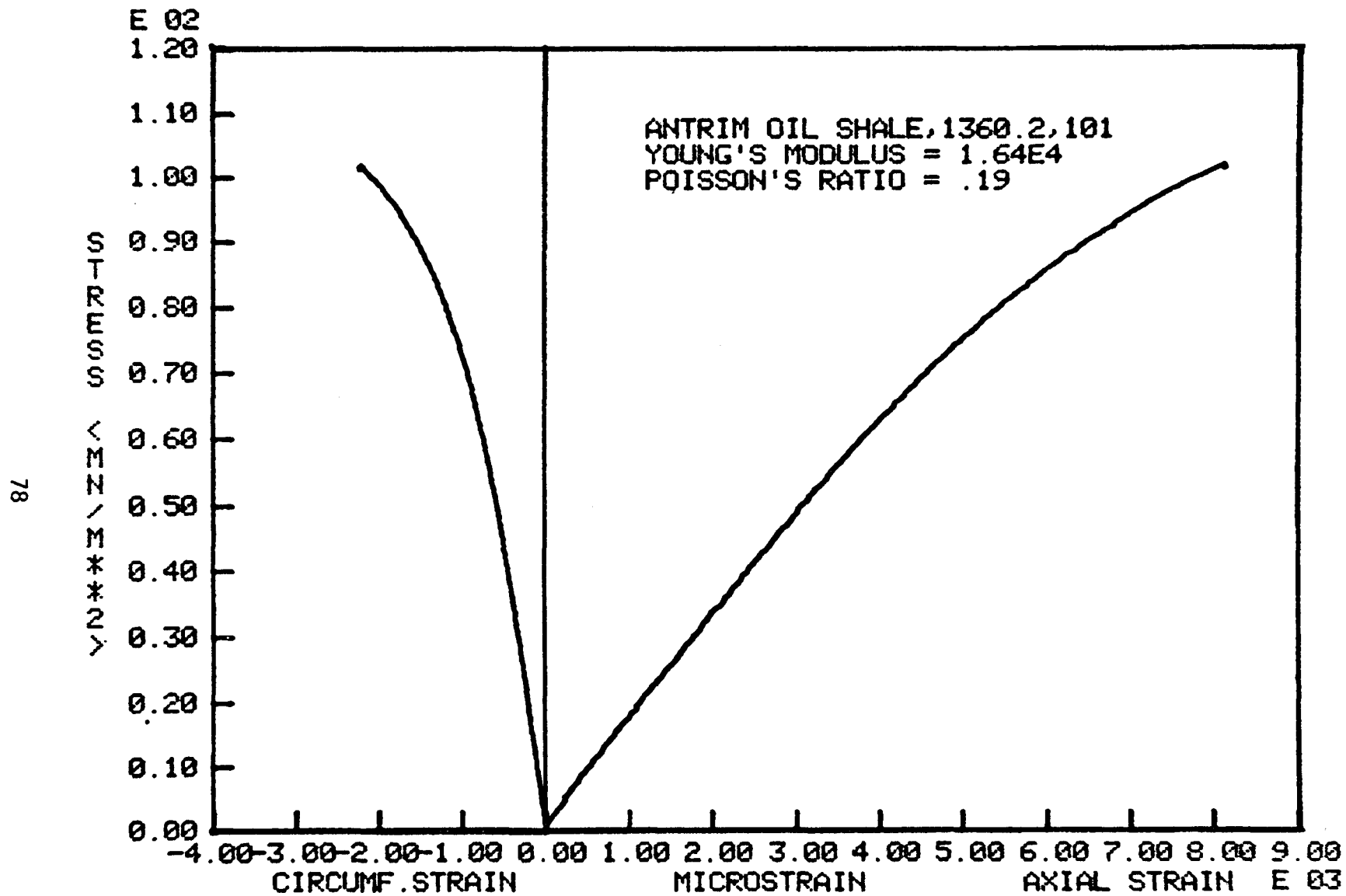
REFERENCES

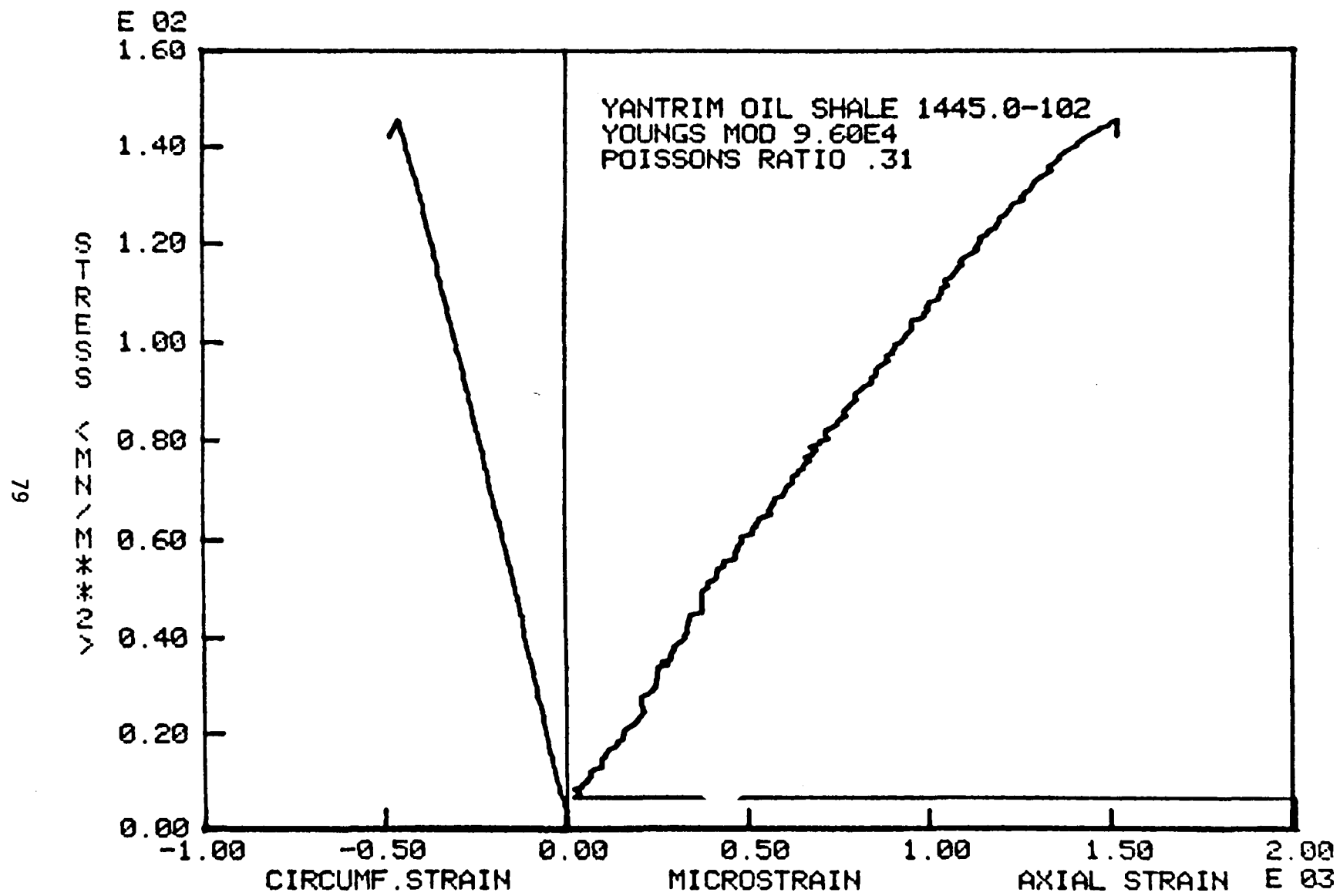
1. ASTM Designation D2938-71, "Standard Method of Test for Unconfined Compressive Strength of Rock Core Specimens".
2. International Society of Rock Mechanics, 1972, "Suggested Methods for Determining the Uniaxial Compressive Strength of Rock Materials and the Point Load Strength Index".
3. ASTM Designation D2845-69, "Standard Method for Laboratory Determination of Pulse Velocities and Ultrasonic Elastic Constants of Rock".
4. Sellers, J. B., G. R. Haworth, and P. G. Zambras, 1972, "Rock Mechanics Research on Oil Shale Mining", SME/AIME Transactions, Vol. 252, No. 2.

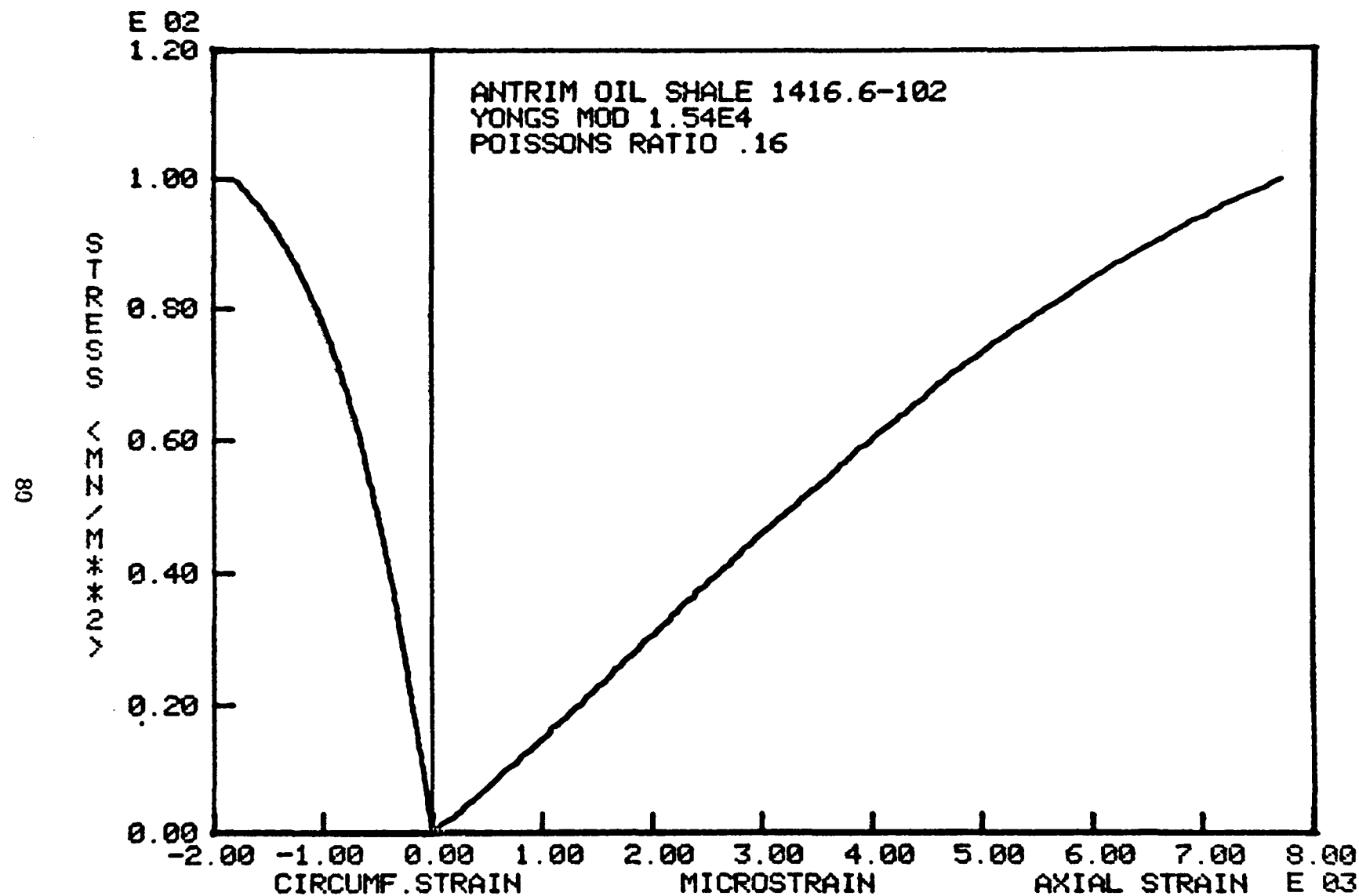
APPENDIX

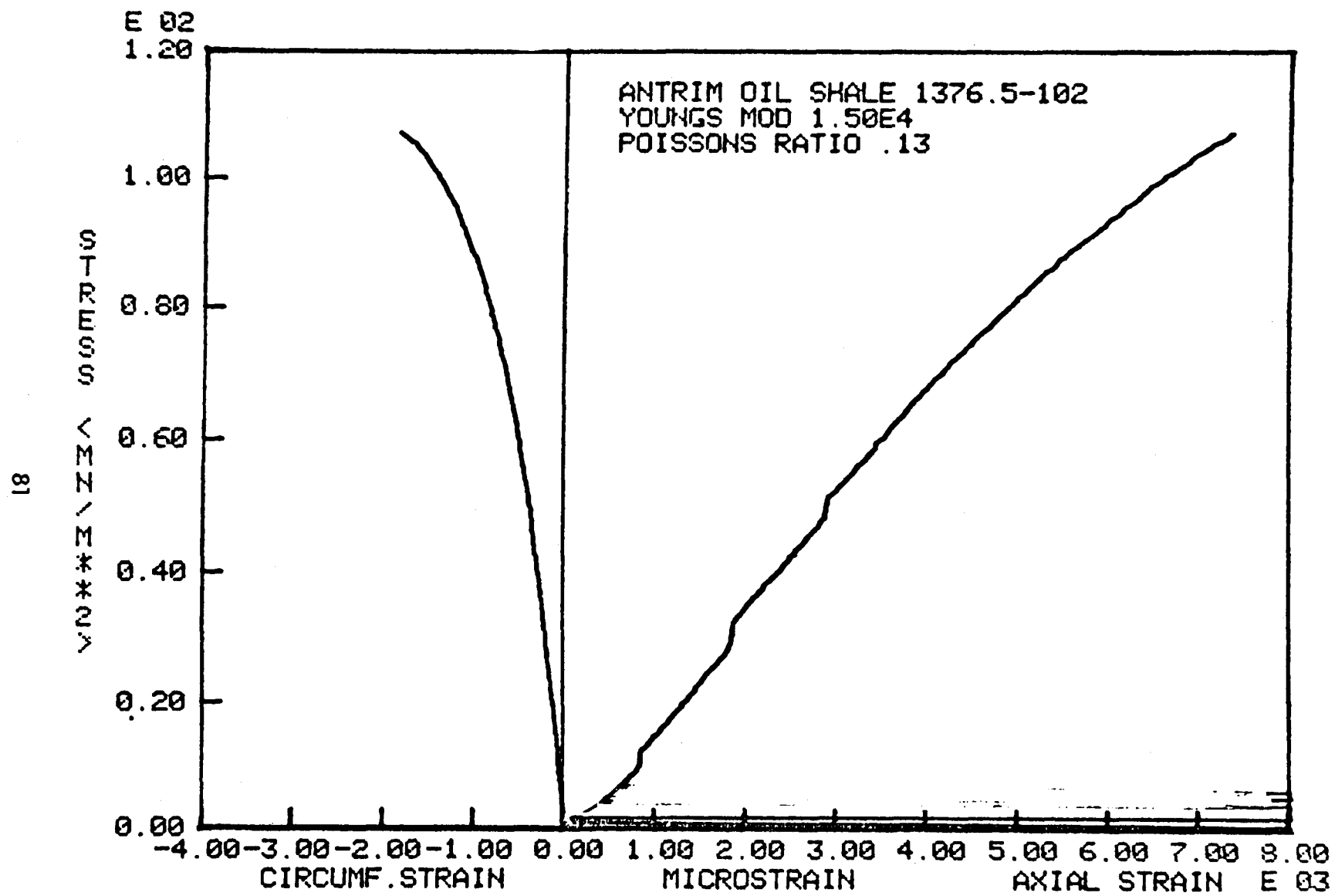
Stress-strain curves of some selected specimens (Specimen numbers, 101/1400.3, 101/1360.2, 102/1445.0, 102/1416.6, 102/1376.5, 102/1306.1, 101/1490.2, 102/1438.0, and 102/1386.4).

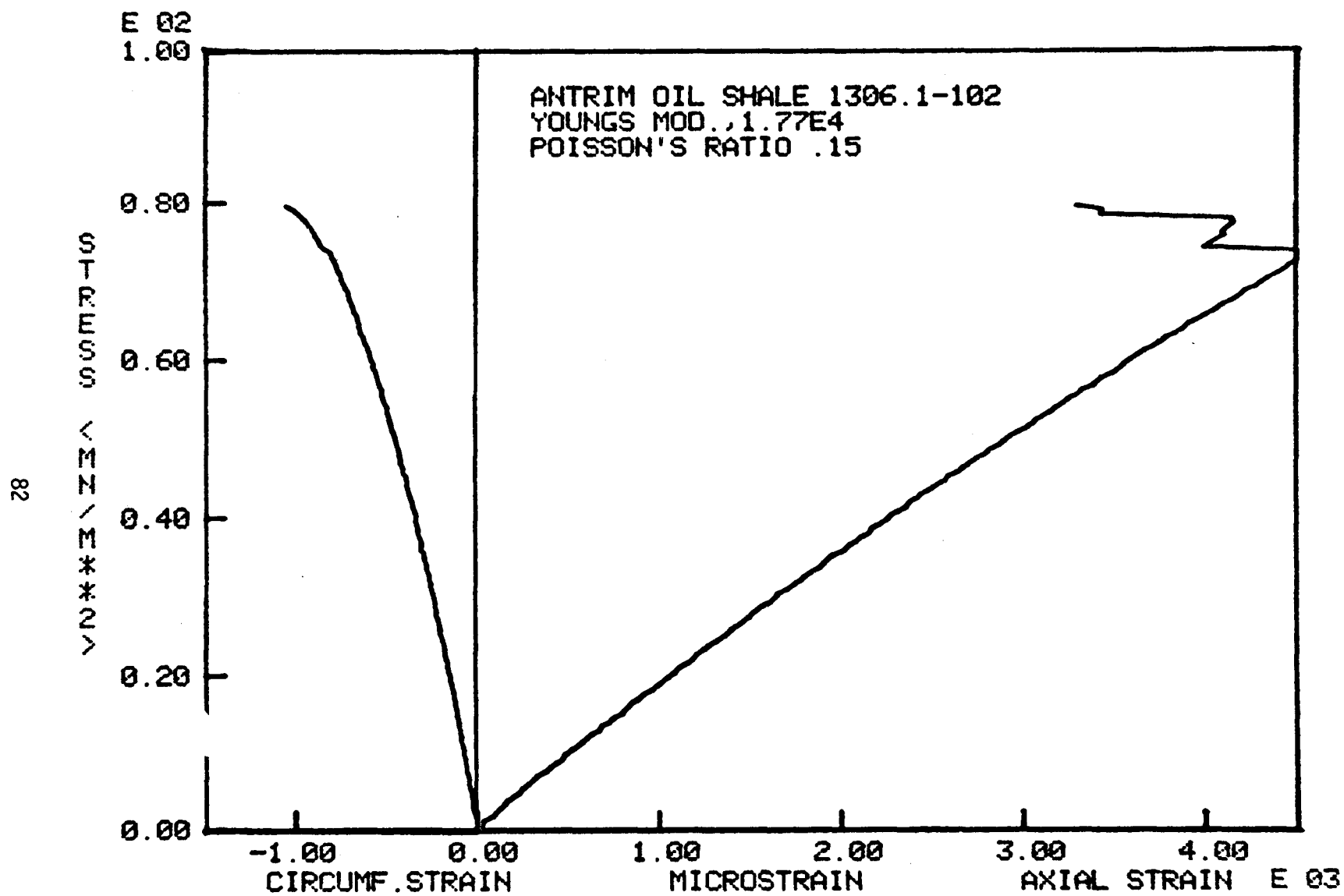












E 02
83

